A CROWDSOURCING TECHNIQUE FOR ROAD SURFACE MONITORING USING SMARTPHONE SENSORS

by

Shahram Sattar

B.Sc., Isfahan University, Isfahan, Iran, 2010

M.A.Sc., Ryerson University, Toronto, Ontario, Canada, 2014

A dissertation

presented to Ryerson University

in partial fulfillment of the

requirements for the degree of

Doctor of Philosophy

in the Program of

Civil Engineering

Toronto, Ontario, Canada, 2018

AUTHOR'S DECLARATION FOR ELECTRONIC SUBMISSION OF A DISSERTATION

I hereby declare that I am the sole author of this dissertation. This is a true copy of the dissertation, including any required final revisions, as accepted by my examiners.

I authorize Ryerson University to lend this dissertation to other institutions or individuals for the purpose of scholarly research

I further authorize Ryerson University to reproduce this dissertation by photocopying or by other means, in total or in part, at the request of other institutions or individuals for the purpose of scholarly research.

I understand that my dissertation may be made electronically available to the public.

Crowdsourcing Technique for Road Surface Monitoring using Smartphone Sensors

Doctor of Philosophy, 2018

Shahram Sattar

Civil Engineering

Ryerson University

Abstract

Road surface monitoring is a key factor in providing safe road infrastructure for road users. As a result, road surface condition monitoring aims to detect road surface anomalies such potholes, cracks and bumps, which affect driving comfort and on-road safety. Road surface anomaly detection is a widely studied problem. Recently, smartphone-based sensing has become popular with the increased amount of available embedded smartphone sensors. Using smartphones to detect road surface anomalies could change the way government agencies monitor and plan for road rehabilitation and maintenance.

Several studies have been developed to utilize smartphone sensors (e.g., Global Positioning system (GPS) and accelerometers) mounted on a moving vehicle to collect and process the data to monitor and tag roadway surface defects. Geotagged images or videos from the roadways have also been used to detect the road surface anomalies. However, existing studies are limited to identifying roadway anomalies mainly from a single source or lack the utility of combined and integrated multi-sensors in terms of accuracy and functionality. Therefore, low-cost, more efficient pavement evaluation technologies and a centralized information system are necessary to provide the most up-to-date information about the road status due to the dynamic changes on the road surface This information will assist transportation authorities to monitor and enhance the road surface condition.

In this research, a probabilistic-based crowdsourcing technique is developed to detect road surface anomalies from smartphone sensors such as linear accelerometers, gyroscopes and GPS to integrate multiple detections accurately. All case studies from the proposed detection approach showed an

approximate 80% detection accuracy (from a single survey) which supports the inclusiveness of the detection approach. In addition, the results of the proposed probabilistic-based integration approach indicated that the detection accuracy can be further improved by 5 to 20% with multiple detections conducted by the same vehicle along the same road segments. Finally, the development of the web-based Geographic Information System (GIS) platform would facilitate the real-time and active monitoring of road surface anomalies and offer further improvement of road surface quality control in large cities like Toronto.

Acknowledgements

Completing this dissertation has been a great milestone I would never have achieved without the support and encouragement of all the individuals mentioned in this section. I have started to note everything that I would like to put here since I started my study at Ryerson University. I would like to express my deepest appreciation to all those who made it possible for me to complete my studies at Ryerson University.

My deepest gratitude is to my supervisor, Professor Songnian Li. Dr. Li is an extremely nice and decent person with whom to share and work with. I have been amazingly fortunate to have him; he gave me the freedom to explore on my own, and at the same time the guidance to recover when my steps faltered. He taught me how to question thoughts and express ideas. His patience and support helped me overcome many crisis situations and helped with finishing this dissertation.

I am so indebted to have a number of senior professors in the department who gave me guidance throughout the study and shared the joy of my research life. I was very fortunate to have Professor Ahmed El-Rabbany as the graduate program director during my first two years of Ph.D. study at Ryerson. I have been very fortunate to have Professor Michael Chapman and Professor Ahmed Shaker in my supervisory committee at Ryerson for their insightful comments and encouragement, and also for the hard questions which incented me to widen my research from various perspectives. I have to specially mention Dr. Chapman who was always available whenever I had a question about my research or writing and generously led me to be in the right direction. This dissertation is in a much better shape as a result of their expertise, for which I am grateful.

I would like to thank administrative and technical staff members at Ryerson who have been kind enough to advise and help in their respective roles. I would like to thank Ms. Dianne Mendonca and Kim Kritzer from the civil engineering department who assisted me throughout my study. Appreciation also goes out to the graduate program administrator, Ms. Rachel (Harpley) Peluso who deserves credit for providing much needed assistance with administrative tasks, reminding us of impending deadlines, and keeping our work running smoothly.

To my best friend Dr. Wai Yeung Yan, thank you for listening, offering me advice, and supporting me through this journey. Your support and care helped me overcome setbacks and stay focused on my graduate study. Your friendly advice, your soothing words and your big heart helped me face all the obstacles and continue with my work. I will never forget your kindness. I also want to deliver my sincere appreciation to all my wonderful lab mates at GIS and Geo-collaboration Laboratory (GGL), Shishuo Xu, Wai Huang, Siyuan Liu, and Richard Wen for their friendships, and I deeply appreciate their support and belief in me. I would like to thank Annie Chow for being supportive throughout my time here and for helping me to proofread my Ph.D. proposal.

The research work was financially supported by the Ontario Graduate Scholarship (OGS), Natural Sciences and Engineering Research Council of Canada (NSERC). Indirect financial support was provided through the student competitions organized by the Association of Ontario Land Surveyor (AOLS). In particular, I would like to specifically mention Ms. Maureen V. Mountjoy from AOLS whose enthusiasm and effort in organizing and supporting different competition events for promoting geomatics education, from which I benefited.

Completing this work would have been impossible without the support and friendship provided by my brilliant friends at Ryerson University for always being there as a friend and colleague. Thanks to my dear friends Hossein Reshadi, Dylan Matin, Maryam Rafierad, Alborz Soltankhah, Keikhosrow Tahmureszadeh and Ali Yeganeh. I have to specially mention Ali Karami who acted like my brother. I never forget all the road trips we had together in his memorable car which definitely helped me to relax and stay focused on my study. I would like to extend my appreciation to my other best friends: Freidoon Attaroodi, Arjang tavassoli and Kaveh Shahbaz with whom I spent joyful days outside the school.

I owe a great debt of gratitude to my instructors during my undergraduate studies at Isfahan University, Iran. I have to specially mention Dr. Jamal Asgari, Dr. Vahab Nafisi, Dr. Mehdi Momeni, Dr. Assadollah Karimi, Dr. Abdolhossein Mousavi-Al-Kazemi, Dr. Saeed Nadi and Dr. Mehran Sattari who created the knowledge foundation which formed the basis of this dissertation. As time goes on, I realize more and more clearly the huge impact that they have had on my academic career.

I always believe it is not easy to get to know true friends when we are grown up which their support and care from all around the world were indispensable to complete this study. They are Majid Sharifi, Nima Mohri, Farshid Hajjarian, Hamed Gholizadeh, Babak Behfrouz, Ehsan Foroutan, Mehdi Naghdi, Hamed Jafari, Mohammad Ebnenassir and Sina Fattholahzadeh. I have to specially mention Majid Sharifi, Nima Mohri, and Farshid Hajarian for all gatherings and trips that we had when I flew back home; Hamed Gholizadeh for his regular text messages, updates and the delightful US trip that we had together. Also, continued moral support from my relatives thousands of miles away. My cousins Sina, Sanaz, Pouya, Sahar, Soheil, Neda, Tannaz, Golnar, Houman, Farnaz, Pejman, Navid, Maral, Araz, Idin, Taraneh, Siavash, Arash, Behnaz Shirin, Mina, Noushin, Iman and Nazanin to provide a loving environment and gathering during my stay in Iran. I have to specially mention Sina who always treats me like a brother.

Most importantly, none of this would have been possible without the endless love and encouragement of my family. I wish to thank my family for providing a loving environment in which I can focus on my study. My dad, Hamid, who is my ultimate role model and source of support, strength and encouragement in my entire life. He teaches me how to live and how to love and inspire me with hope and sense of invincibility. My mom, Afsaneh, for her constant source of love, concern and support in all these years. Mom, dad I do not know how to thank you enough for providing me with the opportunity to be where I am today. My sister, Narges, and my brother, Shahryar, who provide support and unending inspiration. Your devotion, unconditional love and support, sense of humor, patience, optimism and advice was more valuable than you could ever imagine. I am also grateful to my uncles (Amir and Mehdi) for providing lots of gatherings, lunches and dinners with my family here. I love you all dearly.

Last but not least, I want to talk about my lovely family members whom I have lost during my Ph.D. study. My grandmother, Javahar, who was a lovely, honest, courteous, brave and devoted family lady. Even though she was not well educated and lost her husband while she had eight children at a very young age, her enthusiasm and sacrifices to protect and raise her children to be well educated and be successful in their life was extraordinary. She was definitely the roof of the family supporting through her selfless dedication and purest heart. She was always thankful for what she had and certainly never complained. My grandfather, Attaollah, who was a lovely, brave and courteous man. I never forget his smiles, patients and adorable behavior with people around him which taught me how to always treat people in my personal life. My oldest uncle, Mohammad Javad, who was really a gentle and courteous person who passed away very unexpectedly. He was one of the well-known teachers in my hometown who truly served for more than 50 years in this field. And, my youngest uncle, Ebrahim, whom this thesis is humbly dedicated. His kindness, generosity, and selflessness besides of his sense of responsibility and taking care of his surrounding was exemplary. He looked at life in different aspects and was curious about it. Every time I flew back home during my break, I was spending quality time with him as much as I could to talk and exchange our thoughts. I really miss all of you and never forget you.

Shahram Sattar
September 12th, 2018

Dedication

In loving memory of my uncle, Ebrahim,

with all his generosity, humanity, and kindness

(1956-2017)

Table of Contents

List of Acronyms and Abbreviations

API	Application Programming Interface
CPU	Central Processing Unit
CSV	Comma Separated Values
DPGMM	Dirichlet Process Gaussian Mixture Model
DWT	Dynamic Wrapping Time
GIS	Geographic/Geospatial Information System
GML	Geography Markup Language
GMM	Gaussian Mixture Model
GPS	Global Positioning System
GUI	Graphical User Interface
HTTP	Hypertext Transfer Protocol
HTML	Hypertext Markup Language
IDE	Integrated Development Environment
IMU	Inertial Measurement Unit
J2EE	Java Platform, Enterprise Edition
JSON	JavaScript Object Notation
JSP	Java Server Pages
KML	Keyhole Markup Language
MEMS	Microelectromechanical Systems
OS	Operating System
PDF	Probability Density Function
SDK	Software Development Kit
SOAP	Simple Object Access Protocol
SUV	Sport-Utility Vehicle
SVM	Support Vector Machin
XML	Extensible Markup Language

List of Tables

List of Figures

Chapter 1 Introduction

1.1 Research Motivation

Recently, monitoring road surface conditions has become considerably important. Well-maintained road surfaces increase road user safety and comfort levels. Therefore, it is essential to monitor road conditions continuously to enhance the transportation system in terms of driving safety and comfort. For instance, in Canada, authorities responsible for road surface maintenance have to deal with complaints concerning the poor surface conditions of roadways, particularly during winter months. One of the main indicators used to determine road surface condition is the density of road surface anomalies (Strutu et al., 2013).

Traditionally, there has been three main approaches for road surface monitoring: 3D reconstruction, vibration, and vision-based (Buza et al., 2013).

A 3D reconstruction approach relies on 3D laser scanning to create accurate surface models. These models are then compared to a base model to detect road surface anomalies. In this approach, a 3D laser scanner uses reflected laser pulses, which create accurate 3D digital models of existing objects, such as road surface anomalies. Subsequently, the distress features (road surface anomalies) are extracted from the created point clouds (i.e., a collection of points that represent a 3D shape of road surface distress). This approach was widely investigated by Kelvin, (2004), Vijay and Arya (2006), Salari et al., (2012), Moazzam et al., (2013), Hou et al., (2014), Kim et al., (2014), Wang et al. (2015), and Yan et al., (2015). However, the aforementioned approaches require high-cost laser scanners (Kim et al., 2014) and are very costly when monitoring large scale road networks.

A vision-based approach relies on image processing analysis, such as texture extraction and comparison using captured photographs depicting pavement distress features. The principle of this approach primarily utilizes geotagged images captured from a camera/video system mounted downward towards the road surface on a moving vehicle. Any suspicious road surface distress features, including potholes and cracks, can be automatically detected from the collected geotagged video images (Yan et al., 2017) by applying, for example, a Canny edge detection process (Canny, 1986). Vision-based approaches were extensively evaluated by Koch et al. (2013), Jog et al. (2012), Huidrom et al. (2013), Lokeshwor et al. (2013), and Yan et al., (2017). Even though these approaches are cost-effective compared with 3D reconstruction approaches, they depend on certain environmental conditions, such as lighting and shadow influence.

With a vibration-based approach, road surface anomalies are detected from the rate of moving vehicles' vibration captured by motion sensors (e.g., accelerometers and gyroscopes). Theoretically, a vehicle, when passing through any road surface anomaly, such as a pothole, crack, manhole, or expansion joint, will vibrate more than when passing over smooth road surfaces.

Table 1.1 compares the three available approaches for road surface monitoring. It can be seen that the vibration-based approach is more practical approach in terms of developing a broad and low-cost method for road surface anomaly detection.

Table 1.1: Available approaches for road surface monitoring system

Approaches	Pros	Cons
3D reconstruction approach	• Providing geometric measurements (crack width/depth/height) or capable of classifying the crack	• Costly • Computationally intensive • Not widely available for crowdsourcing
Vision-based approach	• More cost effective than 3D reconstruction • Preliminary classify distress feature • Suitable for visual determination of distress feature	• Suffering from determining precise geometric measurements (crack width/depth/height) or classifying the crack • Not widely available for crowdsourcing • Lighting and shadow conditions • Resolution dependent
Vibration-based approach	• Low cost • Widely available (Smartphones) • Capable of evaluating driving comfort of roads surface	• Suffering from determining precise geometric measurements (crack width/depth/height) or classifying the crack • Not suitable for visual determination of distress feature • Sensor and vehicle dependent

Authorities dealing with road surface maintenance are typically rely on statistical data derived from collected road surface information, visual field inspections or vehicles outfitted with special instruments which measure and monitor road surface conditions. For example, ARAN (Automated Road Analyzer), which is widely used for road monitoring in Canada, and ROMDAS (Road Measurement Data Acquisition System), which is used to monitor road surfaces in New Zealand both use combinations of laser as well as ultrasonic and video sensors for high-level road quality assessment (Strutu et al., 2013). However, these methods are labor intensive, costly, and often suffer from insufficient data coverage to generate a complete picture of road surface conditions in large cities such as Toronto, Canada. In addition, local roads maintained by municipalities is mainly rely on traditional visual inspection approach, which is ineffective, time consuming and sometimes subject to error of human judgment.

According to a recent study conducted for the Michigan Department of Transportation, which compared the operational costs using different technologies for road surface monitoring (DMG, 2014), the mobile pavement imagining technique and manual field inspection costs USD $88.5/mile and USD $428.8/mile, respectively. On the other hand, the cost of using multi-sensor hybrid system can range from USD $541/mile to $933/mile, subject to the different service providers. By adding the cost of required equipment (i.e., capital cost) to the aforementioned operational costs for imaging techniques and multi-sensor hybrid systems, it can be concluded that these approaches are costly to monitor low volume and rural roads. In addition, the required storage for the collected video, image and LiDAR data are approximately more than 1 GB per kilometer which should be aggregated during the procedure of data collection and will be processed thereafter once the procedure of data collection is completed to rank each road segment with a number that is occupied less than several bytes. From the viewpoint of the pavement management, these methods (i.e., from recorded images, videos, and LIDAR data) seem to be a data waste to evaluate road surface for low-volume roads (Yan et al., 2017). Based on the aforementioned reasons, transportation authorities, including the Ministry of Transportation, Ontario (MTO), and municipalities are looking for a low-cost, more efficient pavement evaluation technologies and a centralized information system to provide the most up-to-date information about the road status in order to enhance their road surface condition, particularly for low volume and rural roads (Yan et al., 2017).

Recently, due to the introduction of **m**icro**e**lectro**m**echanical systems (MEMS), small and high-performance sensors have been used widely in smartphones (Nomura et al., 2015). Many studies have been carried using collected and processed data from mobile sensing using embedded sensors in moving objects such as vehicles and smartphones. However, processing signals from the embedded sensors of various smartphones is technically challenging due to dissimilar sensor properties and also different vehicle's mechanical properties including vehicle size, weight, length, and suspension system. In addition, the length, depth and location of potholes or cracks on roads and the curvature of roads all affect how accelerometers sense the environment. In fact, different vehicles passing over a pothole or crack would not generate an identical signal (Fox et al., 2015). Further, different vehicle velocities affect accelerometer's response within a single vehicle.

Meanwhile, crowdsourcing is anticipated to be an emerging area where smartphone-based measurements are particularly attractive, widespread, and equipped with several sensing capabilities (Burke et al., 2006). Although such crowdsourcing from smartphone applications presents challenges, such as varieties in sensors characteristics, smartphone orientations, suspension system of vehicles speeds, and users' reliabilities, the trend of smartphone-based sensing and big data also present a valuable research opportunity for the development of distributed road surface condition evaluation technologies using low cost sensor data collected by autonomous vehicle or other on-road users (Dennis et al., 2014). Therefore, in this research, a probabilistic-based crowdsourcing technique was developed to monitor road surface conditions from smartphone sensors. To this end, a free Android-based smartphone application was developed to detect road surface anomalies from smartphone sensors which can be used by publics. The detected anomalies then were accumulated and integrated on the central server based on the proposed probabilistic-based integration approach to infer robust interpretation of each anomalies in terms of the level of discomfort.

1.2 Research Objectives

The primary goal of this thesis research is to develop a crowdsourcing technique for road surface monitoring using smartphone sensors. The research mainly focuses on using smartphone sensors to detect road surface anomalies most likely caused by potholes or cracks. Accordingly, road surface anomaly information from different sources can be processed and integrated continuously to improve the accuracy of anomaly detection and update the hotspot distribution of road surface anomalies to discover the hazardous road segments with accumulated road surface anomalies. Integrated anomaly information stored in a spatiotemporal database can then be visualized in a web-based GIS interface to notify the government authorities which are responsible for the road maintenance and rehabilitation. This also helps to assist drivers by notifying them prior to reaching any anomalies (e.g., potholes) based on information from real-time road surface anomalies in order to avoid accidents or vehicle damages (Madli et al., 2015).

In fact, this study aims to reap the benefits of using smartphones' sensors, crowdsourcing techniques, complex event processing technologies and web-based GIS application to develop a collaborative based monitoring platform to facilitate the road surface condition monitoring. Specifically, the objectives of the research are:

1. To develop a near real-time road surface anomaly detection approach for road surface monitoring (methodological and practical contribution);
2. To develop a probabilistic-based crowdsourcing technique for road surface anomaly integration (methodological and practical contribution); and
3. To develop a web-based GIS prototype of serving as a foundation to incrementally develop a new Sense and Response (S&R) GIS tool (practical contribution).

To meet the first objective, an improved approach, which can continually detect, and distinct various road surface anomalies based on real-time data streams and other geographic data has been developed. The developed method processes data from multiple sensors, infers meaningful events (road surface anomalies) according to the predefined rules and classifies them with respect to their level of discomfort sensed by different vehicles. Furthermore, a smartphone application has been developed based on the developed approach to sense events (road surface anomalies) through real-time data streams from smartphone sensors. Different testing scenarios have been designed and examined on the part of the road networks in the city of Toronto to verify the performance of the proposed approach and the developed application.

The second objective is achieved by developing a probabilistic-based crowdsourcing approach to process real-time streams of events detected from the developed smartphone application employed by multiple users. The underlying principle of this approach is to integrate detected events from multiple users which are not an absolute binary scenario primarily caused by different sensing capabilities of various participators' smartphone sensors and diversity in mechanical properties of vehicles. The outcome from this objective would be either a new potential event such as a new pothole, or continuous improvement toward the accuracy of previously-detected events. The performance of the proposed crowdsourcing technique has been evaluated to insure the effectiveness of the proposed approach.

To fulfill the third objective, a web-based GIS platform was developed based on developed smartphone application defined in **Objective 1** and the probabilistic-based crowdsourcing approach as defined in **Objective 2**. This part focuses on prototyping based on the proposed approach **(Objectives 1 and 2)**, and testing their functionalities and efficiency. This research prototype also includes a web-based GIS interface to visualize and query detected/integrated anomalies, as well as some GIS function, including address matching, hot-spot analysis and access to the attribute values of each event. Furthermore, the integrated sense and response (S&R) GIS tool can be beneficial to the transportation/ infrastructure authorities dealing with road surface maintenance by actively monitoring the current road surface condition for potential maintenance and rehabilitation.

1.3 Scope and Limitations

The scope of this research is to develop a near real-time monitoring system to evaluate the road surface conditions by detecting road surface anomalies, such as cracks, bumps and potholes. In addition, this study aims to classify road surface anomalies that may induce different levels of driving discomfort (severity level). However, classifying cracks, bumps, and potholes according to their type, depth and size are not in the scope of this study. This is because of the differences in the suspension system of vehicles, sensor properties of smartphones, and smartphone placements which all affect how smartphones sense a single anomaly. Therefore, distinguishing road surface anomalies in accordance to their type, depth and size are sophisticated when different vehicle models, smartphones and orientations are employed for road surface anomaly detection. As a result, this study does not cater classification of road surface anomalies in terms of their type, depth and size.

1.4 Structure of the Thesis

The thesis is organized as follows. Chapter 2 presents a literature review of recent advances in road surface anomaly detection from smartphone sensors, followed by a review of parameters affecting the performance of the detection and integration approaches. Chapter 3 introduces the procedures and methodologies for smartphone sensors' data quality analysis, road surface anomaly (event) detection from smartphone sensors, and the probabilistic-based crowdsourcing technique for integrating road surface anomalies detection from multiple users. Details of the processing stages, including analyzing sensors data quality, detecting anomalies from smartphone sensors and integrating anomalies from multi-time survey to update or form newly detected anomalies, are discussed. Concerns associated with each stage are also discussed in this chapter.

Chapter 4 examines the results from the proposed approaches described in Chapter 3. Experimental results are presented to illustrate the validity of the proposed methodologies. Moreover, the employed steps for evaluating the performance of the proposed approaches are presented and discussed.

Chapter 5 describes implementation of the web-based GIS prototype which stores, manipulates, processes and visualizes the detected road surface anomalies from various users. The prototype is developed based on a service-oriented architecture (SOA) to support the S&R GIS tool. For the purpose of proof-of-concept, the implementation of the prototype is based on the available components or modules instead of implementing an entirely fresh system from scratch.

The conclusions of the research are drawn in Chapter 6, along with directions for future work.

Chapter 2 Literature Review

This chapter provides an overview of existing literature related to detecting road surface anomalies from smartphone sensors. As the overall process shown in Figure 2.1, road surface anomaly detection studies consist mainly of five steps: 1) sensing (data collection), 2) preprocessing, 3) processing for feature extraction, 4) post-processing, and 5) performance evaluations.

There are different kinds of sensor data that can be obtained from smartphone sensors. Motion sensor types include accelerometer, gyroscope, linear accelerometer and rotation. Position senor types include GPS, manometer, and orientation. Preprocessing of sensor data aims to filter noises, which contaminate sensors data. The other goal of preprocessing sensor data is to reorient them from device coordinate system to the local level coordinate system. The preprocessed sensor data is then analyzed to discover and extract desired information based on predefined rules (feature extractions). After that, the processed sensor data should be transferred to the central server for data post processing, including their integration with other data from different sources (concept of crowdsourcing). Finally, the performance of the proposed process should be evaluated to determine its functionality and reliability.

The background literature pertaining to the data collection and preprocessing steps is presented in Sections 2.1 and 2.2, respectively. The associated sensors data processing and post-processing procedures are provided in Sections 2.3 and 2.4, respectively. The performance evaluation of each reviewed study is discussed in Section 2.5. Finally, Section 2.6 summarizes and points out the current gaps in detecting road surface anomalies from smartphone sensors for this study.

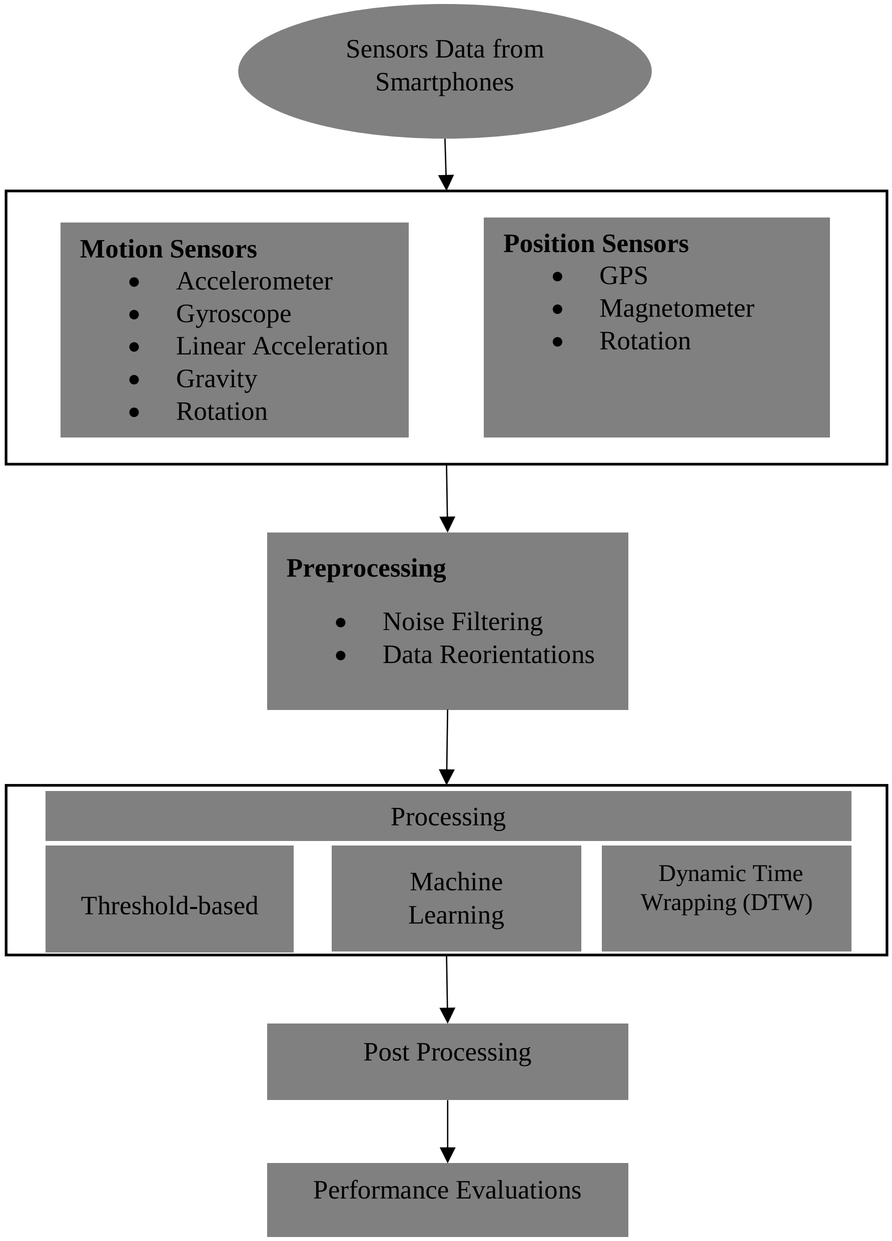

Figure 2.1: The overall process of detecting road surface anomaly from smartphone sensors

Sensors Data Collection

The smartphone sensor framework has open access to many types of built-in sensors. Some of these sensors are hardware-based (physical) and some are software-based (virtual). Hardware-based sensors are the physical, built-in sensors, such as accelerometers, gyroscopes, magnetometers, light, temperature, etc. Physical sensors measure motion, orientation, and environmental conditions, such as acceleration force, physical position of device, illumination, etc. In contrast, software-based sensors use data from one or more of the hardware-based sensors and virtually calculate real-time values based on the desired outcome such as linear acceleration, rotation, gravity, etc. In general, smartphone sensors can be categorized into three different types: motion sensors, position sensors, and environmental sensors.

Motion sensors are suitable for monitoring device's movement and vibration, tilt, shake, rotation, or swing. The movements can directly reflect user interaction as typically happens in game applications (i.e., a user steering a car or a controlling a ball in a game). However, they can also reflect where the device is sitting (i.e., moving with the occupant while they drive their car). With direct user interaction, device movement is monitored relative to the device's coordinate system or a defined local application frame. With physical environmental conditions, the device movement is monitored relative to the local level coordinate system (Figure 2.2).

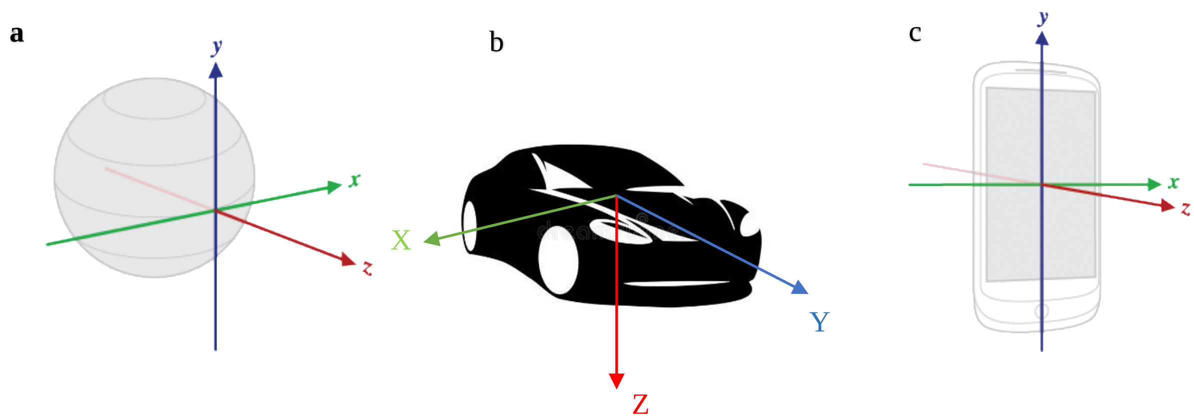

- X axis is defined as the vector product of Y and Z. It is tangential to the ground at the device's current location and points approximately east.
- Y-axis is tangential to the ground at the device's current location and points toward the geomagnetic North Pole.
- Z-axis points upwards and is negative extends down into the ground.

- This body fixed coordinate system is defined such that the X-axis is pointing in a positive direction through the front of the vehicle,
- The Y-axis is positive through the vehicle's right-hand side and
- The Z-axis is positive down through the chassis of the vehicle.

When a device is held in its default orientation:

- The X-axis is horizontal and points to the right
- The Y-axis is vertical and points up, and
- The Z-axis is perpendicular to the face of screen.

Figure 2.2: (a) Local level coordinate system, (b) body-frame coordinate system, and (c) device coordinate system (c)

Position sensors are suitable for specifying a device's physical position in the local level coordinate system. In fact, the geomagnetic field sensor, in combination with accelerometer sensor data, can determine a device's position relative to the local level coordinate system. Environmental sensors measure the environmental properties of surrounding area, such as temperature, humidity, ambient pressure, and illuminance. This type of sensor has very limited contribution to road surface anomalies detection, since it does not seem to have any direct relationship / impact between these factors and the formation of road surface anomalies.

Table 2.1 summarizes and compares a list of sensors commonly found in smartphones for the application of road surface anomalies (Google, 2017). These sensors are used either directly or indirectly for road surface anomaly detection.

For each smartphone-based application, various combinations of sensors (physical or virtual) may be used depending on the desired application criteria. To develop an application for road surface anomaly detection, motion sensor data can be tracked to detect any possible shake or tilt caused by road surface anomalies in a moving vehicle. Previous studies investigating road surface anomaly detection using smartphone sensors have widely employed motions sensors (accelerometers and gyroscopes). Accelerometer sensors measure acceleration force, including gravity force, applied to a device on all three physical axes (m/s^2). Gyroscope sensors measure a device's rate of rotation around each of the three physical axes (rad/s). Previous research (refer to Table 2.1) has frequently used accelerometer sensor data to detect anomalies because road surface anomalies have more influence and are mainly detectable from the acceleration force applied to the vehicles rather than the rotation rate caused by vehicles' vibration. Only a few studies including Yagi et al. (2010) and Douangphachanh et al. (2014) have investigated gyroscope sensor data, particularly frequency domain combined with accelerometer sensor data, which increases the accuracy of detection (as complementary sensor data).

Table 2.1 summarizes and compares a list of sensors commonly found in smartphones for the application of road surface anomalies (Google, 2017). These sensors are used either directly or indirectly for road surface anomaly detection.

Table 2.1: List of sensors used for road surface anomaly detection

Sensor Name	Type	Unit	Description
Accelerometer	Physical	m/s^2	Measures acceleration force
Gyroscope	Physical	rad/s	Measures a device's rate of rotation
Linear Acceleration	Virtual	m/s^2	Measures the acceleration force, excluding the force of gravity.
Magnetometer	Physical	μT (T stands for Tesla)	Measures ambient geomagnetic fields
Gravity	Virtual	m/s^2	Measures the force of gravity
Rotation	Virtual	rad	Measures the orientation of a device
GPS	Hardware	Degree	Obtains location information

To determine the current location information of smartphone or mobile devices including latitude, longitude, bearing of moving direction, and velocity of movement, the location API (Application Program Interface) provides the best available location information of the devices based on the currently available location providers such as GPS (Global Positioning System) and/or Wi-Fi (Global Positioning System). In addition, the API provides the accuracy for each provided location information data.

Preprocessing

The data pre-processing step involves transforming raw data derived from smartphone sensors into a clean and organized data set prior to analysis (Malley et al., 2016). One of the goals of preprocessing is the smoothing of the raw sensor data and noise filtering. There are three major types of smoothing and filtering approaches: moving-average filtering, low/high-pass filtering, and band pass filtering. Moving average filtering is the most common filter in digital signal processing, mainly because it is the easiest to understand and implement since there is no need to have any prior information regarding the sensors data (Smith, 1997). Despite its simplicity, this kind of filter is ideal for some common tasks, such as reducing random noise while retaining major information content. Low/high-pass filters remove some undesired parts of signals based on predetermined cut of frequencies. Band-pass filter passes portions of the signals within a certain range of frequencies and removes the other parts of signals that are outside that range.

Preprocessing may also aim to reorient sensors data values from a device coordinate system (Figure 2.2c) to the local level coordinate system (Figure 2.2a), or to any other preferred local coordinate system. An example would be a body frame (i.e., moving platform) coordinate system (Figure 2.2b) (Noureldin et al., 2013). This process can be accomplished by completing a rotation (using Euler angles) around each of the three axes. The reorientation process reduces issues related to smartphone placement.

Processing

The processing step analyzes the preprocessed sensor values to detect road surface anomalies. The signal pattern is tracked to detect any abnormal changes in sensor values using three main approaches:

1. The threshold-based approach uses simple predefined threshold values based on experiments to detect road surface anomalies from sensors data.
2. The machine learning approach uses more advanced techniques to detect road surface anomalies. Studies (Bhoraskar et al., 2012) have investigated unsupervised approaches, such as K-means clustering, in which a predetermined number of clusters are identified, and data is classified to the same number of clusters. Some other studies including Perttunen et al. (2011) and Jain et al. (2012) have explored supervised approaches, such as support vector machine (SVM) clustering and Gaussian mixture model (GMM) clustering. In the case of supervised approaches, some training datasets should be collected to train the algorithm. The test data is then classified based on the trained dataset.
3. Another approach that was recently investigated is Dynamic Time Wrap (DTW). This approach is predominantly employed in speech recognition studies. DTW compares incoming signal data with predefined templates and measures the similarity of the datasets.

Regarding smartphone applications, the preprocessing and processing steps can be accomplished using two different modes: online and offline. In offline mode, sensor data is collected, and the preprocessing and processing steps are applied locally on computers. In fact, any application developed for sensor data collection is able to collect and store sensor data while a car is passing over potholes or bumps. Next, the sensor data is extracted for further processing. In online mode, data collection, preprocessing, and processing are performed simultaneously as the car is passing over potholes or bumps. Ideally, a specific smartphone application should be designed and developed to collect, preprocess and process the sensor data in an online mode.

Post-Processing

Preprocessing includes crowdsourcing and integrating data from multiple sources (users' collaborations, geographic datasets) to increase the accuracy of detection and scalability. Detection results from various users can be integrated (data fusion), enabling more reliable and precise detection. Due to the dynamic behavior of road surface anomalies, integrating detection results from various users at different times can help evaluate the road surface anomaly's condition more precisely than in the spatiotemporal domain. Moreover, other geographic data, such as road networks, manhole and catchment basin location data, can be integrated through filtration or data analysis to increase the accuracy of the results. As an example, manholes and road joints behave similarly to road surface anomalies on sensor data. Therefore, if the geolocation of man-made anomalies is integrated, sensor-detected road surface anomalies (i.e., manholes or joints) are subsequently able to be filtered.

The central server stores incoming data while also processing parallel incoming data from multiple sources. The completed central processed data can be presented as a geospatial information system (GIS) web-based map to the general users or authorities dealing with road surface maintenance.

2.1. Sensors Data Collection

A major step in developing a viable approach that can detect road surface anomalies is the collection of sample sensor data from smartphones' sensors. As discussed earlier, motion sensors, such as accelerometers and gyroscopes, were widely used in the collection and processing of data for road surface anomaly detection. Data collection from previous studies (refer to Table 2.2) differ in terms of the types of sensors being employed, sampling rates, variety of vehicles, and devices considered for the data collection. These factors are the most critical parameters that affect the performance of a smartphone's ability to detect road surface anomalies. Table 2.2 summarizes sensor data collection properties reviewed in the selected studies.

Table 2.2: Employed sensors for road anomaly detection

Proposed Method	**Employed Sensor(s)**	**Data Sampling Rate (Hz)**	**Vehicle**	**Smartphone Model**	**Distance of Experiment**	**Location of Data Sampling**
Mohan et al (2008)	Accelerometer	310	Toyota Qualis	Windows smartphone	622 KM	Bangalore and Seattle
Yagi et al (2010)	Accelerometer/Gyroscope	100	Toyota PRIUS	iPhone	N/A	Kashiwazaki, Japan
Mednis et al. (2011)	Accelerometer	100	BMW 323 touring	Samsung i5700 Samsung Galaxy s HTC Desire HTC HD2	174 KM	Vairoga iela, Riga, Latvia
Perttunen et al. (2011)	Accelerometer	38	N/A	Nokia N95 8GB	25 KM	Finland
Jain et al. (2012)	Accelerometer	N/A	Bus, Auto rickshaw, cycle rickshaw, motorcycle and car (models were not mentioned)	4 different Android-based smartphones (models were not mentioned)	678 KM	New Delhi, India
Bhoraskar et al. (2012)	Accelerometer	50	Suzuki access 125 Auto-rick-shaw	Google Nexus S, HTC Wildfire S	N/A	IIT Bombay campus
Douangphachanh et al. (2013)	Accelerometer	100	Toyota Vigo 4WD, pick up, Toyota Camry, Toyota Vigo 2WD, Toyota Yaris	Samsung Galaxy Note 3, Galaxy S3, LG 4X HD	N/A	Vientiane, Laos
Sinharay et al. (2013)	Accelerometer	4-6	N/A	Google Nexus S	N/A	Kolkata, India
Douangphachanh et al. (2014)	Accelerometer/Gyroscope	100	Toyota Vigo 4WD, pick up, Toyota Camry, Toyota	Samsung Galaxy Note 3, Galaxy S3, LG 4X HD	N/A	Vientiane, Laos
Sebestyen et al. (2015)	Accelerometer	90	N/A	N/A	N/A	N/A
Wang et al. (2015)	Accelerometer	60				
Nomura et al (2015)	Accelerometer	100	N/A	N/A	N/A	N/A
Yi et al. (2015)	Accelerometer	80	Toyota Camry	Sony Xperia, HTC Desire, HTC Hero	N/A	N/A
Harikrishnan et al. (2017)	Accelerometer	50	Maruti swift	N/A	N/A	India
Singh et al. (2017)	Accelerometer	10	Toyota Etios	Nexus 5, Samsung S5, Samsung Note 3, Moto E, Samsung S4 mini	220 km	Chandigarh, India

According to Table 2.2, accelerometer sensors were widely investigated as a means to develop an approach to detect road surface anomalies. In most previous studies (refer to Table 2.2), accelerometer sensor data was investigated in the time domain for detecting road surface anomalies. However, gyroscope sensor data was transformed to the frequency domain for feature extraction (road surface anomaly detection). Moreover, most of the previous studies only employed accelerometer sensors to detect road surface anomalies. However, Yagi et al., (2010) and Douangphachanh et al., (2014) attempted to combine gyroscope and accelerometer sensor data to increase detection accuracy using a data fusion technique.

Data sampling rates play a significant role in the processing of any detected event. Choosing an appropriate sampling rate is a design decision affected by multiple factors, such as available resources, required accuracy and the type of data being used for event recognition (Shoaib et al., 2015). As an example, if only frequency domain features are used for monitoring road anomalies, the sampling rate should be high enough to capture all relevant frequencies. According to Douangphachanh et al. (2013), the road anomalies most likely have the frequency range of 40-50 Hz are captured in accelerometer data.

A higher sampling rate increases the chances of capturing and detecting road surface distress features. However, it also increases the battery usage of a smartphone, as well as the required capacity to store and process data. Finding proper sampling rates is related to the speed of movement, as well as the mechanical properties of a vehicle. Sinharay et al. (2013) investigated the use of a low sampling rate to develop their approach for road surface anomaly detection.

Various models of vehicles and smartphone devices are factors considered by previous studies when collecting data. According to Table 2.2, Douangphachanh et al. (2014) and Jain et al. (2012) studied both different vehicles (e.g., sedan, SUV (Sport-Utility Vehicle,) trucks) and smartphones (i.e., different manufactures) to ensure their approaches function equally in different circumstances.

2.2. Sensors Data Preprocessing

Preprocessing of sensor data value is important for two major reasons: noise filtering that distorts parts of the signal, and sensor data reorientation. Not all the reviewed studies preprocessed the sensor data. Some reviewed studies only conducted noise filtering and data smoothing as part of their preprocessing, while some other studies only conducted signal data transformation before processing them. Sebestyen et al. (2015) utilized two different filters: one for eliminating noise and one for amplifying acceleration variation caused by road anomalies. Douangphachanh et al. (2014) used a high-pass filter to detect low-frequency information, such as changing speed and vehicle maneuvering and turning, which have lower frequencies than road surface anomalies from sensor data. Harikrishnan et al. (2017) collected data segmented into group of n-samples. Then, a filtering process was conducted to preserve data samples induced by potholes or speed bumps, as well as to minimize the parts of sensor data corresponding to normal roads. To smooth the signal data, Singh et al. (2017) applied a simple moving average and band-pass filter to smooth data values from accelerometer sensor before processing them. The approaches proposed by Mohan et al. (2008), Bhoraskar et al. (2012), Sebestyen et al. (2015), Wang et al. (2015), and Singh et al. (2017) all applied Euler angles (rotation angles) calculated from accelerometer sensor data, to transform signal data values from device coordinate systems to the local level coordinate system orientation.

2.3 Sensors Data Processing

Processing sensor values for the application of road surface anomaly detection has three main approaches: threshold-based, machine learning, and DTW. Table 2.3 summarizes the approaches used by previous studies when processing sensor data and detecting abnormal changes in signal data. Data processing in this application can be reviewed in terms of the feature extraction approach (e.g., threshold-based, machine learning, and DTW), ability to classify road surface anomalies (anomaly classification capability), smartphone orientation dependency in detection, and speed dependency in detection.

Table 2.3: The detection methods using smartphone sensors for road anomaly detection from smartphone sensors

Proposed method	**Employed Technique(s)**	**Approaches**	**Length of analyzing window**
Mohan et al (2008)	Threshold-based	For speed > 25 KM = 0.8 g and for speed <25 z-sus (sustained dip in vertical component of accelerometer data	7 sample for speed of less than 25 Km/h
Yagi et al (2010)	Threshold-based	Standard deviation of z-values with different window time	50 milliseconds
Mednis et al. (2011)	Threshold-based	Z-THERESH = 0.4 g, Z-DIFF = 0.2 g, STDEV(Z) = 0.2 g, and G-ZERO = 0.8 g	1 sample
Perttunen et al. (2011)	Machin learning	Support Vector Machine (SVM)	0.5 second ~ 2 seconds
Jain et al. (2012)	Machin learning	Support Vector Machine (SVM)	N/A
Bhoraskar et al. (2012)	Machin learning	K-means Clustering and Support Vector Machine (SVM)	N/A
Douangphachanh et al. (2013)	Machin learning	Linear Regression	N/A
Sinharay et al. (2013)	Threshold-based	The rate change of z values in acceleration values	1 second
Douangphachanh et al. (2014)	Machin learning	Linear Regression	N/A
Sebestyen et al. (2015)	Threshold-based	Adaptive threshold based on the lowest, highest and average values of accelerometer data in predefined window length	1 sample
Wang et al. (2015)	Threshold-based	Approach proposed by of Mednis et al. (2011) with adaptive threshold	1 sample
Fox et al. (2015)	Machin learning	SVM with radial basis kernel function to discriminate boundaries between pothole and non-pothole regions	N/A
Nomura et al (2015)	Threshold-based	0<RI[1]<1 for σ = 0.0190 m/s^2 and 0<RI< 2 for σ = 0.0428 m/s^2	1 sample
Yi et al. (2015)	Threshold-based	Two steps of pothole verification based on the standard deviation of senor data σ_{i-1}<2 * σ_i and σ_{i-1}<2.5 * σ_{event}	0.5 second
Harikrishnan et al. (2017)	Threshold-based	Fitting Gaussian models to the normal roads and comparing the accelerometer sensor data value in the z direction with the mean of fitted model.	
Singh et al (2017)	Dynamic Time Wrapping (DWT)	Measuring signal pattern similarity	N/A

2.3.1 Feature Extraction Method

Threshold-Based Approach

In order to detect road surface anomalies using threshold-based approaches, sensors' changing data value patterns, or statistical values (e.g., standard deviations), taken from sensor data values, were analyzed. The amplitude of accelerometer signals was monitored and the anomaly's patterns in the signal were identified

[1] RI = Roughness Index

(anomaly's patterns in digital signals occur when the power of the signal exceeds a specific value). Threshold-based approaches were reviewed from three different perspectives: length of interval for window function, fixed vs. flexible threshold determination, and amplitude of signal vs. other properties of signal amplitude (e.g., mean and standard deviation).

Determining interval length for window function on spectral analysis is challenging as it is related to various factors, such as speed of vehicles and distance from front to rear wheels. Window function considers predefined intervals of signal data for analysis and feature extraction as opposed to looking at signal data individually. Table 2.3 summarizes the length of interval for window function for each of the studies that explored window function.

Defining proper threshold values in a statistical approach is an intensive process since values are affected by variable conditions. The suspension system of a car, sensor properties of smartphones, and smartphone placement all affect how smartphones sense a single anomaly. Studies conducted by Mohan et al. (2008), Mednis et al. (2011), Sinharay et al. (2013) and Yi et al. (2015) determined fixed-threshold values from some experiments studying road surface anomaly detection. However, studies conducted by Sebestyen et al. (2015), Wang et al., (2015), and Harikrishnan et al. (2017) utilized dynamic threshold values to overcome unsteady signal patterns caused by various sensor and mechanical properties. Dynamically assigned threshold values are desirable when developing methods for detecting road surface anomalies, as they can be adapted to different circumstances.

Mohan et al. (2008), Mednis et al. (2011), Sebestyen et al. (2015), Wang et al. (2015), and Harikrishnan et al. (2017) determined thresholds based on the amplitude of the signal. However, other studies, such as Yagi et al. (2010), Nomura et al. (2015), and Yi et al. (2015) determined thresholds based on the statistical value (such as the standard deviation) derived from signal values. Mednis et al. (2011) confirmed that the standard deviation is the most important parameter in detecting road surface anomalies from accelerometer sensor data.

Machine Learning Approach

There are two prevalent approaches using machine-learning techniques: supervised learning and unsupervised learning. Reviewed studies that involved machine learning techniques can also be categorized based on these two approaches. Bhoraskar et al. (2012) used k-means, an unsupervised method, to classify sensor data on smooth and bumpy roads, as well as using them to train the SVM algorithm. In this approach, the outcomes from the k-means classification approach were manually labeled to classes (bumpy or smooth) in order to train the SVM approach. Perttunen et al. (2011) and Jain et al. (2012) employed SVM to classify sensor data. Although these methods successfully classified the sensor data, a sample of labeled data was required to train the SVM algorithm first, which is impractical for real-time or near real-time application.

Dynamic Time Wrapping Approach (DTW)

In time series signal processing, the DTW approach measures the similarity between any two patterns of signals and extracts features from signal data. For example, Singh et al. (2017) proposed a DTW-based approach to detect road surface anomalies from accelerometer sensor data. In this approach, time series values captured accelerometer sensor data for every pothole and bump, and then stored them in a central server as templates. Next, incoming sensor data was compared with the stored templates to detect similarities. The accuracy of this approach was greatly correlated to the quality of the reference template. Therefore, this approach was both computationally intensive and unreliable, as it required reference templates for each different condition (i.e., various vehicles, road conditions, and speed of driving).

2.3.2 Differentiating Various Forms of Road Surface Anomalies

Anomalies existing on road surfaces can be categorized into two major forms:

1) Actual road surface anomalies, including potholes and cracks

2) Man-made road surface anomalies, including manholes, road joints, catchment basins, and speed bumps

A comprehensive pothole detection approach should be able to differentiate actual road surface anomalies (such as potholes and cracks) successfully from a variety of man-made anomalies (such as manholes and speed bumps). However, this is challenging as they both generate similar signal patterns especially in the case of manholes and catchment basins.

In an approach proposed by Sebestyen et al. (2015), potholes can be distinguished from other man-made speed bumps. If a car runs over a pothole, the car first drops, and then, climbs back up. Conversely, if a car runs over a man-made bump, the car first climbs, and then, drops. Therefore, by setting these rules within the signal pattern these anomalies were detected and separated. Sinharay et al. (2013) suggested that the standard of deviation values calculated from sensors data were able to distinguish potholes from bumps. Harikrishnan et al., (2017) used an X-Z filter proposed by Eriksson et al. (2008) to differentiate potholes and speed bumps. Eriksson et al. (2008) claimed that potholes are mainly caused by the impact on one side of the vehicle, resulting in a relatively large variation on the x direction of the accelerometer sensor data. However, speed bumps cause impact on *both* sides of a vehicle, leading to small variations on the x direction of the data value from accelerometer sensors. Such a mechanism can then be used to distinguish between potholes and speed bumps.

2.3.3 Smartphone Orientation Dependency

Road anomaly detection results are sensitive to the sensors' orientation. Most of the reviewed studies, such as Yagi et al. (2010), Mednis et al. (2011), Perttunen et al. (2011), and Sinharay et al. (2013), assumed fixed and predetermined positions for analyzing smartphone sensor data. They required users to place their mobile device at a specific orientation and restricted them from using their mobile devices freely. As such, smartphones lack of orientation independence. In order to find a practical road surface anomaly detection solution, smartphones should be freely placed. To develop an approach independent from smartphone orientation, two methods have been investigated:

- **Signal transformation**. In this method, the sensors' values are transferred from device coordinate system to another geometric coordinate system (e.g., local level coordinate system or body-frame coordinate system).
- **Orientation-independent features**. In this method, the magnitude of the sensor data value on all three axes is considered instead of considering their individual values on three separate axes.

The method proposed by Mohan et al. (2008), Bhoraskar et al. (2012), Sebestyen et al. (2015), Wang et al. (2015), and Singh et al. (2017) applied a signal transformation method, which uses the Euler angles (computed from accelerometer sensor data) for coordinate transformations. Conversely, the approaches proposed by Jain et al. (2012), Sinharay et al. (2013), and Yi et al. (2015) utilized orientation-independent features of acceleration data (i.e., vector sum, mean, and standard of deviation) to become independent from smartphone orientation.

2.3.4 Speed Dependency

Another factor that influences road anomaly detection using smartphone sensors is the speed of the vehicle. Douangphachanh et al. (2013) demonstrated that average speed plays an important role in road roughness estimation. When a car passes over a specific road anomaly, such as a pothole, at different speeds, the amplitude of the collected acceleration signal reacts in a different manner, which should be modeled. Fox et al. (2015) investigated the effect of velocity as a component for detecting road surface anomalies from an on-board accelerometer sensor. Their investigations revealed that at high speeds discriminating between normal roads and pothole regions was difficult. Sebestyen et al. (2015) collected sensor data at three different speeds: 15, 30, and 60 km/h. All values from different speeds were normalized to a value of 30 km/h to develop and verify the proposed approach. Yi et al. (2015) examined the effect of vehicle velocity discussed in their approach by creating a lookup table, as well as categorizing the speed into different ranges. Then, each event was indexed according to the ratio of standard deviation, as well as standard deviation of stable periods of the speed interval during which the event had been detected. Sinharay et al.

(2013) normalized the feature values based on the speed of the vehicle. Speed was categorized three ways: lower than 2 km/h, between 2 km/h and 30 km/h, and more than 30 km/h. In addition, Perttunen et al. (2011) adopted an approach by Tanaka et al. (2000) that removed the effects of speed on signal data. Mednis et al. (2011) used different algorithms for different speeds. For instance, for a speed of less than 25 km/h, the z-sus algorithm was implemented. For the speed of more than 25 km/h, the z-peak algorithm was implemented. Mohan et al. (2008) used the z-sus method for speeds less than 25 km/h and z-peak for speeds more than 25 km/h. To minimize the false positive detection rate, Harikrishnan et al. (2017) proposed to specify a velocity-dependent variable. This variable was adjusted to the threshold value based on the current vehicle's velocity. Different studies used various methods to deal with the effects of vehicle speed on the performance of their approaches to road anomaly detection. However, none of them provided a technique robust enough to account for the effect of a vehicle's velocity

2.4 Post Processing of Detected Road Surface Anomalies

In this section, studies investigating data integration and approaches used to process detected road surface anomalies from various users (i.e., data fusions) are reviewed and discussed.

Chen et al. (2013) and Fox et al. (2015) transferred identified potholes information for each selected region in their study to the cloud for further analysis in their proposed approach. Then, a voting algorithm was applied on the study area for final decision making. In fact, the voting algorithm counts the number of reports made for each phenomenon from different sources. If the number of reported anomalies from various sources, for each predefined slice of the road, is more than a predefined threshold, those anomalies are considered as true detection. Otherwise, they are rejected and assumed as false detection. Fox et al. (2015) considered a sliding window of 10 meters for evaluating the number of reports from smartphones on-board vehicles in order to minimize the false positive rate of detection.

Unfortunately, in both studies, this simple voting algorithm ignores the fact that sources have different degrees of trustworthiness (Zhang et al., 2018). In addition, this binary-based algorithm does not consider the temporal and probabilistic nature of the anomalies. The results from Fox et al. (2015) indicated that at least ten vehicles operated at a speed of 50 km/h were required for data collection in order to reach the accuracy of 90%. Furthermore, Chen et al. (2013) claimed 90% accuracy with nearly zero false positive alarms for their Crowdsourcing Based Road Surface Monitoring (CRSM) system.

Yi et al. (2015) adopted a grid-based clustering algorithm called DENCLUE (DENsity CLUstering) to filter out false detections using the reporting frequency of events in a five-meter grid zone. Neighboring grids were grouped together if the frequency of reported anomalies for each neighbor grid was more than three. Otherwise, the grid was assumed to noisy and was removed. The drawback of this strategy is that some anomalies close to each other were treated as a single anomaly. In addition, threshold-based approaches for data integration are similar to the voting algorithm, which suffers from considering the temporal and probabilistic nature of any road surface anomaly detecting from smartphones. Moreover, there is always a trade-off between reducing false detection and missing detecting anomalies at the same time. In this study, only the position accuracy of detected road surface anomalies was investigated, and the overall accuracy of detection was not studied.

Alessandroni et al. (2014) proposed the “SmartRoadSense” system. Roughness information was collected in a central server. Then, the average of all roughness values within the predefined buffers of the detected location was considered as the roughness value for that region. Sebestyen et al. (2015) proposed a method of taking an average to combine incoming information from multiple users. In this method, a weighted sum between the available evaluations was computed, as well as integrated multiple surveys from various incidents. This method, similar to the voting algorithm suffers from the ignorance of the temporal aspect of road surface anomalies and the inherent uncertainty of incoming data. In addition, defining the proper buffer distance is challenging because it significantly affects the detection rate.

2.5 Performance Evaluations

To evaluate the performance of road surface anomaly detection approaches, performance metrics are required, including accuracy ratio, precision, false positives ratio and false negatives ratio. The choice of a specific performance metric or a combination of different performance metrics depends on the type of application needed, as well as its performance requirements. Table 2.4 summarizes overall performance evaluations for each approach based on the provided performance metrics. In addition to the overall accuracy of analysis, some studies investigated performance evaluations in different smartphone placements.

Table 2.4: Performance evaluation of reviewed studies investigating road surface anomalies from smartphone sensors

Proposed Method	**Performance Evaluation**
Mohan et al (2008)	For the speed of less than 25 km/h the rate of the false negative is 29% (well-oriented sensor) and 37% (virtually oriented). However, for the speed of more than 25 km/h, the rate of false negative is 41% (well-oriented sensor) and 51% (virtually oriented).
Yagi et al (2010)	Not provided.
Mednis et al. (2011)	The accuracy of the overall system is approximately 90%. However, the outcome of Z-DIFF and STDEV-Z approaches are highly dependent on the frequency and timing of data.
Perttunen et al. (2011)	The confusion matrix for the best result indicates that this approach has approximately 80 % accuracy.
Jain et al. (2012)	The results indicate approximately 75% accuracy.
Bhoraskar et al. (2012)	For bump detection, the algorithm gets zero false positives and 10% false negatives.
Douangphachanh et al. (2013)	The R^2 values in their estimation was between 0.721 and 0.869 for different cars when the smartphones were located in the box near gearshift.
Sinharay et al. (2013)	The accuracy of the system is 80% with 20% false positives.
Douangphachanh et al. (2014)	The R^2 values in their estimation indicated significant improvement compared to the previous study.
Sebestyen et al. (2015)	The accuracy of the anomaly detection algorithm implemented in this study is about 80%.
Wang et al. (2015)	In experiments, the results represent the accuracy of the proposed approach is 100% without false positive.
Nomura et al (2015)	94% accuracy rate for classifying road segments into different roughness levels (detection rate for road surface anomaly detection was not provided).
Yi et al. (2015)	Numerically, compared with z-component, the RMSEs (Root Mean Square Deviation) are 0.01m/s^2 of the batch mode and 0.03 m/s^2 of online mode
Harikrishnan et al. (2017)	The estimation error is 34.8% for the speed of 15 km/h and 1.6% for the speed of 20 km/h. The estimation error increases as the speed goes above 20 km/h.
Singh et al. (2017)	88.66% detection rate for potholes and 88.89% detection rate for bumps.

Smartphone Placement

One of the challenges in road surface anomaly detection is that smartphone sensors are sensitive to the placement of the device. In most studies, the placement of mobile phones was considered fixed to a mount on the windshield or attached to the dashboard. However, few studies have investigated the performance of their approaches with smartphones in different locations in a vehicle, such as in driver's pocket or in the console near the gearbox. Different drivers have different habits and the ideal approach should consider any circumstance that could result in a change in placement of a smartphone and its impact on the loss of recognition performance. Table 2.5 indicates that only three studies investigated the performance of their respective approaches with different placements in moving vehicles (Jain et al. (2012), Douangphachanh et al. (2013), and Yi et al. (2015)). Douangphachanh et al. (2013) confirmed that smartphones located in a driver's pocket or in the console caused lower detection rates.

Table 2.5: Smartphone placement dependency considerations for each approach

Proposed method	**Considering smartphone mounting dependency**
Mohan et al. (2008)	Back and middle seats, dashboard and hand-rest of vehicle
Yagi et al. (2010)	Front dashboard
Mednis et al. (2011)	Front dashboard
Perttunen et al. (2011)	Windshield rack
Jain et al. (2012)	Pants pocket, front dashboard, near the gearbox, near the rear car speakers
Bhoraskar et al. (2012)	Not defined
Douangphachanh et al. (2013)	Front dashboard, near the gearshift, inside driver's pocket
Sinharay et al. (2013)	Front dashboard
Douangphachanh et al. (2014)	On the dashboard, In the box near the gearshift, and inside driver's pocket
Sebestyen et al. (2015)	Front dashboard
Wang et al. (2015)	Not defined
Yi et al. (2015)	Front dashboard and windshield rack
Harikrishnan et al. (2017)	Not defined
Singh et al. (2017)	Not defined

2.6. Discussion

In this review, existing studies investigating approaches for road surface anomaly detection using smartphone sensors have been reviewed and compared. The existing approaches have been compared in five aspects: sensor data collection, preprocessing, processing, post processing, and performance evaluations.

Data collection is the one of the most important considerations when developing any approach to road surface anomaly detection with smartphone sensors. It is essential that the detection process consider all relevant aspects including smartphone sensor properties, smartphone mounting location, vehicle suspension system, driving behavior, and speed. Therefore, to guarantee an approach is compatible with different conditions, sensor data should be collected in various situations: various models of cars, smartphones, and speeds. However, due to the limitation of resources, only certain vehicles and smartphone devices have been selected and used for data collection in the reviewed studies.

Preprocessing is also an important task for any application using sensor data to extract features such as road surface anomalies. Preprocessing has two major objectives:

1) To smooth the sensor data, to amplify the parts of the sensor data caused by the event (road surface anomaly), and to attenuate or remove parts of sensor data caused by noise or undesired input.
2) Reorienting the sensor data from a device coordinate system to the body-frame (vehicle coordinate system) or local level coordinate system.

In fact, the preprocessing step can increase the accuracy of detection and decreases the false detection rate. In most reviewed studies, it was assumed that the general location of a smartphone was in a rigid holder. It was also assumed to be fixed, both position- and rotation-wise, with respect to the body frame (vehicle) coordinate system. Unfortunately, when the smartphone is positioned in its holder or placed on the dashboard, there is no guarantee that the direction of the sensor data measurements will align with the vehicle's body-frame coordinate system. The relative direction between the device's coordinate system and the body frame's coordinate system is therefore considered unknown (Wallin and Zachrisson, 2013). In fact, the desired approach should give freedom to users concerning smartphone placement. Several studies considered sensor data reorientation using accelerometer sensor data to approximate rotation angles (employing Euler angles). However, the calculated rotation angles from accelerometer sensor data is both biased and contaminated by variant noises caused by thermal and mechanical fluctuations inside the sensor. Most modern smartphones using MEMS such as inertial measurement units (IMU), which contains a three-axis gyroscope for measuring angular velocities around three axes (i.e., pitch, roll and heading), a three-axis accelerometer for measuring acceleration, and a three-axis magnetometer for measuring magnetic fields. The data from the IMU can be fused to obtain unbiased rotation angles that can then be applied for the purpose of coordinate system transformations.

Developing processing algorithms to detect road surface anomalies from smartphone sensor data is quite challenging. Smartphone sensor properties, car suspension systems, driving behavior and speed all affect signal patterns when passing over any road anomaly since they are contaminated with biases and noise. Threshold-based approaches have been examined to minimize these problems and they have been evaluated in several studies. Results of these studies were not reliable as a robust and inclusive detection approach. The machine-learning approach, which has been applied by some studies, was able to overcome some limitations encountered by threshold-based approaches. However, the proposed methods were not inclusive and did not yield a robust solution. For example, supervised approaches, such as SVM, required many trained datasets to cover all possible scenarios for classification.

Additionally, as seen in Table 2.1, most of the studies employed a single sensor (e.g., an accelerometer) to detect road surface anomalies. Figure 2.3 illustrates all available motion sensors on current trending smartphones. Linear acceleration and gravity are the new software-based (virtual) sensors that have been recently integrated in high-end smartphone devices. To improve the system performance, sensor fusion techniques can be used. For example, gyroscope or gravity sensors can be combined with accelerometer sensor data to strengthen the detection of road surface anomalies. In addition, accelerometer, magnetic and gyroscope sensor data are combined in order to derive the isolated gravity vector and to exclude it from accelerometer data. Most new and high-end smartphone devices are capable of calculating linear acceleration from their sensors. Linear acceleration is the effect of acceleration on the smartphone devices excluding the earth's gravity. As a result, actual acceleration of the device can be determined irrespective of the device orientation.

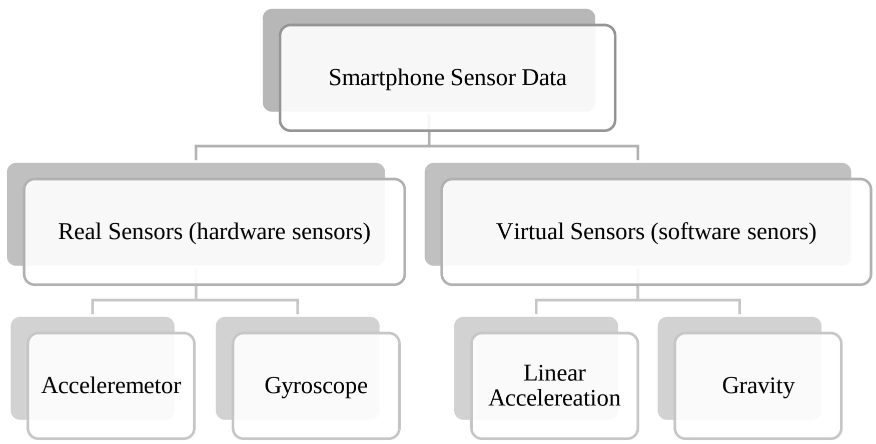

Figure 2.3: Available motion sensors on current smartphones

Most studies reviewed have implemented and verified their methods in an offline mode. However, with the continued release of powerful smartphones, few studies have both developed and verified their approaches in an online mode. Mednis et al. (2011) and Wang et al. (2015) implemented the proposed method on Android OS (Operating System) for real-time pothole detection. However, in major studies, entire preprocessing and processing steps which have been done on computers and smartphones have only been used for sensor data collection. Due to the popularity of smartphones embedded with high-performance sensors, as well as the recent enhancement of smartphone's capability complex analysis and processing of streamed data from smartphone sensors in real time are now possible and practical (Dunkel et al., 2015). For online road surface anomaly detection approaches, the feasibility of implementing an online mode for smartphones should be investigated. In addition, a proper evaluation of implemented approaches for road surface monitoring on smartphones is desirable. Smartphone resource consumption analysis, such as CPU (central processing unit), memory, and battery usage are topics of further interest.

Due to the complexity of the processing step, post-processing using multiple sources is able to increase both detection accuracy and decrease the rate of false detection. Some studies investigated data crowdsourcing techniques for road surface monitoring and indicated considerable improvement of the detection accuracy rate. Unfortunately, their recommended approaches were in the very early stages of development and suffered from the unreliability of smartphone detection and the variable nature of road surface anomalies.

Moreover, the participatory sensing from smartphone applications presents challenges, such as flawed client-server communication due to unreliable vehicular networks, limited connectivity time, and high packet rate (Fernandez et al., 2012). GPS errors also complicate data accumulation because of erratic sampling (Fox et al., 2015). In fact, the detected location derived from GPS sensor of the smartphones has uncertainty. For instance, some existing studies proved that the cellular and/or GPS positioning can result in error ranging from several meters to hundred meters (Mok et al., 2004; Pun-cheng et al., 2007; Zandbergen, 2009) Therefore, the detected location from various smartphone users for any road surface anomaly varies due to the data uncertainty. As a result, the best approach to crowd-source road surface anomalies from multiple sources would be a probabilistic and spatiotemporal-based approach that would overcome both uncertainty and variability of road surface anomalies. In addition, novel technologies of data transferring such as RESTful (representational state transfer) architecture and data formats such as JSON (JavaScript object notation) data format can be utilized to minimize the packet rate and overcome the challenges in participatory sensing using smartphones.

Chapter 3 Methodology

This chapter presents the methodological steps for analysis of smartphone sensors' data quality, detection of road surface anomalies (events) from smartphone sensors, and integration of detected events from multiple road users. The procedures related to data collections and pre-processing required for each step of the analysis is described in Section 3.1. The developed approaches for road surface anomaly detection from smartphone sensors and a probabilistic-based crowdsourcing technique for road surface anomaly integration are presented in Sections 3.2 and 3.3. Finally, the steps required to validate the performance of the proposed approaches are described in Section 3.4.

3.1 Data Collection and Pre-Processing

The data collection and preprocessing steps had three different phases: data collection for exploring sensors data quality, data collection for evaluating the road surface anomaly detection approach from smartphone sensors, and data collection for validating the proposed approach for the probabilistic-based crowdsourcing technique for road surface anomaly integration.

To collect the required sensor data, an Android-based smartphone app was developed to access and collect sensor data from the devices (e.g., smartphones or tablets). All sensors' data that are available in any Android device can be accessed using the "SensorManager" class, which is a part of the hardware package of the Software Development Kit (SDK)[2]. Some of these sensors, such as the accelerometer, gyroscope, magnetometer, light and temperature, are physical sensors. While some other sensors are virtual sensors, where these virtual sensors acquire data from one or more of the physical sensors and virtually calculate (using software) their real-time values, such as linear acceleration, rotation and gravity, based on the desired outcome.

[2] https://developer.android.com/guide/topics/sensors/sensors_overview.html

The sensor availability varies among Android versions. This is because the fact that the sensors have been introduced over the development of several platform releases. For example, many sensors were introduced in Android 1.5 (API Level 3), but some of them were not implemented and were not available in the market for use until Android 2.3 (API Level 9). Table 3.1 summarizes the availability of each sensor on a platform-by-platform basis. Only the platforms that involved sensor changes are listed. Based on the sensor requirements for the developed app in this study, the app is executable on the Android devices having API Level 9 (Android 2.3) or higher.

Table 3.1: Sensors availability by platform utilized for road surface anomaly detection (Google, 2017)

Type of Sensor	**Android 4.0 (API Level 14)**	**Android 2.3 (API Level 9)**	**Android 2.2 (API Level 8)**	**Android 1.5 (API Level 3)**
Accelerometer	**Yes**	**Yes**	**Yes**	**Yes**
Gravity	**Yes**	**Yes**	N/A	N/A
Gyroscope	**Yes**	**Yes**	N/A	N/A
Linear acceleration	**Yes**	**Yes**	N/A	N/A
Magnetic field	**Yes**	**Yes**	**Yes**	**Yes**
Rotation vector	**Yes**	**Yes**	N/A	N/A

An Android API was utilized to obtain current location information, including longitude, latitude, bearing and the vehicle's velocity. The Android API provides the best available location information based on location providers such as Wi-Fi and GPS (Global Positioning System) available on each smartphone. Furthermore, the API can deliver the accuracy of the reported location information determined by the available location providers.

The sensor's sampling rate indicates the rate which sensor events are provided. According to the Android documents, there are four prevalent sampling rates defined in Android API. Table 3.2 summarizes the sampling rate's name and the predefined delay for each of the predefined sampling rate. In addition, the Android API enables users to determine any preferred delay in microseconds between events for the

Android version 2.3 (API Level 9) or higher. In fact, the data delay (or latency) controls the interval at which sensor events are sent to the application through the "onSensorChanged()" callback method. This callback method triggers when new sensor data is available.

Table 3.2: Sampling rate for sensors data collection predefined by Android API

Sampling rate name	**Predefined Delay (in microseconds)**
SENSOR_DELAY_NORMAL	200,000
SENSOR_DELAY_UI	60,000
SENSOR_DELAY_GAME	20,000
SENSOR_DELAY_FASTEST	0

In this research, the SENSOR_DELAY_FASTEST sampling rate was used to obtain sensors' data from smartphones with highest available sampling rate (i.e., without any delay) in every device in order to provide the highest resolution of sensors' data found in every smartphone to serve the objective of road surface anomaly detection. This indeed increased the possibility of detecting anomaly events with regards to the uneven distribution of road anomaly found in any road. In this case, one can have a control to interpret and manipulate the data in a way so that the data/result can be down-sampled at either the data level or decision level, if necessary.

3.1.1 Data Collection for Sensors Data Quality Analysis

The essential thing to know about the employed sensors is the data quality (i.e., types of errors and their magnitudes). The sensitivity of integrated sensor data should be investigated, and the existing errors should be identified in order to model and filter them. According to Gustafsson (2010), typical errors that exist in the accelerometers and gyroscopes sensors are bias errors, scaling errors and random noise errors.

To this end, sensor data being used in this study such as, linear accelerometer, gyroscope and rotation (in X, Y and Z direction), as well as the time intervals between each consecutive generated signals and location information were collected by a mobile app specifically developed to support the experimental testing. The process of data collection was conducted for two different devices' orientations (vertical and horizontal positions) and logged for approximately 10 minutes. The collected data was separately stored in a CSV comma-separated values (CSV) file format in the local storage of the device.

3.1.2 Data Collection for Road Surface Anomaly Detection from Smartphone Sensors

After exploring the sensors data quality, the second phase of data collection was performed to evaluate the proposed approach for road surface anomaly detection from smartphone sensors data. The data collection of this phase had two stages. First stage included collecting raw sensor data and location information using the developed mobile app. In this stage of data collection, linear accelerometer, rotation vector and location information data were retrieved. Linear accelerometer sensor data were collected to monitor the acceleration values caused by vehicle's vibration. To eliminate the smartphone orientation dependency in the proposed approach, the process first utilized the smartphone API to retrieve the three rotation parameters (i.e., azimuth, roll and pitch), which are computed from the three accelerometer, magnetometer and gyroscope sensors (where the process is deemed to be a black box in terms of the end-users). The three retrieved rotation parameters were utilized to perform coordinate transformation of the linear acceleration from the smart-phone (internal/local) coordinate system to the local level coordinate system. Also, the collected data was utilized to compare the improved approach which was proposed in this study with an existing approach (Yi et al., 2015) which was adopted.

After validating the results from applying the proposed approach for road surface anomaly detection from smartphone sensors on the collected data from the first stage of data collection, the second stage of data collection was accomplished to test and verify the performance of the developed mobile app (based on the proposed approach in Section 3.2.1).

3.1.3 Data Collection for Probabilistic Based Crowdsourcing Technique for Road Surface Anomaly Integration

After validating the performance of the proposed approach and the developed mobile app for road surface anomaly detection from smartphone sensors, the mobile app was modified in order to function as a part of proposed mobile crowdsourcing approach. For instance, the classification process (i.e., GMM method) was removed from the mobile app and transferred to a central server and substituted with an unsupervised classification approach (i.e., Dirichlet Process Gaussian Mixture Model (DPGMM) method) which is more suitable and practical for road surface anomalies classification (in terms of levels of discomfort sensed by each vehicle). This modification also helps to decrease the processing intensity of the mobile app, which is one of the critical factors that should be considered in any mobile crowdsourcing approaches.

3.2 Road Surface Anomaly Detection from Smartphone Sensors

In this section, an improved approach based on the approach proposed by Yi et al., (2015) was developed to detect road surface anomalies from smartphone sensors. The improved approach, which is a hybrid approach, integrates both adaptive threshold-based approach and machine learning-based approach to automatically adapt itself to any condition, including different smartphones with dissimilar sensor properties and different mechanical properties of the vehicles to detect road surface anomalies. In addition, the developed approach utilized a sensor fusion technique to improve the system performance and coordinate transformation technique in order to eliminate the dependency of the smartphone orientation on detection process. A Gaussian Mixture Model (GMM), which is a supervised fuzzy classification approach, was utilized to classify detected road surface anomalies into two different classes according to their severity level by taking into account that the road surface anomalies have a fuzzy nature.

3.2.1 Road Surface Anomaly Detection Approach

To detect road surface anomalies from smartphone sensors, the threshold-based method proposed by Yi et al. (2015) was adopted and improved. The following developments were accomplished to modify their method to a robust and inclusive one that is capable of implementation on smartphone devices.

- Instead of using accelerometer sensor data for anomaly detection, the linear acceleration sensor data was utilized. The data value of linear accelerometer sensor, which are virtual sensor data, is mainly computed by a sensor fusion technique. Data from magnetometer and gyroscope sensors are fused to determine the acceleration value caused by gravity. Then, the calculated gravity value is excluded from the data values of accelerometer sensor. Since the effect of gravity is excluded from the accelerometer sensor data, the accuracy of detection can be improved.
- Instead of completely implementing threshold-based detection decision approach, a complementary machine learning-based approach was implemented to improve the detection decision based on the dynamic nature of vehicles and smartphones sensors.
- Rotation parameter values (roll, pitch and azimuth) about smartphones axes were obtained to reorient the linear accelerometer sensor values from device coordinate system to the local level coordinate system.

Figure 3.1 summarizes the overall process for the proposed road surface anomaly detection. The process has two phases of processing. The first phase aims to obtain real-time senor data (i.e., linear acceleration), reorient them and compare them with the updated threshold values driven from the other phase of process to detect any suspicious vibrations caused by road surface anomalies. The second phase of the process aims to calculate the real-time standard deviation and average values of three-minute windows of sensor data values in the stable period (i.e., normal road surface conditions). Figure 3.1 shows the steps that have been implemented to complete a potential road anomaly detection approach.

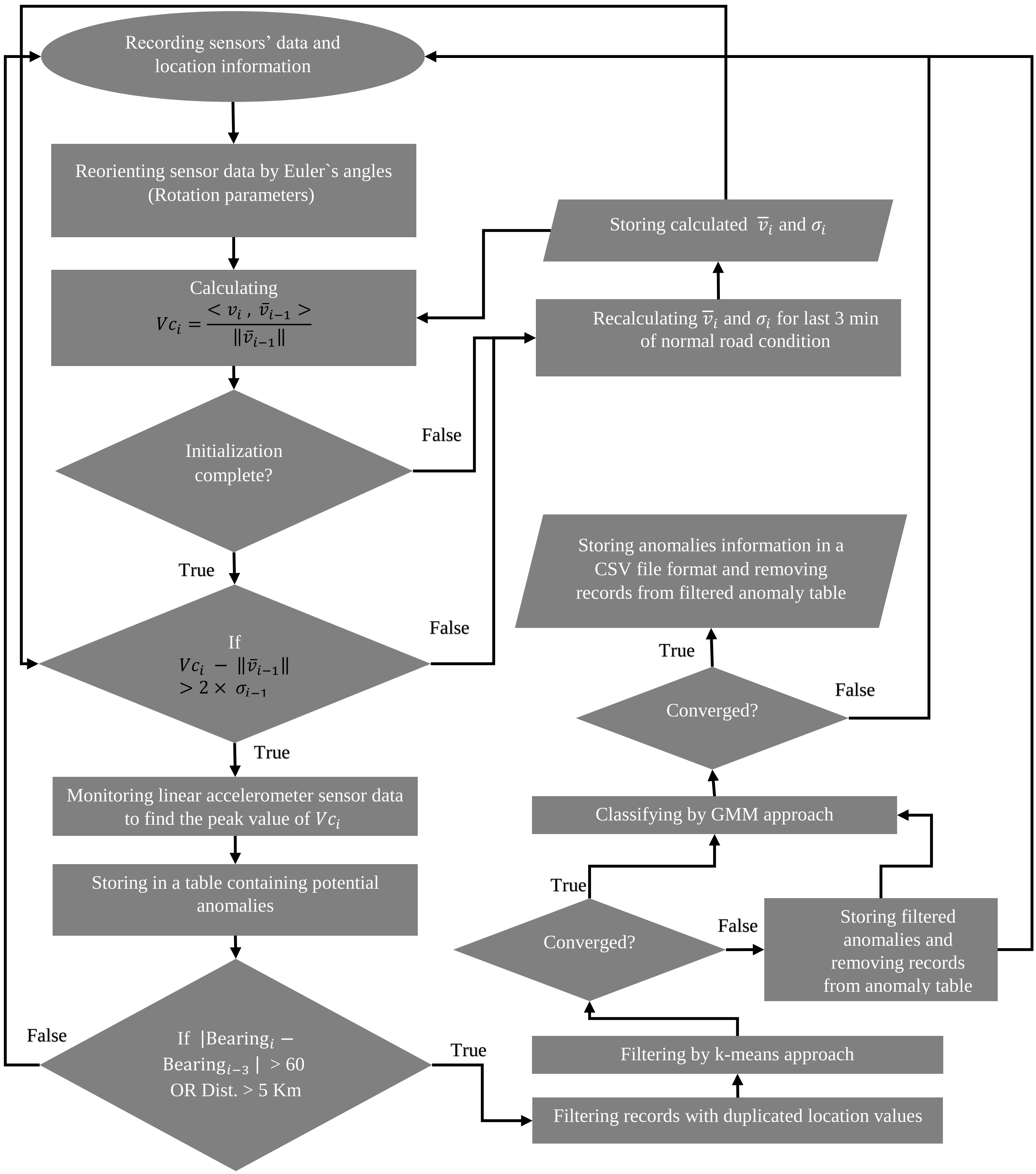

Figure 3.1: The proposed road surface anomaly detection process

According to Figure 3.1, the following steps were accomplished by generating required portions of the sensor data:

1. The system was initialized by listening to the required sensor data and waiting for 30 seconds before storage begins. This is due to the unstable behavior of generated sensors data caused by the embedded sensors' properties (i.e., 30 seconds is considered an adequate warm-up time).
2. System then started to collect linear accelerometer sensor data and applied the reorientation process by obtaining the orientation parameter values to transfer the data values of linear accelerometer sensor from device coordinate system to the local level coordinate system. The transformation equation was employed here to perform the coordinate transformation is given in Equation 3.1.

$$\begin{bmatrix} LinAcc_x \\ LinAcc_y \\ LinAcc_z \end{bmatrix}_{local\ level} = R_x R_y R_z \begin{bmatrix} LinAcc_x \\ LinAcc_y \\ LinAcc_z \end{bmatrix}_{device} \quad (3.1)$$

According to Equation 3.1, $\begin{bmatrix} LinAcc_x \\ LinAcc_y \\ LinAcc_z \end{bmatrix}_{local\ level}$ is the transformed vector of linear accelerometer sensor data values (in m/s^2) along the three axes in the local level coordinate system (refer to Figure 2.2a) and $R_x, R_y, and\ R_z$ are the rotation matrices about the X, Y, and Z axes, respectively. In addition, $\begin{bmatrix} LinAcc_x \\ LinAcc_y \\ LinAcc_z \end{bmatrix}_{device}$ is the data values linear accelerometer sensor (in m/s^2) along the three axes in the device coordinate system (refer to Figure 2.2c).

3. Then, the Vc_i, which is the vertical component of the linear acceleration value (m/s^2) at the current statue (t_i), was computed using Equation 3.2. According to Equation 3.2, the v_i is the current linear accelerometer vector value (in m/s^2) and the $\bar{v}_{i-1}$ is the average vector value of the linear accelerometer sensor data values (m/s^2) corresponding to the normal road condition at the previous state t_{i-1}. The $\|\bar{v}_{i-1}\|$ denotes the norm value of the average vector value of the linear accelerometer sensor data values corresponded to the normal road condition (a three-minute window was considered).

$$Vc_i = \frac{<v_i , \overline{v_{i-1}}>}{\|\overline{v_{i-1}}\|} \tag{3.2}$$

4. For the first 30 seconds of collecting data, the calculated Vc_i and reoriented v_i values were utilized to calculate the σ_i (standard deviation of Vc_i) and $\overline{v}_i$ (average value of v_i) before beginning to detect potential road surface anomalies (i.e., value initialization).
5. To start detecting potential road surface anomalies, the value of the $Vc_i - \|\bar{v}_{i-1}\|$ should be calculated. If $Vc_i - \|\bar{v}_{i-1}\| < 2 \times \sigma_{i-1}$ (based on the desired 95% confidence level / sensitivity level), the Vc_i value and corresponded v_i value were considered as the value corresponding to normal road conditions and were passed to the process for updating the average and standard deviation values. However, if the $Vc_i - \|\bar{v}_{i-1}\| \geq 2 \times \sigma_{i-1}$, Vc_i values and corresponded v_i value were suspected as a potential road surface anomaly, they were monitored for another 0.5 second (Step 6).
6. Any suspected road surface anomaly detected from Step 6 was monitored for a period of 0.5 second (called an event period) to capture the time, when the maximum Vc_i value occurred. Also, the standard deviation ($\sigma_{(event)}$) of Vc_i values in the event period was computed.
7. The maximum captured value of the Vc_i during the event period and the ratio of $C_{(ratio)} = {}^{\sigma_{(event)}}/_{\sigma_{i-1}}$ were the considered variables for each suspected road surface anomaly for further filtration and classification purposes. These values were accumulated in a table (i.e., an anomaly table).
8. To partition the detected anomalies with respect to the road segment two different strategies were proposed. These strategies helped to prevent accumulation of excessive amount of data on the memories of the mobile devices and reduce the computational processing. One of the strategy was tracking every four sequences of the bearing values of the moving vehicle continuously and if a substantial change was identified, it was determined that the vehicle possibly turned into another road segment (i.e., the difference of the first and the fourth values were more than > 60 degrees). The other strategy was slicing the detected anomalies if the driver continued driving in the same

direction (i.e., no substantial change happened in the moving direction based on the first strategy) for every five kilometers to manage the data volumes. If any of the described conditions occurred, the detected anomalies stored in a table were passed to the filtration process (i.e., Steps 9 to 11). Otherwise, the process was stopped, and it waited for new incoming sensor data.

9. Since the frequency of the generated data from the location sensor was less than those from the motion sensors, in some occasions, two records might have similar location values (i.e., longitude and latitude). To filter out the duplicated records with similar geographic location values, only the record with higher value of Vc_i was selected and the rest were removed from the Anomaly table.
10. To perform the developed k-means filtration process, a minimum of three anomalies should be in the table of anomalies. If the number of anomalies in the Anomaly table was less than three, the process should be stopped, and the process should wait for incoming sensor data.
11. To filter the other incidents (non-road surface anomalies such as breaking, turning and accelerating) which were mixed with the detected road surface anomalies from the detected suspected road surface anomalies, a k-means clustering approach was applied to partition the stored data stored into three different categorizes. Generally, the cluster which has the lowest centroid value was likely caused by a non-road surface anomaly incident which should be filtered from the detection list (e.g., road noise). It is essential to note that since the $C_{(ratio)}$ and Vc_i values were in different scales and they should be standardized before applying the filtration process. Therefore, the Z-score values of $C_{(ratio)}$ and Vc_i data were considered as the standardized values for classification purpose. If this process has not converged, the process would be stopped at this point and it would wait for incoming sensor data. However, if the process converged the filtered anomalies were stored in a table (i.e., filtered anomaly table) and passed to the GMM classification algorithm. In addition, the records that were stored in potential anomaly table were all removed after successfully applying k-means process.

The rationale of applying k-means prior to any probabilistic-based classification approach is because such a mechanism can aid in filtering out any superfluous data belonging to turns, deceleration and acceleration incidents, which all do not represent the road surface anomaly data. In this case, after the raw data being filtered out by k-means, it can help to improve the data transmission efficiency, resulting in sending those road surface anomalies data to the subsequent data processing on the server side, as described in the following Sections 3.2.2 and 3.3.1.

3.2.2 Road Surface Anomaly Classification Approach

To classify road surface anomalies into two different classes based on the severity level (i.e., discomfort level) of the anomalies, a Gaussian mixture model (GMM) with a maximum expectation model (EM) was applied. Therefore, the outcomes from the filtration process (i.e., Step 11 in Section 4.2) are passed to the GMM model. This approach fits a fixed number of Gaussian models (determined to be 2 for the mobile app) to the data points in such a way that the classes have the parameters with the maximum likelihood estimates.

The formed class from the GMM process, which had the lower centroid value, is labeled as “Class 1”, which includes small cracks, even manholes and road joints. In contrast, the other class, which had higher centroid value compared to “Class 1”, is labeled as “Class 2” which includes big cracks, uneven manholes and potholes. Since the GMM classification approach is a fuzzy (soft) classification approach, it assigns a probability distribution to road surface anomalies instead of assigning them to particular clusters.

In some situations, the GMM algorithm might suffer from a lack of convergence (i.e., a singular covariance matrix). This was because the number of data points (i.e., road surface anomalies) were insufficient to fit a GMM model or some of the data points, which were discrete in the space, caused a singularity in the covariance matrix. To solve this issue, this set of anomalies was accumulated with the other sets of the detected road surface anomalies from the following road segment. This process was repeated until the GMM model converged. If the GMM process converged, the classification results as well as the corresponded location information were stored in a CSV file format. In addition, the records associated with the other road segments, which the GMM process was unable to converge and were stored in the filtered anomaly table, were all removed after successfully applying GMM classification process.

3.3 Probabilistic-Based Crowdsourcing Technique for Road Surface Anomaly Integration

A novel probabilistic-based crowdsourcing approach was proposed to classify and integrate detected road surface anomalies from multiple users and/or multiple passes of any road segment. The proposed approach was built upon a real-time probabilistic-based approach to overcome the inherent uncertainty existing in the application of detecting road surface anomalies from smartphone sensors. Figure 3.2 illustrates the overall process of the proposed crowdsourcing approach. According to this approach, the DPGMM is an unsupervised classification approach, was utilized to classify detected road surface anomalies. The detected road surface anomalies are the outcomes of the developed mobile app as described in Section 3.2. Then, the classified data should be accumulated and integrated with other possible classified data, which has been detected and reported from the other road users for the corresponded road segment with similar moving direction. In addition, the accumulated road surface anomalies from multiple surveys are grouped in different clusters. Each cluster represents a road surface anomaly.

To store and query historical classified data, formed clusters and integrated anomalies' information, a database was established. After classifying incoming road surface anomaly data, the developed database should be queried. If any related historically formed cluster existed in the database, the new classified data was assigned to the proper clusters according to the approach described in Section 3.3.3. Subsequently, updated clusters with the newly added events were processed in the spatiotemporal domain in order to update the cluster information (i.e., integrated road surface anomaly data) according to the proposed approach described in Section 3.3.4. Then, the integrated data was entered into the database to update the road surface anomaly information related to the surveyed road segment. However, if no historical cluster existed for the surveyed road segment with the similar moving direction, the newly data events were used to form new clusters and stored in the database. The aforementioned process runs autonomously by receiving any set of detected road surface anomalies, which is reported from the developed smartphone app.

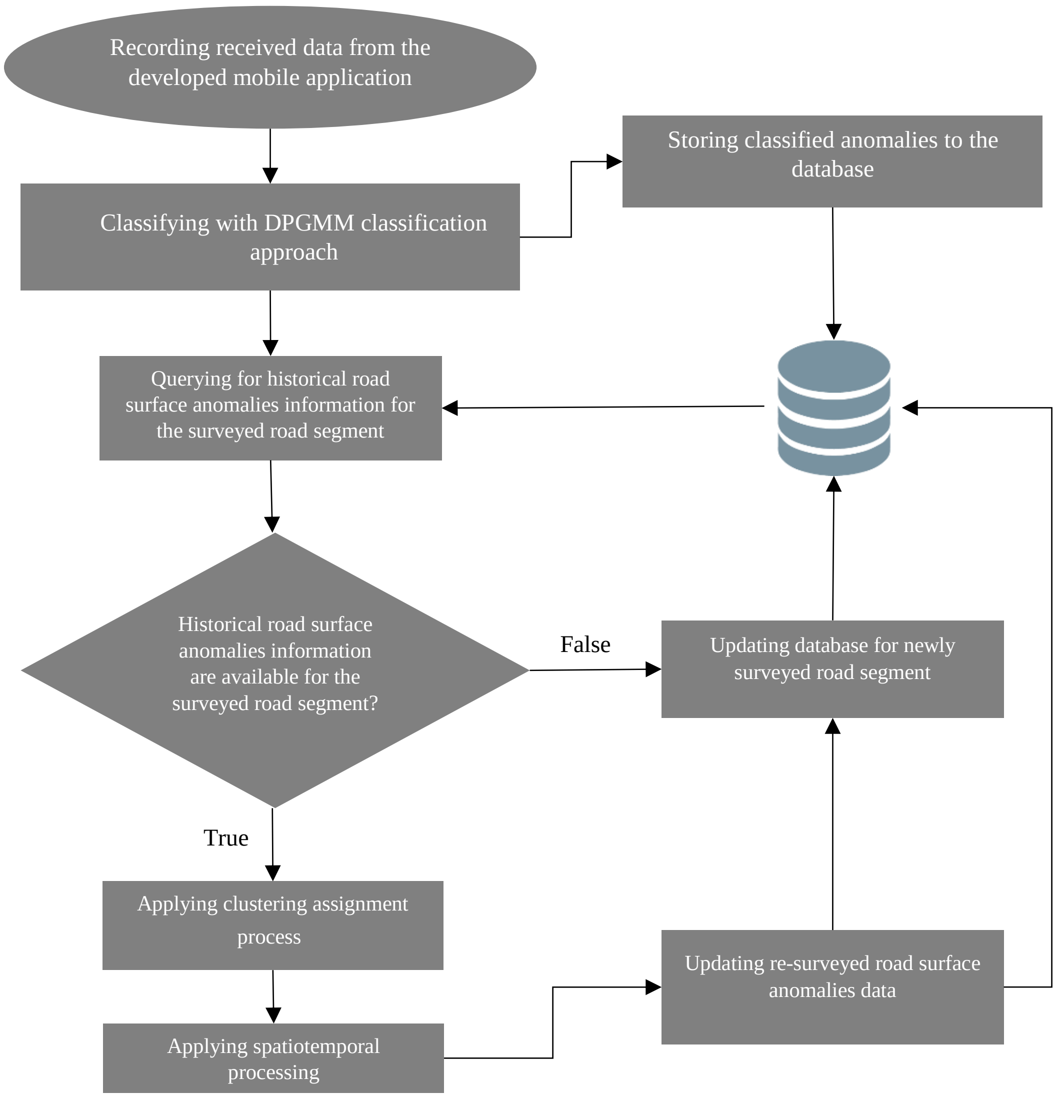

Figure 3.2: The proposed spatiotemporal crowdsourcing procedure

The main benefits of the proposed crowdsourcing approach are two-fold. First, anomalies that cannot be detected by a single source/survey can be possibly identified by other sources/surveys. Second, the proposed approach aids to improve the detected location of road surface anomalies and infer more robust and reliable illustration regarding the severity level of each road surface anomaly.

3.3.1 DPGMM Classification

The collected data from the third phase of data collection procedure (Section 3.1.3), which were stored in CSV file format, were imported to the MATLAB V. R2017b environment. Each file contains detected road surface anomalies information for every surveyed road segment. To classify the detected road surface anomalies into different classes, the DPGMM approach was applied.

DPGMM, which is an unsupervised, nonparametric Bayesian clustering model, was adopted to classify data events (i.e., detected road surface anomalies from mobile app) to infinite Gaussian mixture models. This model adopts the concept of Dirichlet Process (DP) and Chinese Restaurant Process Mixture (CRPM) to partition the data. The Gibbs sampler approach, which is a simple and widely applicable Markov chain Monte Carlo algorithm, was applied to control the sampling process and to maximize the likelihood of classification (Christopher, 2016). The Gaussian mixture model with K components can be derived from the Equation 3.3.

$$P(x|\theta_1 + \theta_2 + \ldots + \theta_n) = \sum_{i=1}^{K} \pi_i \, N(x|\mu_i, S_i) \tag{3.3}$$

where $\theta_i = \{\mu_i, S_i, \pi_i\}$ is the set of parameters for component i, π is the mixing proportion (Subject to: $\sum_{i=1}^{k} \pi_i = 1, \pi_i > 0$), μ_i is the mean vector for component i, and S_i is its precision matrix (i.e. inverse of the covariance matrix). The detail computational procedure to apply DPGMM is described in Chapters 9 and 11 of the book written by Christopher (2016).

The DPGMM approach aims to classify road surface anomalies according to the severity level of each anomaly sensed by vehicles. Since $C_{(ratio)}$ and V values are correlated with speed values, these values were normalized by dividing them to their respective speed values to reduce the correlation. Then, the normalized values of $C_{(ratio)}$ and V were standardized (by calculating z-score values) before applying DPGMM classification algorithm.

3.3.2 Browsing the Developed Database

The purpose of the developed database was to store the information about classified road surface anomaly and to form clusters, required for the cluster assignment and data integration processes. For each classified road surface anomaly, the probability distribution information and location information were recorded in the developed database. For each formed cluster, the updated values of integrated probability distribution information and averaged values of geographic location (longitude and latitude) were recorded (as per Section 3.3.4).

Once the newly detected road surface anomalies were classified (the outcomes from Section 3.3.1), the database should be queried to discover any possible formed cluster from prior road survey in order to combine them with possible historical information. If any formed cluster was discovered, the new classified road surface anomaly was assigned to the associated cluster based on the proposed assignment approach described in Section 3.3.3. Conversely, if no formed cluster was found in the database, the new classified road surface anomaly was stored in the database as a newly detected road surface anomaly, which formed a new cluster.

3.3.3 Cluster Assignment Processing

To assign new classified data events (i.e., road surface anomalies) to any possible formed clusters, which were stored in the developed database, the geographic location of the new classified data events and the formed clusters were utilized to find any potential geographic intersection. Due to the uncertainty of detected geographic location, two steps of geo-query were conducted to find the possible related clusters which new classified event can be assigned:

1. The absolute accuracy value reported by Android API for each detected anomaly’s geographic location was used to create a buffer area and discover the formed clusters intersected with buffer area.

2. The bearing value of direction for each classified data event was used to filter out the intersected clusters from the previous stage, which had dissimilar moving directions.

According to the Android API documentation, both the absolute accuracy estimated for each detected geographic location and the bearing of moving direction have a 68% confidence level (1 σ). However, in this study, 95% confidence level (2σ) values of estimated accuracy values for both geographic location and bearing values were considered to search for intersected clusters.

Each newly classified data event was buffered at the radius of 2σ (based on the estimated accuracy for detected geographic location). If any intersected cluster was identified in the first step of query, the bearing values of the intersected cluster and the new classified data event were compared to filter out the unrelated clusters. Therefore, the difference value of the bearing for each intersected cluster and the bearing value of the new classified data event should be in the range of ±2σ (i.e., estimated accuracy value obtained for the new classified data event) in order to assume that the queried cluster and the newly classified data event were in the similar direction. However, if no cluster was found in the database, the newly classified data event was considered as a new formed cluster and stored in the database.

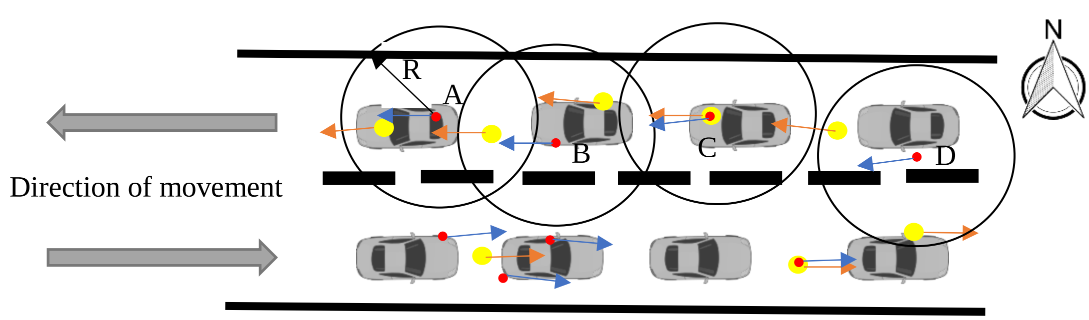

Figure 3.3: The illustration of the clustering and assignment process

Figure 3.3 illustrates the overall concept behind the clustering assignment process in order to assign new classified data event to the most possible relevant clusters formed from the previously detected road surface anomalies. According to the Figure 3.3, the red points denote new classified data events and yellow points denote the existing clusters formed from the integration of former classified data events in different times.

In addition, the orange arrows indicate the average of bearing values specifying the moving direction, in which the data events grouped in a cluster, is detected. The blue arrows indicate the direction in which each individual data event is detected. “R” indicates the buffer radius and the black circles represent the buffer area with provided “R” radius, which is used to find possible intersections with previously formed clusters.

According to Figure 3.3, the buffered area around the red points labelled with “A” and “B” encounter two formed clusters with similar moving directions. Therefore, these newly detected events should be assigned to the both of the formed clusters which they are encountered. The buffered area around the red point labelled with “C” dose not encounter any formed cluster. Therefore, it forms a cluster and stores as a new formed cluster in the database. In addition, the red point labelled with “D” encounters two formed clusters; however, one of the intersected clusters has dissimilar moving direction which should be discarded. Therefore, point “D” should be assigned to the cluster with similar moving direction.

3.3.4 Spatiotemporal Data Processing

This step aims to consider spatiotemporal behavior of road surface anomalies (i.e., data events) for the data integration process. Various road surface anomaly data detected by different smartphones on-board vehicles at different times should be integrated to infer the most probable and updated information for each road surface anomaly existing on the road surface. As discussed in Chapter 2, different vehicles’ mechanical properties and different devices’ sensor properties cause diverse sensitivity responses for any road surface anomaly. Therefore, road surface anomalies may be sensed differently when multiple users are involved for the application of road surface anomaly detection. Moreover, due to the detected geographic locations’ uncertainty, road surface anomalies are potentially assigned to different formed clusters as described in Section 3.3.3. Furthermore, road surface anomalies have dynamic characteristics and may change in terms of their shapes and sizes over time. For example, road defects may be repaired by authorities dealing with road surface maintenance or deterioration due to adverse weather conditions, the influence of passing vehicles or pavement mechanistic failure.

To consider all the aforementioned concerns in order to integrate detected road surface anomalies from multiple road users, a spatiotemporal Dirichlet process was developed. This approach consists of various steps. First, to determine the spatiotemporal weight of each anomaly grouped within a cluster, the Gaussian Radial Basis kernel function (RBF) was utilized. RBF calculates both spatial and temporal distance from the centroid of that cluster and all observations within the cluster. RBF is one of the widely used kernel function of Gaussian Processing (GP), which is continuous and flexible enough to be positive or negative in various region of space (Rasmussen, 2014). Equation 3.3 describes the formulation of RBF kernel function:

$$\mathrm{k}(\mathrm{l}, \mathrm{l}') = \exp\left(\frac{-\|\mathrm{l}-\mathrm{l}'\|^2}{2\sigma_{\mathrm{l}}^2}\right) = \exp(-\gamma\|\mathrm{l} - \mathrm{l}'\|^2) \tag{3.3}$$

According to Equation 3.3, $\|\mathrm{l} - \mathrm{l}'\|$ calculates the Euclidean distance of both time and location for each anomaly within a cluster from the current time and the centroid geographic location of the cluster. "l" denotes the array containing geographic location and the time stamp values of each detected anomaly within a cluster. "l'" denotes the array containing the geographic location centroid of each cluster and the latest time recorded for the detected anomaly grouped within a cluster. In this study, $\frac{1}{2\sigma_{\mathrm{l}}^2} = \gamma$, which defines the width of the bell-shaped curve, is calculated based on the standard deviation of the computed time and geographic location distances for each member of a cluster. The results after applying the RBF are considered as the weight values (for both time and location) for each detected anomaly. In fact, the closest event to the centroid location of the cluster or the latest detected anomaly, which have lower distance values (i.e., in terms of location and time), essentially obtains higher weight values in accordance to the RBF.

To combine both spatial and temporal weight values of an anomaly in order to determine the spatiotemporal weight factor, the weight values of time and location computed from Equation 3.3 were summed. In order to normalize all computed weigh factors to fall between 0 and 1 and sum to 1, the calculated spatiotemporal weight factors are each divided by the sum of all weight factors. These normalized weight factors were applied to each corresponding anomaly probability distribution in order to form a weighted-probability matrix.

To estimate the probability distribution of each cluster from the composed frequency weighted-probability, a Dirichlet multinomial mixture (DMM) model, which is a family of discrete multivariate probability distribution, was applied. The Dirichlet-multinomial distribution is a compound distribution where the probability vector is drawn from a Dirichlet distribution and then a sample of discrete outcomes is drawn from a multinomial probability vector. In order to fit DMM to the composed frequency matrix, the proposed approach by Minka (2000) with detail computational procedure was adopted and applied.

To infer the most probable value for the geographic location and bearing value of moving direction in which the anomalies within a cluster were detected, the values of the geographic location and the bearing values of the clustered anomalies were averaged.

3.4 Performance Evaluations

The proposed approaches were validated by performance evaluation, which was conducted in two different phases. For both phases, multiple road segments within the boundary of the City of Toronto were selected. They consisted of number of road surface anomalies (e.g., potholes and cracks) and were driven when the developed mobile app was installed and ran on the smartphone or tablet. Verification of the proposed approaches was made visually by comparing detection results with the geotagged referenced images and videos captured during the field inspection and data collection.

To conduct the first phase of the performance evaluation to investigate the functionality of the proposed approach described in Section 3.2, three different case studies were conducted. The accuracy of detection for each case study was evaluated to ensure the functionality of the proposed approach and developed mobile app in various conditions (e.g., different smartphone devices, different vehicles, different placements of smartphone and different vehicle velocities). To do so, the developed mobile app was utilized to collect the desired data for the performance evaluation.

Although this study did not aim to classify the type of road anomaly, each studied road segment was visually inspected with respect to the number (instead of the anomaly type) of existing anomalies, including potholes, cracks, manholes and bumps. In addition, geotagged images and estimated location of anomalies were recorded during site inspections. All these recorded data and associated information were used for the accuracy assessment.

The first case study aimed to verify the performance of the developed mobile app on different devices. Two different devices, i.e., a Nexus 6 (smartphone) and a Nexus 7 (tablet), were used to perform this part of evaluation task. Both devices employed the Android operating system and were compatible with the developed mobile app.

The second case study aimed to evaluate the performance of the developed mobile app while operating on-board three different types of vehicles. Three different available vehicles (i.e., Infinity QX60, Acura MDX and Honda Civic) were employed to perform the second case study to ensure the functionality of the developed mobile app when different vehicles with dissimilar mechanical properties were involved. In this experiment, the Nexus 6 was placed on the available smartphone holder, which was attached to the windshield of all three vehicles.

Finally, the third case study aimed to validate the performance of the mobile app for different speeds of moving vehicles. The study area has three different maximum allowable speeds: 40, 50 and 60 km/h. However, only minimum and maximum speeds were investigated to ensure the capability of the developed mobile app in various speeds of vehicle. This case study was intentionally conducted in late evening minimize the traffic in order to keep the speed constant during the experiments. However, the vehicles stopped in some cases due to encountered traffic lights or stop signs. The selected road segment for the first and second case studies had a maximum allowable speed limit of 40 km/h. Therefore, a similar road segment was chosen to evaluate the performance of the developed mobile app for the speed of 40 km/h. In addition, to evaluate the accuracy of detection for a speed of 60 km/h another road segments (i.e., Finch

Avenue between Leslie Street and Bayview Avenue) were chosen since they had the maximum allowable speed of 60 km/h.

The second phase of performance evaluation was expected to assess the performance of the developed probabilistic-based crowdsourcing approach to integrate road surface anomalies detected from various road users. However, due to the lack of volunteers in this research study, the collection of road surface anomalies was repeated a few times in the defined study area by a single user and the results of the assessment were used to measure the accuracy of detection. The detection rate from multiple road surveys was evaluated and compared with the detection rates of the previous phase of performance evaluation, which were from a single user. The improved version of the developed mobile app was employed to fulfill the second phase of accuracy assessment.

To assess and verify the accuracy of detection in the second phase of performance evaluation, a field inspection was carried out to define the number of existing road surface anomalies for every studied road segment. To validate the accuracy of detected geographic location of road surface anomalies for each studied road segment, the outcomes from the proposed approach were compared with those from the smaller road segments. Each of the four studied road segments was sliced into the smaller segments based on the number of intersections existed within each main road segment. For example, parts of Cummer Avenue, Leslie Avenue, Finch Avenue, and Bayview Avenue, which were selected for this phase of performance evaluation, composed of twelve, eight, six, and three smaller road segments, respectively. During the field inspection, the number of road surface anomalies in each portioned road segment was counted and recorded. In addition, geotagged images from the road surface anomalies were captured.

Chapter 4 Experimental Results

Given the proposed approaches for road surface anomaly detection from smartphone sensors and a probabilistic-based crowdsourcing approach to integrate multiple detections from various road users, the objective of this chapter is to describe in detail the experiment results, which are the outcomes of applying the proposed approaches to case studies and assessment of the performance of the proposed approaches. Section 4.1 defines the selected study area for this thesis research, as well as the collected data for each phase of data collection. The outcomes from applying the proposed approaches are presented in Sections 4.2 and 4.3. Section 4.4 describes the performance evaluation outcomes for each proposed approach.

4.1 Study Area and Data Collection

4.1.1 Study area

Multiple road segments with different surface conditions were selected in the North York region of the City of Toronto, Ontario, Canada. The selected study area, shown in Figure 4.1, consists of four different major road segments: a part of Leslie Street from the Leslie and Cummer intersection to the Leslie and Finch intersection (i.e., a north-south direction), a part of Finch Avenue from Leslie Street and Bayview Avenue (i.e., an east-west direction), a part of Bayview Avenue between Finch Avenue and Cummer Avenue (i.e., south-north direction), and Cummer Avenue between Bayview Avenue and Leslie Street (i.e., a west-east direction). These four major road segments had different surface conditions. For example, the selected part of Bayview Avenue had been recently paved and was quite smooth, so there were no cracks and potholes existing except for two existing uneven manholes. However, a large number of cracks, small potholes, two road joints, and uneven manholes existed on the surface of Cummer Avenue compared to the other selected road segments. The selected part of Leslie Street had only few small cracks and some even manholes. The selected part of Finch Avenue also had few cracks, some even and uneven manholes and two road joints, in addition to two uneven surface areas due to the ongoing construction operation during the second phase of data collection. However, these two uneven areas had been rehabilitated before conducting the third phase of the data collection. Table 4.1 provides the maximum allowable speed, length and total number of lanes of the selected street segments. In all phases of data collection, for the selected road segments that had more than one lane in each direction, the right-hand lanes were considered for the data collection.

Figure 4.1: Location of the study area

Table 4.1: The properties of the studied road segments

Road segment	Speed (Km/h)	Length (Km)	Number of lanes
Leslie Street	60	1.3	4
Finch avenue	60	2.0	4
Bayview avenue	60	0.85	4
Cummer avenue	40~50	2.2	2

4.1.2 Data Collection for Sensors Data Quality Analysis (First Phase)

To the study sensors' data quality, the Nexus 7, which was used widely for different phases of data collection, was placed both on a flat surface and a vertical position and kept static while data was logged for approximately ten minutes (in both positions). In both cases, the corresponding sensors data were continuously being captured including linear accelerometer, gyroscope, rotation, and location data. The sampling rate of the employed device sensors was set approximately 100 Hz, though the specification claimed that the maximum sampling rate can yield up to 200 Hz. A total of 55679 data samples were generated in the horizontal position and 53821 data samples were generated in the vertical position from each of the studied sensors. However, the location sensor that was updated less frequent than the other sensors (1 Hz).

Figure 4.2 demonstrates time interval between every consecutive generated sensors data (in the horizontal position). In the Android, sensor events are generated every time the sensor values are changed. According to Figure 4.2, the time intervals of generated sensors data vary. However, most of the data were generated in the range of 0 to 50 milliseconds (time interval) such that sensors data had a sufficient sampling rate to detect road surface anomalies (refer to Figure 4.3). Table 4.2 summarizes the statistical analysis of the sampling rate of the collected sensor data. According to Table 4.2, the average of sampling rate was approximately 10.77 milliseconds with minimum and maximum values ranging from 3.60 to 860.81, resulting in a standard deviation of 37.06 from 55679 number of data samples.

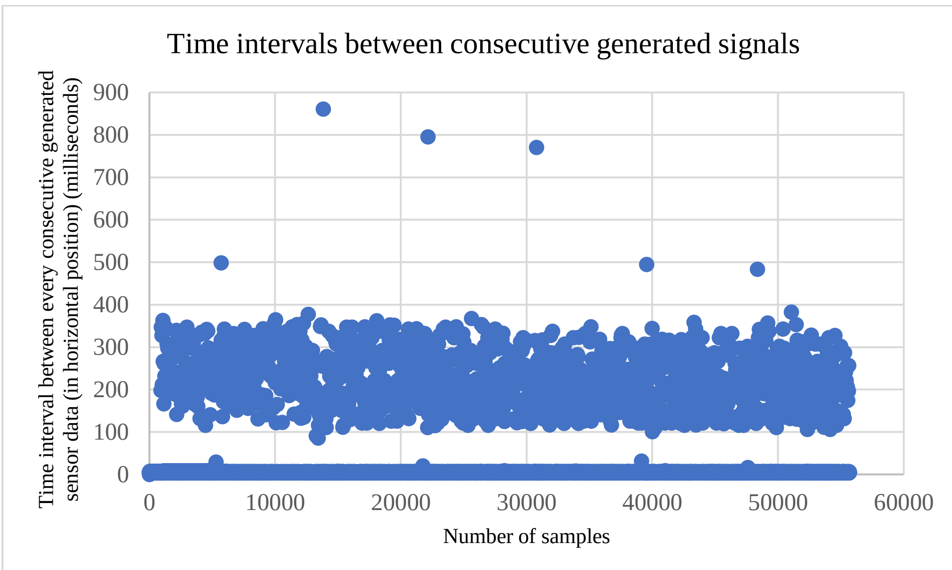

Figure 4.2: The time intervals between consecutive generated signals (sampling frequency) of the collected data (fastest mode)

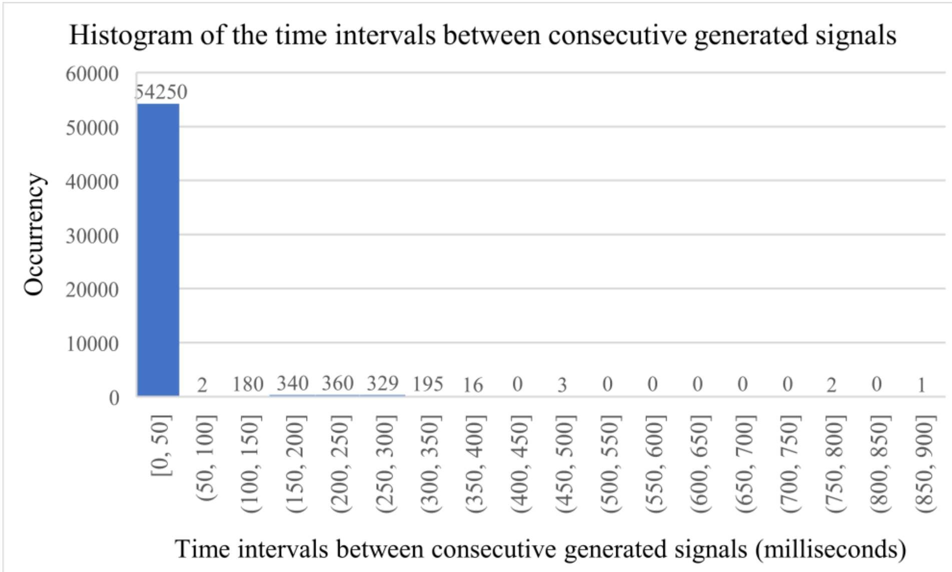

Figure 4.3: Histogram of the time intervals between consecutive generated signals (sampling frequency) of the collected data (fastest mode)

Table 4.2: Statistics analysis for the sampling frequency of the collected data (fastest mode)

	Mean (milliseconds)	**Min (milliseconds)**	**Max (milliseconds)**	**Standard deviation (milliseconds)**
Time between each consecutive reading	10.77	3.60	860.81	37.06

Figure 4.4 illustrates the amplitude of the collected sensors data while the device was in stationary mode and in the horizontal position. The amplitude of the linear accelerometer sensor data along the “Z” axis, the rate of rotation about “Z” axis derived from the gyroscope sensor, and the rate change of the rotation angle about “Z” axis (azimuth) are illustrated in Figure 4.4a, Figure 4.4b, and Figure 4.4c, respectively. Tables 4.3 and 4.4 summarize the mean and the standard deviation derived from the collected sample data of the studied sensors from two modes of smartphone positions (vertical and horizontal modes).

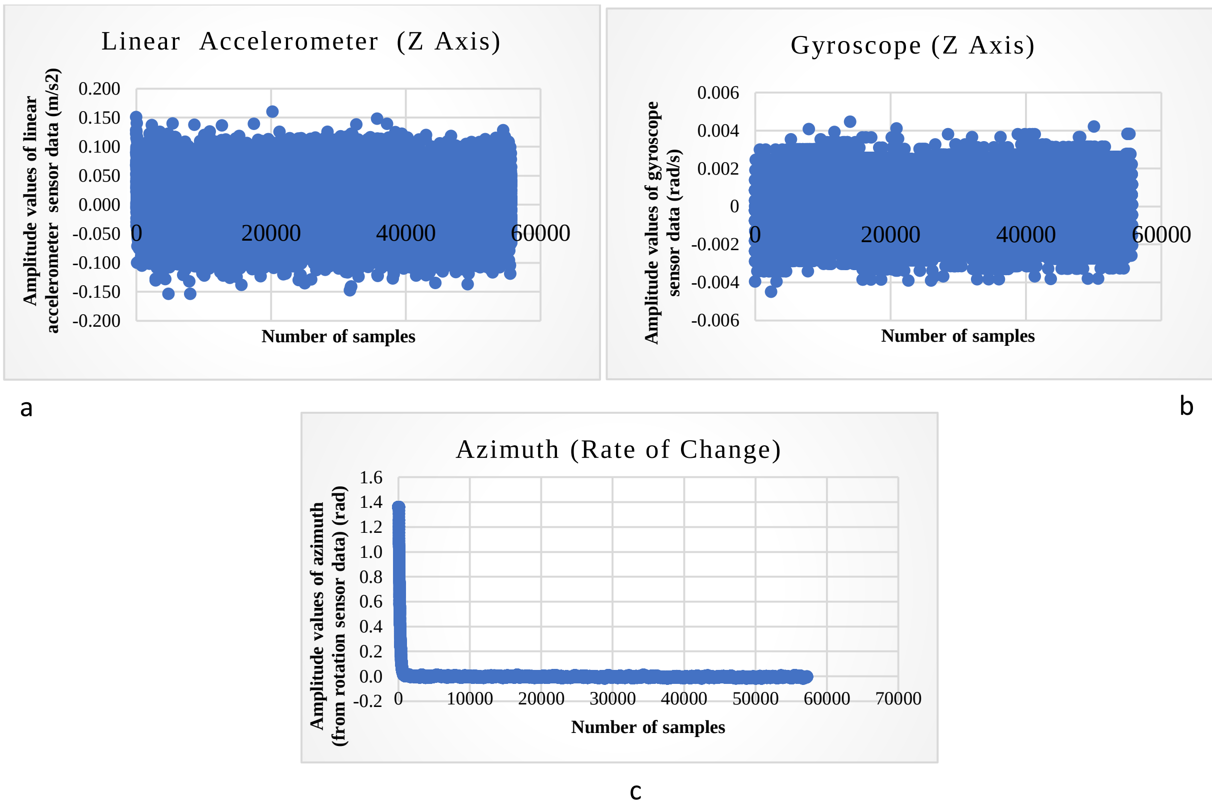

Figure 4.4: (a) The plot of linear accelerometer sensor data values (along Z axis) in stationary mode of the device, (b) the plot of gyroscope sensor data values (along Z axis) in stationary mode of the device, and (c) the plot of azimuth values (from rotation sensor data) in stationary mode of the device

Table 4.3: Mean and standard deviation values for logged sensors' data (horizontal position)

	Linear accelerometer (m/s²)			Gyroscope (degree/s)			Rotation (degree)		
Direction	X	Y	Z	X	Y	Z	Azimuth	Pitch	Roll
Mean	0.001	-0.0005	0.000	0° 0' 0.30"	0° 0' 0.06"	0° 0' 0.20"	0° 0' 0.00"	0° 0' 0.00"	0° 0' 0.00"
Standard deviation	0.0194	0.0191	0.0365	0° 0' 04.62"	0° 0' 04.24"	0° 0' 03.76"	0° 0' 24.30"	0° 0' 02.40"	0° 0' 01.43"

Table 4.4: Mean and standard deviation values for logged sensors' data (vertical position)

	Linear accelerometer (m/s²)			Gyroscope (degree/s)			Rotation (degree)		
Direction	X	Y	Z	X	Y	Z	Azimuth	Pitch	Roll
Mean	0.002	-0.0001	0.001	0° 0' 0.05"	0° 0' 00.06"	0° 0' 0.05"	0° 0' 0.00"	0° 0' 0.00"	0° 0' 0.00"
Standard deviation	0.0189	0.0195	0.0358	0° 0' 4.72"	0° 0' 04.27"	0° 0' 03.72"	0° 03' 22.68"	0° 0' 02.78"	0° 03' 15.34"

According to Table 4.3 and 4.4, the mean and standard deviation values indicate that the smartphone sensors' data contained certain level of errors. These errors include bias and scaling errors found in each of the sensors. However, the error values generated from sensors were relatively insignificant for the application of road surface anomaly detection and can be smoothed or filtered by a preprocessing mechanism. According to the amplitude of sensors data depicted in Figure 4.4, the sensors data are not stable for the first few samples due to the warm-up drift, since the sensors should reach a certain operational temperature in order to properly operate and minimize the produced bias. In order to account for warmup drift in this research study, the entire system should be allowed to stabilize for a short period of time before beginning data collection. The results from this part of study indicate that warm-up usually takes between 20 to 30 seconds for the smartphone sensors to stabilize.

To assess the GPS sensor data values including longitude and latitude values and to evaluate the accuracy of detected location while the device was in the stationary mode, the collected location data values (total of 57218 samples) were first subtracted from their respective sample mean values to obtain the rate of change. The sample rate for GPS sensor was approximately 1Hz, indicating that the sensor data values were changed every second. Figure 4.5 represents the rate of change values for both longitude and latitude data values. Table 4.5 summarizes the mean and standard deviation values derived from the collected location sample data, as well as the calculated values for the relative accuracy. The estimated ground distance values with respect to their calculated standard deviation and relative accuracy values are also summarized in Table 4.5.

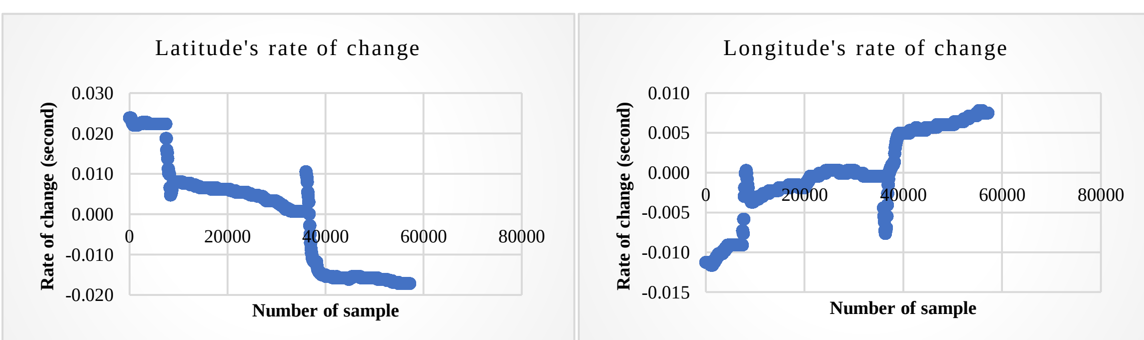

Figure 4.5: (a) The plot of rate of change values of latitude data, and (b) the plot of rate of change values of longitude data

Table 4.5: Standard deviation and relative accuracy values for rate of change values of latitude and longitude, as well as the estimated ground lengths

	Standard deviation (degree)	Standard deviation (m)	Relative Accuracy (degree)	Relative Accuracy (m)
Latitude (Difference from mean)	**0° 0' 0.0130"**	**0.40**	**0° 0' 0.0410"**	**1.27**
Longitude (Difference from mean)	**0° 0' 0.0007"**	**0.17**	**0° 0' 0.0194"**	**0.60**

The accuracy analysis of the collected location data obtained from the GPS sensor indicates that even though the relative accuracies of latitude and longitude were about 1.27 and 0.6 meters (ground distance), respectively, these biases were relatively small and can be neglected for the application of road surface anomalies; all of them were grouped based on each individual road segments (> 100 m).

4.1.3 Data Collection for Road Surface Anomaly Detection from Smartphone Sensors (Second Phase)

To assess and evaluate the proposed approach for road surface anomaly detection from smartphone sensors, a first stage of the data collection was conducted, the Nexus 7 tablet was attached to the dashboard of the Infinity QX60 to collect raw sensor data. The sample rate was set to the fastest mode, which generated data at approximately 100Hz. The collected data included linear accelerometer orientation and location information, which were stored in a CSV file format on the local storage of the device. Linear accelerometer sensor data was collected to monitor the vehicle's vibration in order to detect any significant changes in acceleration values possibly caused by road surface anomalies. Orientation vector data was used to reorient sensors data values and to eliminate the smartphone orientation dependency. An Android API was utilized to retrieve the three rotation parameters (i.e., azimuth, roll and pitch), which were computed from a data fusion technique involving the accelerometer, magnetometer and gyroscope sensors (where the process is deemed to be a black box to end-users). The three retrieved rotation parameters were utilized to perform a coordinate transformation of the linear accelerometer data from the smartphone (internal/local) coordinate system to a local level projective coordinate system.

This stage of data collection was completed on 7 August 2017. The collected data were imported to a MATLAB VR2017b environment for further analysis and model verification. The collected data was preprocessed to filter out the records that were captured when the vehicle was in a stationary mode. Speed values, which was a part of location information and derived from GPS sensor, were utilized to eliminate the records captured in a stationary mode. In fact, these records did not represent any information concerning the road surface condition.

A total of 47756 data points was collected in the study area. Figure 4.6 illustrates the amplitude of linear accelerometer sensor data along three axes (X, Y and Z). As depicted in Figure 4.6a, Figure 4.6b and Figure 4.6c, certain peaks can be found along the time profile, where these peaks may represent the suggested location of the cracks, potholes and bumps along the surveyed area. Figure 4.6d represents the captured images from two selected road surface anomalies, which were located along Bayview Avenue (A) and Cummer Avenue (B). Specified peaks (i.e., A and B) denoted in Figure 4.6a, Figure 4.63b and Figure 4.63c are associated with the selected anomalies.

Both the improved approach for road surface anomaly detection developed in this research and the existing approach (Yi et al., 2015) which was adopted were applied on the collected data by considering different lengths of the window time period and compared. The number of existing road surface anomalies on the surface of the portion of Bayview Avenue and Cummer Avenue was compared with the total number of detected road surface anomalies from both approaches. There were total of 77 anomalies on both portions of road segments. Table 4.6 summarizes the number of detected road surface anomalies with respect to different lengths of window time periods. According to Table 4.6, the approach proposed by Yi et al. (2015) is highly dependent on the length of window time periods. In fact, by increasing the length of time window the detection rate is decreased. However, the results from the approach proposed in this study indicates that the accuracy of detection dose not rely on the length of time window. In addition, the outcomes from the approach proposed in this research study shows that the detection rates are higher than all of those proposed by Yi et al. (2015). In fact, the proposed modifications and improvements which were applied on the existing approach resulted in an enhancement of the detection approach by approximately 20%.

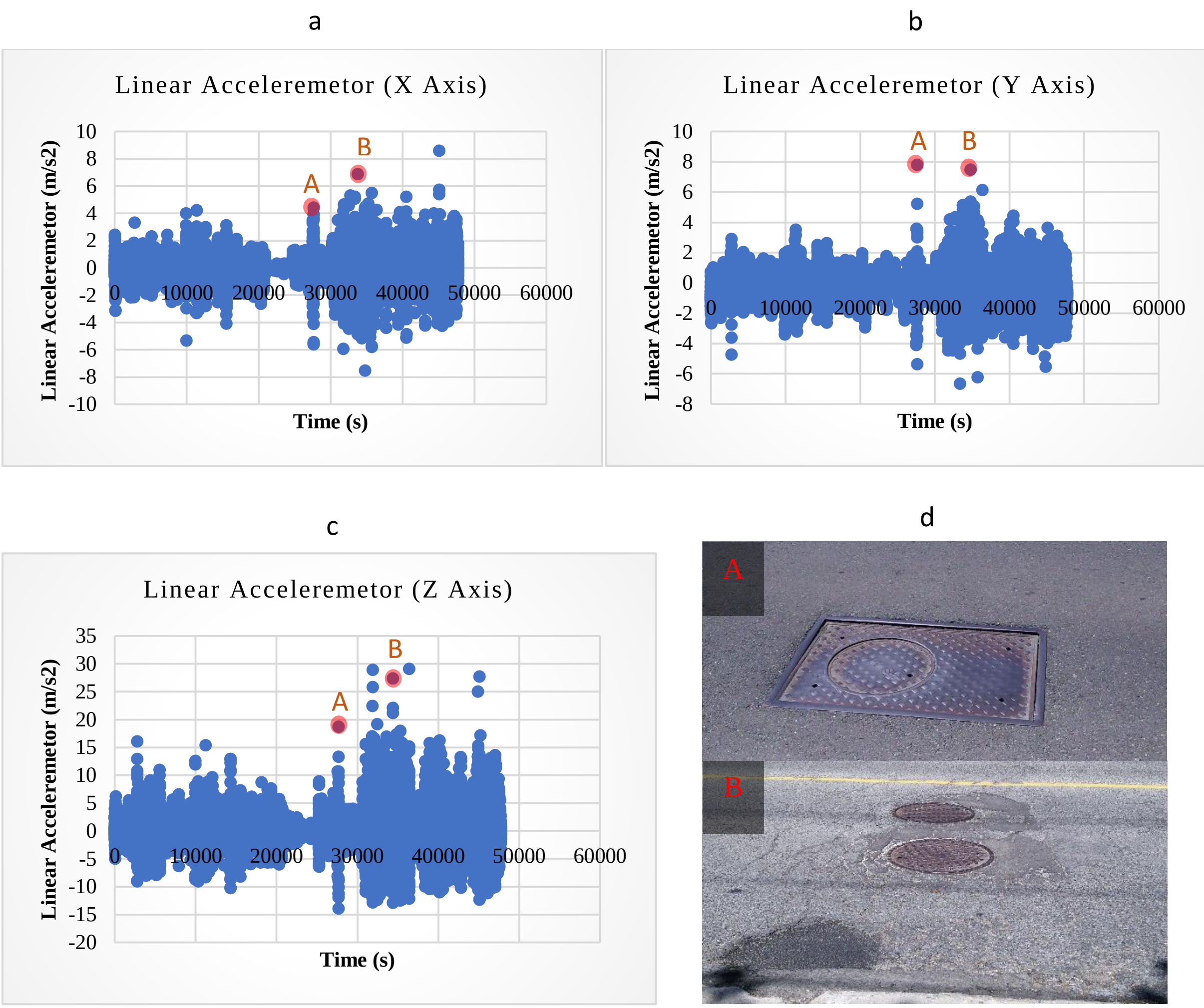

Figure 4.6: (a) Power of the linear accelerometer signal in time domain (x direction), (b) power of the linear accelerometer signal in time domain (y direction), (c) power of the linear accelerometer signal in time domain (z direction), and (d) captured images from field inspections

To test and validate the proposed approach for road surface anomaly detection from smartphone sensors, the collected data from the second phase of data collection (first stage) was preprocessed in order to remove the records while the vehicles were not moving (for example stopping at traffic lights or stop signs). A total of 100 data points was removed from the data file. Subsequently, the filtered data were processed according to the proposed approach described in Sections 3.2.1 and 3.2.2. After validating the results, a mobile app was developed based on the verified proposed approach and the second stage of data collection was completed to evaluate the performance of the mobile app.

Table 4.6: Detection results by the proposed approach and the approach from Yi et al. (2015) under different time windows

Approaches	**Proposed approach**		**Approach by Yi et al. (2015)**	
Time window (seconds)	**Total number of detection**	**Accuracy (%)**	**Total number of detection**	**Accuracy (%)**
30	50	65%	45	58%
60	49	64%	41	53%
90	46	60%	41	53%
120	53	69%	37	48%
180	51	66%	35	45%
210	54	70%	36	47%
270	49	64%	39	51%
300	52	68%	35	45%

For the second stage of data collection, an Android-based mobile app was developed based on the proposed approach for road surface anomaly detection from smartphone sensors, which was verified from the first stage of data collection. The outcome information, including location information and probability distribution information of the detected road surface anomalies, was stored locally on the device in a CSV file format. Then, the stored CSV files were imported in an ESRI ArcGIS environment and analyzed in terms of the approximate locations of detected anomalies and the capability of classifying anomalies compared with collected information from existing road surface anomalies during the field inspections.

Two different devices, including one smartphone (Nexus 6) with a 230 Hz nominal sampling rate and one tablet (Nexus 7) with a 200 Hz nominal sampling rate, were employed in this stage of data collection.

During the data collection, the Nexus 6 was mounted on the phone holder attached to the windshield and the Nexus 7 was attached on the dashboard. In addition, three different vehicles were utilized, including a 2008 Acura MDX, a 2017 Infinity QX 60 and a 2007 Honda Civic. The data collection process was conducted once for each studied vehicle but in different days of the week (between September 26, 2017 and October 2, 2017).

Tables 4.7 and 4.8 summarize the outcomes from the second stage of data collection. Table 4.7 summarizes the number of road surface anomalies detected by the Nexus 6. Table 4.8 summarizes the road surface anomalies detected from Nexus 7. The detected anomalies were also categorized into two different classes (which induced the discomfort level associated with the anomalies) by GMM classification. According to Tables 4.7 and 4.8, although the parts of Cummer Avenue and Finch Avenue have approximately equal length, the number of detected road surface anomalies along Cummer Avenue is about 5 times greater than that along Finch Avenue. Similarly, the parts of Leslie Street and Bayview Avenue have approximately similar lengths even though the number of detected road surface anomalies on Leslie Street is about 8 times higher than those of Bayview Avenue. Visual inspections and captured geotagged videos can justify these assessments. The summarized detected anomaly data from the Nexus 6 and the Nexus 7 indicates that the number of detected anomalies by both devices are approximately the same to each studied road segment.

Table 4.7: Classification results of the detected road surface anomalies detected from the Nexus 6

	Infinity QX60 (2017)			**Acura MDX (2008)**			**Honda Civic (2007)**		
	Class 1	**Class 2**	**Total**	**Class 1**	**Class 2**	**Total**	**Class 1**	**Class 2**	**Total**
Leslie Street	19	5	**24**	25	5	**30**	13	9	**22**
Finch Avenue	15	4	**19**	14	4	**18**	13	4	**17**
Bayview Avenue	3	0	**3**	1	2	**3**	1	1	**2**
Cummer Ave.	56	30	**86**	62	23	**85**	73	19	**92**

Table 4.8: Classification results of the detected road surface anomalies detected from the Nexus 7

	Infinity QX60 (2017)			**Acura MDX (2008)**			**Honda Civic (2007)**		
	Class 1	**Class 2**	**Total**	**Class 1**	**Class 2**	**Total**	**Class 1**	**Class 2**	**Total**
Leslie St.	13	6	**19**	10	6	**16**	2	0	**2**
Finch Avenue	7	3	**10**	7	3	**10**	4	5	**9**
Bayview Avenue	3	2	**5**	1	1	**2**	1	1	**2**
Cummer Avenue	54	35	**89**	71	19	**99**	55	28	**83**

Figure 4.7 and Figure 4.8 shows the geographic location of detected road surface anomalies for each studied road segment captured by the Nexus 6 and the Nexus 7. The yellow points illustrate the anomalies that have a high probability of belonging to Class 1 (i.e., a lower severity level) and the red points show the anomalies that have higher probability of belonging to the Class 2 (i.e., a higher severity level).

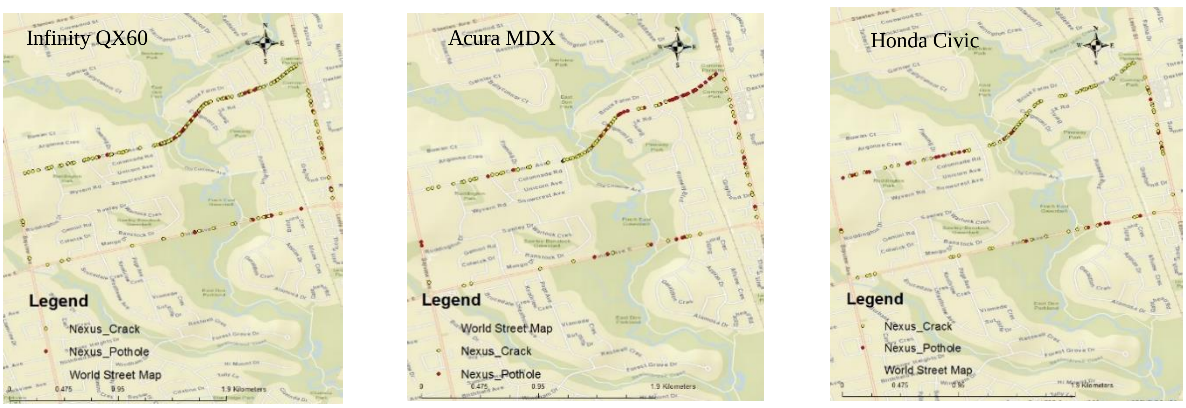

Figure 4.7: The geographic location of the detected road surface anomalies by the Nexus 6

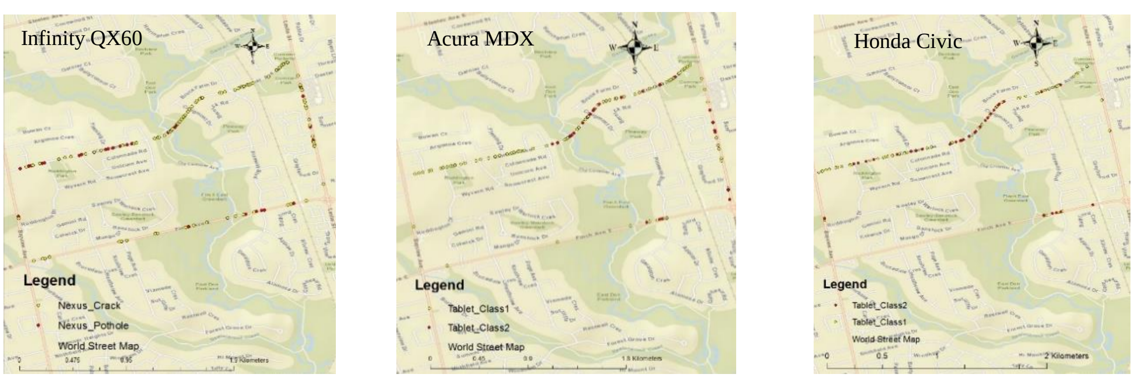

Figure 4.8 The geographic location of the detected road surface anomalies by the Nexus 7

By comparing the location of detected road anomalies with different devices and different vehicles, it is evident that the major road surface anomalies were detected in all scenarios. The difference of detection rates in each scenario were related to the differences in sensors properties, mechanical properties of vehicles, smartphone device placements or speed of the vehicle. For example, in certain cases, manholes were detected as road surface anomalies; however, in certain cases, they were not detected. Similarly, in some cases certain small cracks were not detected, but in some cases they were detected.

4.1.4 Data Collection for Probabilistic based Crowdsourcing Technique for Road Surface Anomaly Integration (Third Phase)

This phase of data collection was completed on days between 21 March 2018 and 30 March 2018 with the Nexus 7 attached on the dashboard of the Infinity QX60 in order to simulate the data collection model operated by different users. The modified version of the developed mobile app, which was employed for this phase of data collection, had the capability to process the generated sensor data from the smartphone sensors and filter out the irrelevant incidents, such as breaking, turning, and accelerating.

For each detected road surface anomaly, its geographic location (longitude and latitude), vehicle's velocity at the time of detection, bearing of the moving direction at the time of detection, location accuracy, $C_{(ratio)}$ value, " $\mathrm{Vc_i}$ " value, and the date and time of detection were stored in a CSV file format on the internal storage of the mobile device.

Table 4.9 demonstrates the collected data from some of the detected road surface anomalies processed by the Nexus 7. The illustrated sample data shows a part of the road surface anomalies detected along Leslie Street.

Table 4.9 : Samples of collected road surface anomaly information

Latitude (Degree)	Longitude (Degree)	Speed (m/s)	Bearing (rad)	Accuracy of detected location (m)	$C_{(ratio)}$	V_i	Time of Detection (Date and time)
43.80073	-79.3707	13.29	169	10	0.48	1.67	21/03/2018 23:18:43
43.80061	-79.3706	14.04	168	10	0.63	2.09	21/03/2018 23:18:44
43.80022	-79.3705	14.78	167	11	0.50	1.30	21/03/2018 23:18:48
43.79995	-79.3705	14.78	168	10	1.52	5.21	21/03/2018 23:18:49
43.79968	-79.3704	15.53	169	10	1.35	5.77	21/03/2018 23:18:51
43.79939	-79.3703	16.03	169	10	0.40	1.45	21/03/2018 23:18:53
43.79925	-79.3703	15.53	169	10	0.42	1.34	21/03/2018 23:18:54
43.7991	-79.3702	16.28	170	10	1.04	3.55	21/03/2018 23:18:55
43.79895	-79.3702	17.03	170	10	0.57	2.23	21/03/2018 23:19:01

To illustrate the geographic location of detected anomalies, ESRI ArcGIS software was utilized to visually display the results according to their reported longitude and latitude values. Figure 4.9 represents the location of the detected anomalies for each road segment. As shown, the data points are clustered in some areas, representing the possibility of existing road surface anomalies being detected every time of a road survey was completed. For example, a large number of congested areas along the Cummer Avenue could be the reason numerous anomalies existed on the surface of this road segment. By integrating this multi-time detection of anomalies from multi-time surveys, more robust and accurate information regarding the existing road surface anomalies can be inferred in terms of intensity and precise geographic location of the road surface anomalies.

Figure 4.9: The collected road surface anomalies after five-time of road survey

Table 4.10 summarizes the number of detected road surface anomalies of the studied road segments for each time of road survey. According to Table 4.10, the differences in the detection rates on every round of survey (anomaly data collection) was due to the dissimilar vehicle maneuvering resulting in the vehicle not passing over all existing road surface anomalies for each time of survey, or due to deceleration caused by traffic congestion and passing with very low speed on some of the road surface anomalies. Also, the contact point of every anomaly may not be similar every time a vehicle passes over any specific road surface anomaly. Even though the detection rate were varied, the pattern of detection is relatively similar for all surveys. By combining and integrating these multi-time detected anomalies, not only the detection rate is increased but also the accuracy of the anomaly classification (i.e., in terms of their level of discomfort) is enhanced.

Table 4.10: Total detected road surface anomalies for each road segment in each time of survey

Time of survey	**Cummer Ave**	**Leslie St.**	**Finch Ave.**	**Bayview Ave.**
March 21, 2018	86	13	26	6
March 23, 2018	72	14	19	6
March 24, 2018	87	9	20	7
March 28, 2018	72	13	27	4
March 30, 2018	77	10	18	6

In order to demonstrate the detected road surface anomalies in a temporal domain, the ESRI’s ArcScene software was utilized. The detected road surface anomalies are displayed in a way that the vertical dimension of each detected road surface anomaly illustrates the time of detection. For example, red data points which are at shorter lengths than the other data points were collected in March 21, 2018 and purple data points which are at longer lengths were collected in the last survey conducted on March 30, 2018 (refer to Figure 4.10).

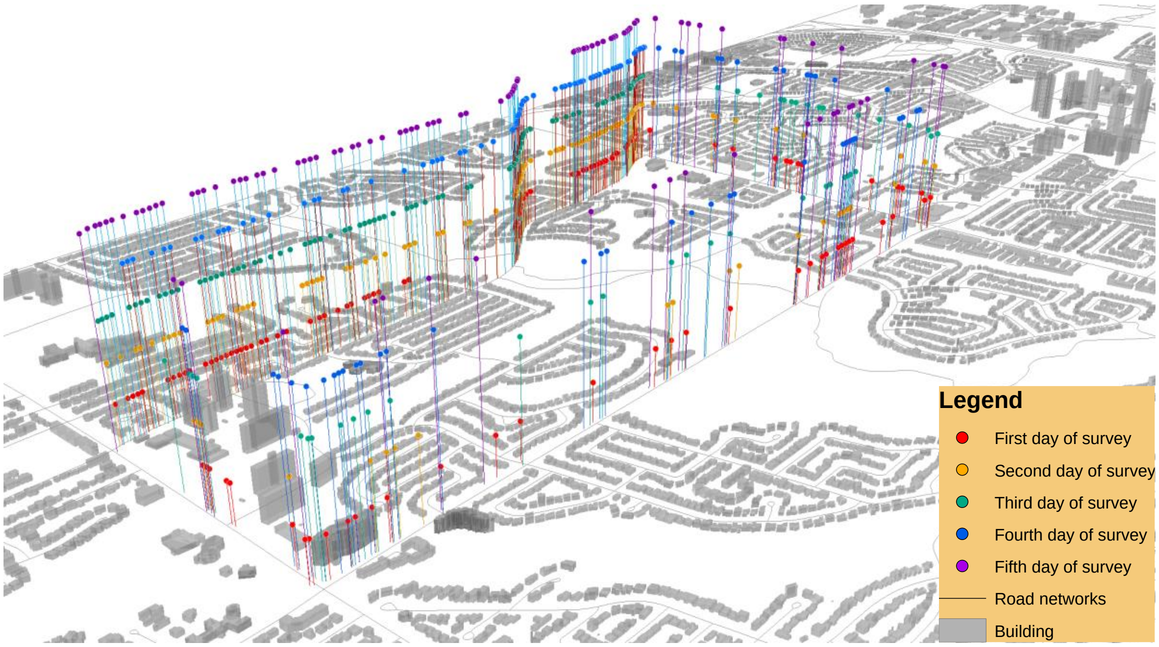

Figure 4.10: Spatiotemporal representation of the detected road surface anomalies

4.2 Road Surface Anomaly Detection from Smartphone Sensors

4.2.1 Road Surface Anomaly Detection

Figure 4.11 shows the outcomes from the road surface anomaly detection process applied during the first stage of data collection. Figure 4.11a illustrates the geographic location of the detected anomalies (before the k-means filtration process), overlaid on the street map provided by ESRI ArcGIS. Figure 4.11b demonstrates the 2D plot representing the standardized values (z-score values) of $C_{(ratio)}$ and the standardized values (z-score values) of Vc_i for each detected anomaly before filtration process. Afterwards, these detected anomalies were filtered according to the proposed k-mean based approach to filter out the incidents caused by non-road surface anomalies, such as accelerating, decelerating, breaking, maneuvering or turning (see Section 3.2).

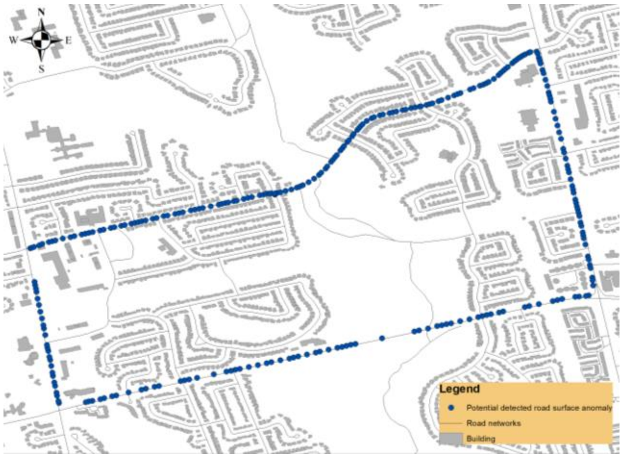

a

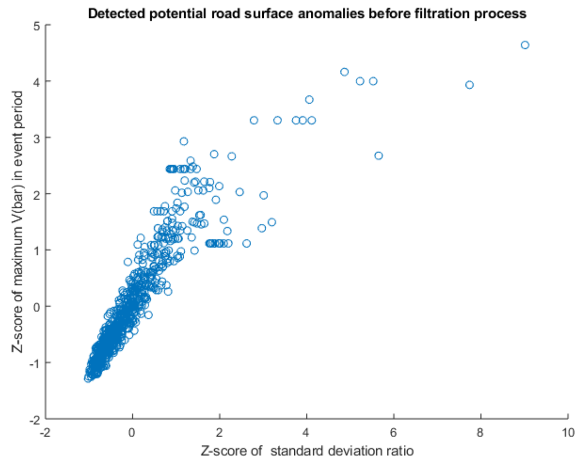

b

Figure 4.11: (a) Location of raw anomaly data from Infinity QX 60 test, and (b) the 2D plot of z-score value of maximum Vc_i *value and the z-score value of the standard deviation ratio*

Figure 4.12 demonstrates the result from k-means based filtration approach for the studied area. In fact, k-means approach partitioned anomalies data into three different classes. For example, according to Figure 4.12a, the anomalies detected from Leslie Street are partitioned to three classes (i.e., red, purple, blue). The cluster containing red data points, which has the lowest centroid value, was filtered because these data primarily caused by non-road surface anomaly incidents. Table 4.11 summarizes the total number of the detected road surface anomalies after k-means filtration process and the number of filtered incidents for each studied road segment.

According to Table 4.11, an average of 65% of the detected potential road surface anomalies were filtered based on the k-means as discussed in Section 3.2.1 for each studied road segment. As a result, it not only justified the rationale of reducing the amount of data being transferred to the central server (for applying required post-processing in the concept of crowdsourcing), but also relieved the computational demand of the probabilistic-based classification process (such as GMM and DPGMM).

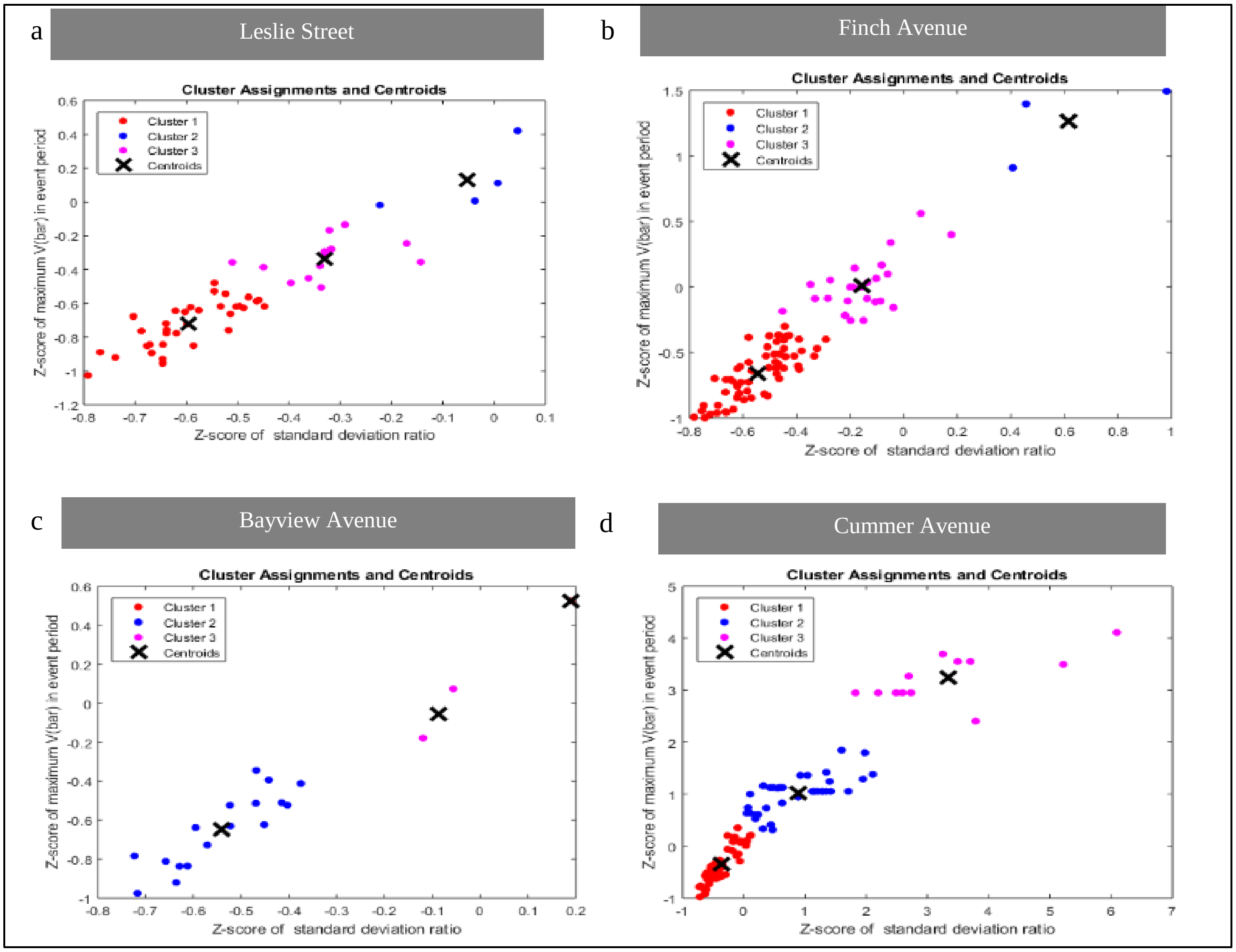

Figure 4.12: Outcomes result from k-means classification approach

Table 4.11: The number of the detected road surface anomalies before and after filtration along with no. of filtered anomalies

	No. of detected potential road surface anomalies (Before filtration)	No. of filtered data	No. of road surface anomalies (After filtration)
Leslie Street	44	23	21
Finch Avenue	109	84	25
Bayview Avenue	24	20	4
Cummer Avenue	148	63	88

4.2.2 Road Surface Anomaly Classification

To classify the road surface anomalies into two severity levels, the GMM approach was applied to the filtered anomalies data. Figure 4.13 shows the outcomes from this classification approach. Figure 4.13a illustrates the 2D plot of the probability density function (PDF) for the fitted Gaussian models. Figure 4.13b illustrates the 3D plot of the PDF of the fitted Gaussian models to the data events. As discussed in Section 3.2.2, since the GMM may not converge for the detected anomalies of some road segments, the detected anomalies were accumulated with the subsequent road segment anomalies in order to ensure convergence. For example, the detected anomalies from Leslie Street were accumulated with the anomalies detected from Finch Avenue since the GMM process was unable to converge for the detected anomalies on Leslie Street. However, once the detected anomalies from Leslie Street were accumulated with those detected on Finch Avenue, the GMM process converged. In addition, the detected anomalies from Bayview Avenue exhibited a similar condition; therefore, by accumulating the detected anomalies from Bayview Avenue with the ones on Cummer Avenue, the GMM classification process converged.

According to Figure 4.13b, it is evident that the peak value of the “Class 1” (i.e., lower severity level mainly caused by small cracks and even manholes) is higher than the one associated with “Class 2” (i.e., higher severity level mainly caused by big cracks, uneven manholes and potholes). This indicates that the number of data points assigned to the first class (Class 1) is more than the number of data points assigned to the second class (Class 2). Moreover, the distribution of the second class (Class 2) is less clustered than that of the first class (Class1), because the response from the vehicle’s vibration becomes more heterogeneous when increasing the severity level of the road surface anomalies.

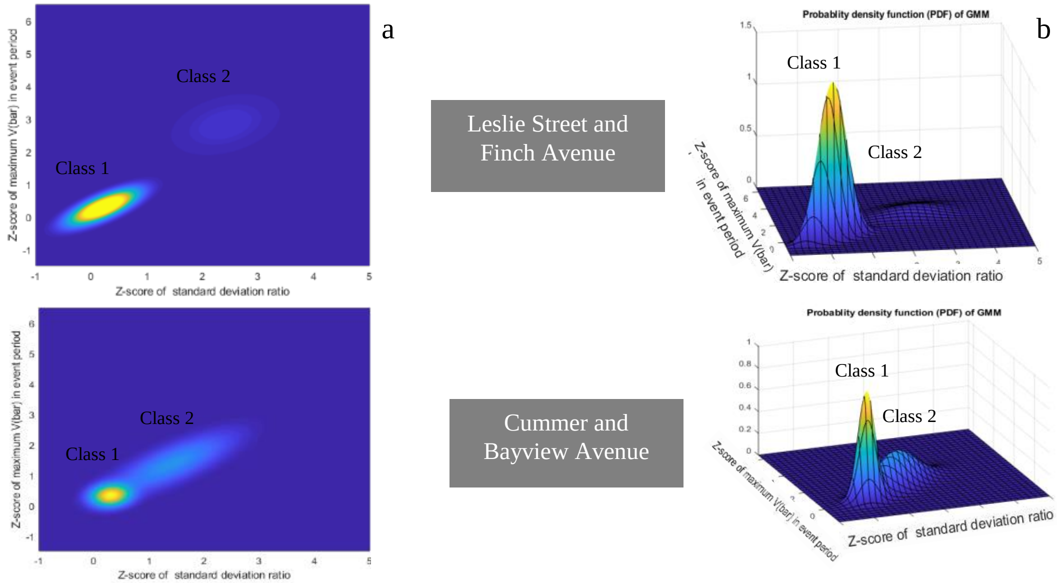

Figure 4.13: (a) 2D plot of PDF for fitted Gaussian models, and (b) 3D plot of PDF for fitted Gaussian models

Since Class 1 and Class 2 do not have clear distinct boundary, by comparing the membership values (probability distribution) of each classified anomaly to every produced Gaussian model, the probability distribution of each anomaly associated with the classes can be investigated. Such a fuzzy property of GMM helps to prevent some occasional misjudgment for class assignment due to the complex and fuzzy boundary situation occurring in road anomaly classification scenarios. In fact, the higher the membership value, the more the probability of being a member of that class.

Figure 4.14 illustrates the membership values (derived from the GMM) for one of the selected anomaly detected along Cummer Avenue. Figure 4.14a represents the selected anomaly detected using an Infinity QX60 with the associated membership values and Figure 4.14b represents the selected anomaly detected by an Acura MDX with the associated membership values belonging to that anomaly. In addition, Figure 4.14c illustrates the image of the selected anomaly captured during the filed inspection. According to Figure 4.14a and 4.14b, yellow points illustrate the anomalies classified as “Class 1” with higher probability, and the red points are the ones classified as “Class 2” with a higher probability. As seen in Figure 4.14, the classification results for the selected anomaly indicate a membership value of 0.02 (~38%) for Class 1 and 0.10 (~62%) for Class 2 (from collected data by an Acura MDX). However, the classification outcomes from a similar anomaly but detected with different vehicle (Infinity QX60) indicate that the membership value for the Class 1 was 0.35 (~98%) and for the Class 2 was 0.02 (~2%). Although the selected anomaly has a dissimilar probability distribution when it was sensed by different vehicles, there is also a possibility where such anomaly belongs to the other class in both cases.

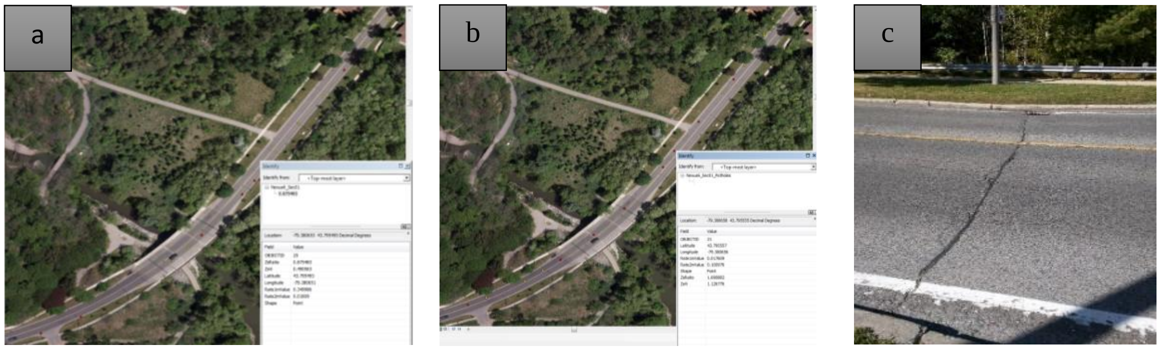

Figure 4.14: (a) the selected anomaly detected by Infinity QX60, (b) the selected anomaly detected by Acura MDX, and (c) the image of the selected anomaly captured during the field inspection

The outcomes from the classification process indicate that the GMM was able to distinguish between two different classes and was able to fit Gaussian models to each class. However, to validate the performance of the proposed approach, a comprehensive evaluation process was conducted based on the second stage of data collection.

This approach which, was implemented as a part of the developed mobile app for the classification purpose, should be replaced by an unsupervised classification approach to meet the requirement for the crowdsourcing purpose since every road segment surface has an exclusive surface condition and every combination of smartphone and vehicle has an exclusive sensing capability. Therefore, unsupervised classification approaches aid in the classification of detected road surface anomalies to more manageable number of classes (i.e. level of severity) leading to better classification outcomes and accurate inference for every single anomaly. This thus leads to the idea of using DPGMM for road surface anomaly classification on the server- side.

4.3 Probabilistic-Based Crowdsourcing Technique for Road Surface Anomaly Classification

4.3.1 Dirichlet Process Gaussian Mixture Model

To classify the detected road surface anomalies to different classes in terms of the level of severity, a DPGMM approach was adopted and applied to the collected data for each road segment. Table 4.12 summarizes the number of formed clusters for each road segment after applying the DPGMM approach.

Table 4.12: The number of the formed clusters for each road segment

Time of survey	Cummer Ave.	Leslie St.	Finch Ave.	Bayview Ave.
March 21, 2018	3	1	2	2
March 23, 2018	3	3	2	1
March 24, 2018	3	1	3	2
March 28, 2018	4	3	3	1
March 30, 2018	3	2	2	3

It is evident that the DPGMM is effective for handling the dissimilarities of the available road surface anomalies existing on every road segment and was able to classify them to the most appropriate classes. For example, the detected road surface anomalies on Cummer Avenue, which had the most defective road surface condition among all the other studied road segments, were classified into either three or four classes. However, the detected road surface anomalies on Bayview Avenue, which had the greatest road surface condition among all those studied road segments, were classified into mostly one or two classes. The outcomes from the DPGMM classification approach specifies that the number of the formed clusters be highly correlated with the quality of the roads surface.

4.3.2 Cluster Assignment Processing

Classified road surface anomalies for different time of survey should be integrated in order to obtain more accurate and reliable results. Figure 4.15 illustrates the two formed clusters and all associated members from detected anomalies along Cummer Avenue after five- repetitions of the road surveys. Blue and yellow points illustrate the assigned road surface anomalies to these two formed clusters, which were the outcomes of the cluster assignment process. Furthermore, the red points represent the centroid locations of these two formed clusters.

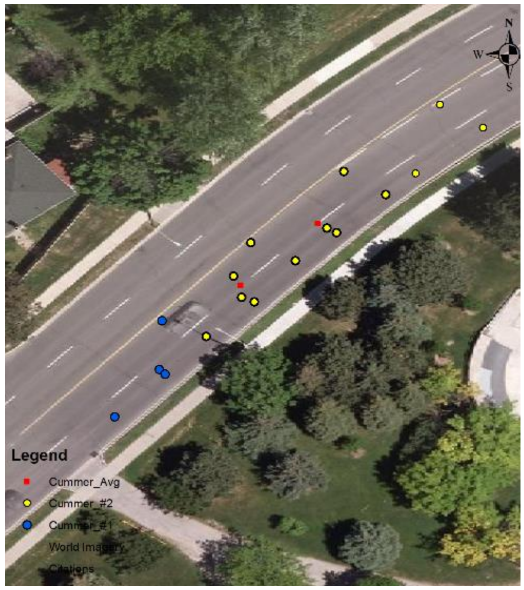

Figure 4.15: Two formed clusters with their associated members along Cummer Avenue

It is obvious that some of the detected road surface anomalies were grouped into more than one cluster due to the detected location uncertainty. Table 4.13 summarizes the inputs and outputs of the cluster assignment process after five-time of surveys. The first column represents the surveyed road segments and the second column summarizes the total number of anomalies derived from five surveys. The third column summarizes the number of the formed clusters after applying the cluster assignment processing approach. Figure 4.16 illustrates the location of cluster centroids formed in this part of processing. According to Figure 4.16, more road surface anomalies were detected and, as a result, more clusters were formed along Cummer Avenue compared to the other surveyed road segments.

Table 4.13: The total number detected road surface anomalies and formed clusters

Road segment	Total number of detected anomalies	Grouped number of anomalies
Cummer Avenue	394	132
Leslie Street	55	21
Finch Avenue	89	38
Bayview Avenue	27	10

Although the geographic locations and the number of detected anomalies existing in every road segment are critical for road surface monitoring purposes, it is also crucial that the severity of each anomaly is defined. Even though inferring the level of severity of each road surface anomaly is challenging using the smartphone sensors, by integrating multiple anomaly information derived from multiple detections of various users' in the spatiotemporal domain, the most reliable information and the identification of every road surface anomaly can be inferred in terms of the level of severity.

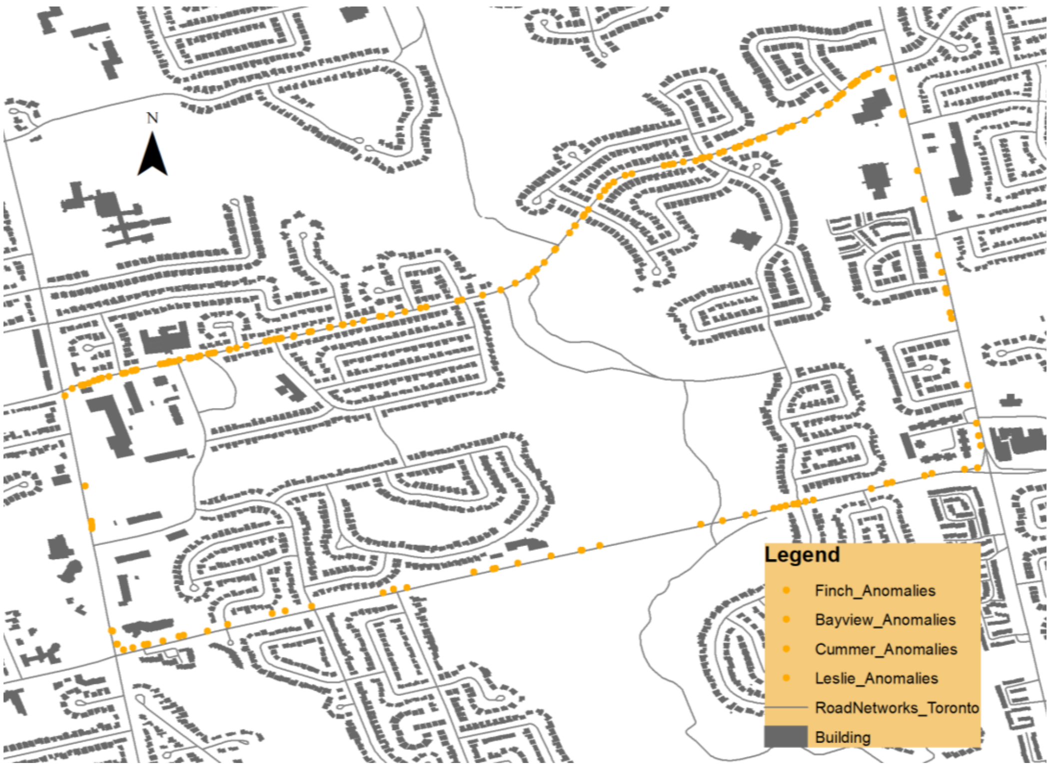

Figure 4.16: The centroids' location of the formed clusters after five-time road survey

4.3.3 Spatiotemporal Data Processing

This step of processing is aimed at integrating the multiple probability distributions of multi-time detections of any road surface anomaly. They were grouped as a cluster resulting from the cluster assigning process in order to update the level of the severity probability distribution for a detected anomaly as more evidence becomes available. Figure 4.17 represents the 3D view of the results by integrating road surface anomalies according to their classes which have high probability. According to Figure 4.17, the height of each anomaly indicates the severity level of the anomaly (with high probability), which were sensed and integrated after five repetitions of the road surveys. The anomalies which were clustered in Class 1 (first level of severity) with higher probability specifies the least level of severity which were mainly caused by small cracks, even manholes, or road joints. However, the anomalies, which were clustered in other classes (i.e., Class 1, Class 2 and Class 3) with higher probabilities, are essentially resulted from potholes, big cracks, or uneven manholes and should be inspected for further verification.

Figure 4.17: Outcomes of the spatiotemporal processing of the formed clusters

To illustrate the spatiotemporal processing procedure applied to each formed cluster, one of the clusters which was formed along Cummer Avenue (labelled “A “) was chosen and discussed (refer to Figure 4.17). Table 4.14 summarizes the probability distribution, detected geographic location, detection time, spatial and temporal distances and weight factor associated to each member (anomaly) of the formed cluster.

According to Table 4.14, the anomaly, which was detected later, obtained more temporal weight comparing to the other anomalies detected previously. For instance, the most recent detection, which was detected on March 30th, obtained the highest temporal weight comparing to the other detections that were detected before the day. Furthermore, the furthest the detections are from the centroid’s location, the lowest spatial weight values were assigned. For example, the third detection, which was detected on Mach 23rd, was approximately 13 meters away from the centroid of the cluster and has the furthest distance from the centroid among all other anomalies. Therefore, the spatial weight for this observation was assigned to be zero.

Table 4.14: Outcomes results from spatiotemporal processing of the selected cluster

Class #1	Class #2	Class #3	Class #4	Longitude	Latitude	Time of Detection	Temporal Distance	Spatial Distance	Temporal Weight	Spatial Weight	Accumulated Weight
0.00	0.00	1.00	0.00	-79.3848	43.79442	'21/03/2018 23:23:59'	9.00	3.83	0.00	0.17	0.06
0.00	0.98	0.02	0.00	-79.3847	43.79433	'21/03/2018 23:24:00'	9.00	6.43	0.00	0.01	0.00
0.93	0.07	0.00	0.00	-79.3849	43.79429	'23/03/2018 23:13:36'	7.01	12.84	0.00	0.00	0.00
0.00	0.00	1.00	0.00	-79.3847	43.79434	'24/03/2018 22:47:56'	6.03	5.13	0.01	0.04	0.02
0.00	0.00	0.02	0.97	-79.3848	43.79435	'28/03/2018 22:41:10'	2.03	4.16	0.58	0.12	0.24
0.00	0.00	1.00	0.00	-79.3848	43.79436	'30/03/2018 23:24:43'	0.00	0.49	1.00	0.97	0.68

Table 4.15: Weighted probability matrix for the selected cluster

Class #1	Class #2	Class #3	Class #4
0.00	0.00	0.06	0.00
0.00	0.00	0.00	0.00
0.00	0.00	0.00	0.00
0.00	0.00	0.02	0.00
0.00	0.00	0.01	0.23
0.00	0.00	0.68	0.00

To generate the weighted-probability matrix, the accumulated weights were multiplied to the probability distribution of each anomaly (refer to Table 4.15). Then, the DMM model was applied on the generated weighted-probability matrix to infer the integrated probability distribution belonging to the selected cluster.

Table 4.16 represents the integrated probability distribution results for the selected clusters. These clusters are indicated as “A”, “B”, “C”, and “D” as depicted in Figure 4.17. One of the clusters is located in Leslie Street and has higher likelihood of being in Class 1. The other one is located in Finch Avenue and has higher likelihood of being in Class 2. The last selected cluster is located in Bayview Avenue and has more likelihood of being in Class 1. However, in all four selected clusters, there is the possibility of such anomalies belonging to other classes in all selected clusters. Figure 4.18 shows the captured images of those selected road surface anomalies recorded during the filed inspections.

Table 4.16: Probability distribution of four selected clusters illustrating four individual road surface anomalies in four different road segments

	Class #1	Class #2	Class #3	Class #4
A	0%	0%	76%	24%
B	53%	25%	22%	0%
C	35%	47%	18%	0%
D	96%	3%	1%	0%

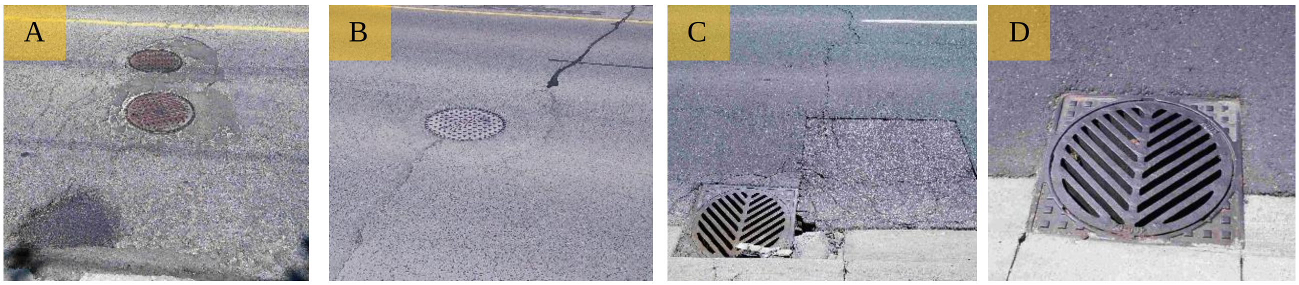

Figure 4.18: Captured geotagged images from studied road surface anomalies

4.4 Performance Evaluations

This section evaluated the performance of the proposed approaches, which was accomplished in two different phases. The first phase evaluated the performance of the proposed approach for detecting road surface anomalies from smartphone sensors, which was implemented as a mobile app. The second phase evaluated the functionality of the probabilistic-based crowdsourcing approach for anomaly integration, which was implemented in a central server after verifying the results.

4.4.1 Road Surface Anomaly Detection from Smartphone Sensors

Case Study (1)

To evaluate the accuracy of detection for the first case study, a portion of Cummer Avenue was selected and visually inspected. This segment had a total of 76 anomalies including 2 potholes, 5 even-manholes, 22 uneven- manholes, 45 cracks and 2 road joints. The Nexus 6 detected 62 anomalies in total, with 35 belonging to Class 1 and 27 belonging to Class 2 with higher probability. The Nexus 7 detected 65 anomalies in total, with 34 classified as Class 1 and 31 classified as Class 2 with higher probability. Table 4.17 summarizes the results from the first case study.

Table 4.17: The number of detected road surface anomalies employing different devices

	Nexus 6			Nexus 7			Existing anomalies
	Class 1	Class 2	Total	Class 1	Class 2	Total	Total
No. of anomalies	35	27	62	34	31	65	76

By comparing the results with from the records from the field inspection and the captured geotagged videos and images, it was concluded that the detection rate for the Nexus 6 and the Nexus 7 were approximately 82% and 86%, respectively. For both devices, the false negative and false positive rate were zero.

Case study (2)

Figure 4.19 summarizes the number of detected road surface anomalies by employing different types of vehicles. With Infinity QX60, totally 62 anomalies were detected, including 35 Class 1 anomalies and 27 Class 2 anomalies. By Acura MDX, 66 anomalies, including 44 Class 1 anomalies and 22 Class 2 anomalies, were detected. With Honda Civic, a total of 67 anomalies were detected, including 61 anomalies classified as Class 1 and 6 of them classified as Class 2. The results indicate that the accuracies of detection for the Infinity QX60, Acura MDX and Honda Civic were 82%, 87% and 88%, respectively. In addition, the outcomes illustrate that the mobile app functioned with optimum performance, even if different types of vehicles were involved.

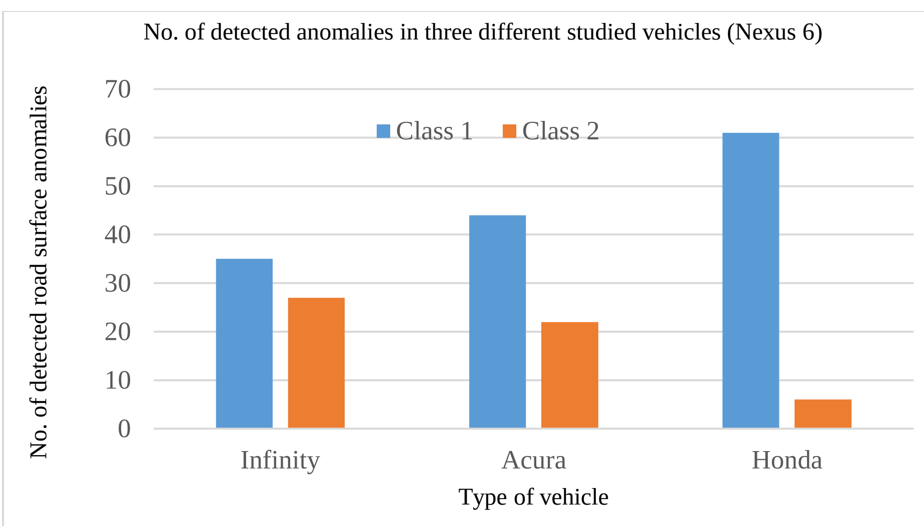

Figure 4.19: The classified number of detected road surface in three different studied vehicles

Figure 4.20a illustrates the detected anomalies from the three vehicles used on the portion of Finch Avenue. As shown, the three involved vehicles were well able to detect existing anomalies in this portion of Finch Avenue. However, due to the limited positioning accuracy available from each smartphone's GPS sensor, the detected geographic location for each anomaly was biased by a few meters (due to the location uncertainty). Figure 4.20b shows the captured images taken from the selected area during the field inspection.

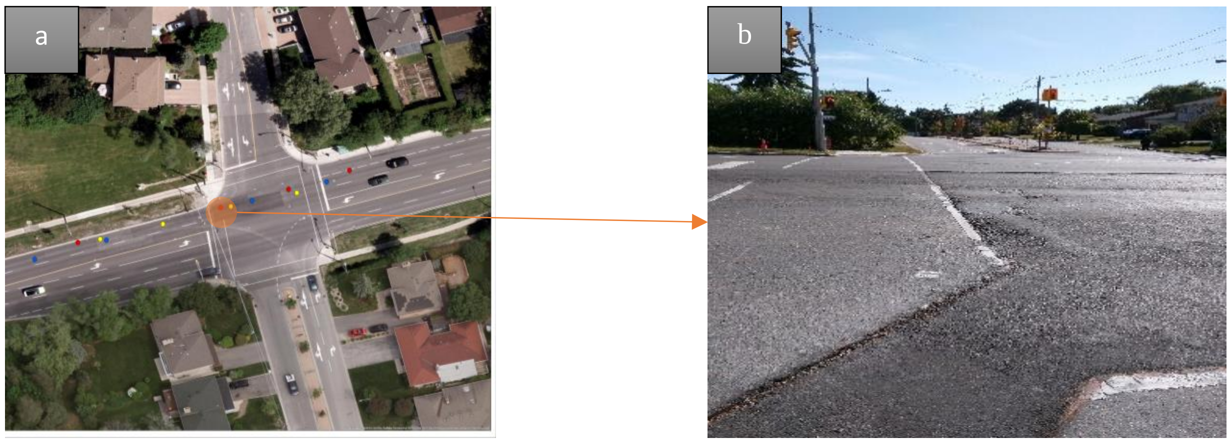

Figure 4.20: (a) The road surface anomaly detected by all three studied vehicles along Finch Avenue, and (b) the captured image recorded from the selected anomaly during the field inspection

Case study (3)

Table 4.18 summarizes the number of the detected anomalies for this case study. The region was selected for both first and second case study had the speed limit of 40 Km/h. However, to assess the accuracy of detection in different speeds and compare the results while the vehicles were moving with different speeds, a portion of Finch Avenue, which had the speed limit of 60 km/h, was selected for the performance evaluation. This selected portion of Finch Avenue had 26 anomalies, including 3 potholes, 5 cracks, 4 uneven-manholes, 12 even manholes and 2 road joints.

Table 4.18: The number of detected road surface anomalies in two different speeds

	Infinity QX60			Acura MDX			Honda Civic		
	Class 1	Class 2	Total	Class 1	Class 2	Total	Class 1	Class 2	Total
40 Km/h	35	27	62	44	20	64	61	6	67
60 Km/h	15	4	19	14	4	18	19	6	25

The detection rates for the road segment which had a 40 km/h speed limit were 82%,87% and 88% for the Infinity QX60, Acura MDX and Honda Civic, respectively, as reported in the second case study. The accuracy of detection for the road segment which had a 60 km/h speed limit were 74%, 70% and 96% for Infinity QX60, Acura MDX and Honda Civic, respectively. It is clear that the developed application based on the proposed approach works reasonably well for various speeds; however, speed seems to have a direct proportional impact on the detection rate. For example, with higher speed discriminating between even-manholes or small cracks and normal roads regions is complicated due to the mechanical properties of the vehicles.

4.4.2 Probabilistic-Based Crowdsourcing Technique for Road Surface Anomaly Classification

Table 4.19 summarizes the number of existing anomalies on the surface of each road segment and the outcomes from road surface anomalies integration approach. The first column outlines the number of existed smaller road segments within the four studied major road segments and the second column summarizes the number of road surface anomalies existing on each road segment, which was recorded from the field inspections. The existed anomalies on each road segment consisted of all existing cracks, potholes, manholes and catchment basins. In addition, columns three to seven summarize the number of integrated road surface anomalies by combining anomaly data from each round of survey. By comparing the number of integrated road surface anomalies and the number of existed road surface anomalies on each road segment, it can be verified that the proposed approach for anomaly integration is able to detect nearly all of the existing anomalies on the road surface after a few surveys.

Table 4.19: The number of detected road surface anomalies in each time of survey, as well as the existing anomalies recorded from the field inspection

Cummer Avenue

Road Segment	No of anomalies	1st	2nd	3rd	4th	5th
1	11	5	7	8	10	10
2	11	9	10	10	11	11
3	13	9	9	10	12	12
4	6	3	4	5	5	5
5	10	7	8	9	8	8
6	9	3	6	8	9	9
7	4	0	3	3	4	4
8	2	0	2	2	2	2
9	14	6	7	11	12	12
10	18	7	12	15	17	17
11	26	15	23	24	24	24
12	9	4	5	8	8	8
Total	**133**	**86**	**102**	**123**	**129**	**132**

Leslie Street

Road Segment	No of anomalies	1st	2nd	3rd	4th	5th
1	3	3	3	3	3	3
2	4	2	4	4	5	4
3	4	2	3	3	3	4
4	2	1	2	2	2	2
5	1	0	0	0	1	1
6	2	1	2	2	2	2
7	0	0	0	0	0	0
8	1	1	1	1	1	1
9	4	3	4	4	4	4
Total	**21**	**13**	**19**	**19**	**21**	**21**

Finch Avenue

Road Segment	No of anomalies	1st	2nd	3rd	4th	5th
1	8	5	5	5	8	8
2	17	12	15	16	17	17
3	2	2	2	2	2	2
4	3	2	2	2	3	3
5	6	4	6	6	6	6
6	2	1	1	1	2	2
Total	**38**	**26**	**31**	**32**	**38**	**38**

Bayview Avenue

Road Segment	No of anomalies	1st	2nd	3rd	4th	5th
1	4	3	3	3	4	4
2	5	3	3	5	5	5
3	1	0	0	0	0	1
Total	**8**	**6**	**6**	**8**	**9**	**9**

According to Figure 4.21, it is evident that the detection rate improves drastically using the proposed crowdsourcing approach. On Cummer Avenue, the first round of survey was able to detect road anomalies with an overall accuracy of 65%. With one additional survey, the accuracy improved to 77%. The overall accuracy yielded better than 90% whenever Cummer Avenue was surveyed for more than three times. A similar occurred on Finch Avenue and Leslie Street. The first survey was able to detect the anomaly features with accuracy over 68% and 62%, respectively. While the second and the third surveys improved the detection over 80% and 90% for the respective two roads. Additional surveys increased the accuracy to almost 100%. On Bayview Street, since the road has been recently rehabilitated, there exists less road anomaly features along the road. As a result, a drastic improvement of road anomaly detection can be achieved after three rounds of survey with overall accuracy improving from 67% to almost 100%.

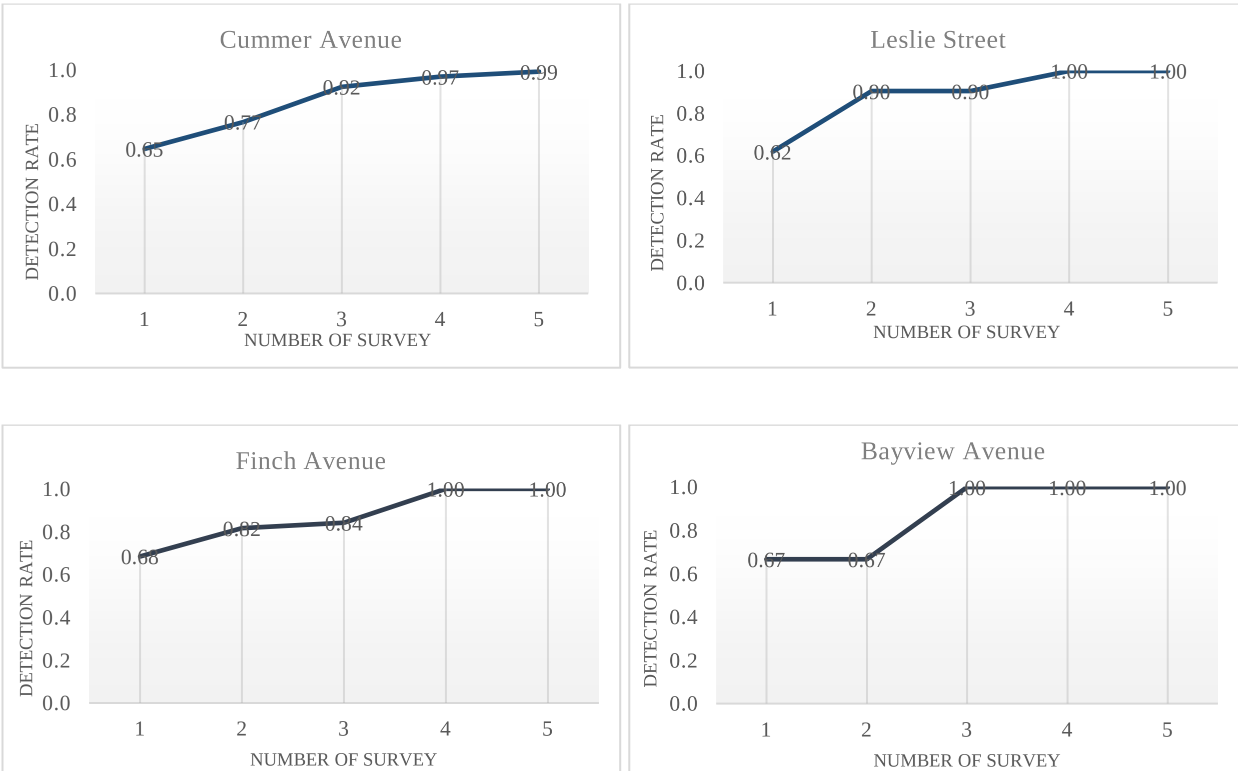

Figure 4.21: Detection rate after every time of road survey and data integration

4.5 Discussions

Currently, smartphone-based sensing is becoming widespread since the mobile devices are equipped with different sensors such as cameras, accelerometers, gyroscopes, GPS, microphones, etc. Participatory sensing is anticipated to be an emerging area where smartphone-based measurements seems particularly attractive and they are not only widespread but also equipped by several sensing capabilities (Burke et al., 2006). However, the measured signal amplitudes from various smartphones may diverge depending on the various reasons: characteristics and quality of the sensors, the position of the smartphone, the suspension system and the speed of the car (Sinharay et al., 2015).

Detection of road anomalies from smartphones is a complex and challenging process. Different vehicles have different responses while passing over the same road anomaly due to the difference in their suspension systems. Further, different smartphones may induce a diverse sensitivity response since they have different sensor properties. Moreover, the wheels of a vehicle rolling over the road anomalies react differently due to their vibration response. Furthermore, each road anomaly different from the others in terms of size, depth or height. Therefore, not only is the response from each road anomaly different from other road anomalies but also due to various devices and vehicles sensing them differently.

Previous studies did not have the ability to implement such a robust approach for road surface anomaly detection. For instance, threshold-based approaches were developed based on certain limited experimental conducted by researchers. However, those limited experimental results cannot represent the entire available scenarios for road surface anomaly detection from smartphone sensors. The machine learning approaches proposed by previous studies required vast amounts of training data sets to cover all possible scenarios. However, the proposed approach in this study considers all these matters in order to be compatible with multiple devices, vehicles and many road surface conditions. In fact, the proposed robust machine learning approach is automatic and self-adapting with every circumstance (i.e., various devices and various vehicles) for road surface anomaly detection.

In addition, the proposed method requires minimal user interaction and offers widespread user freedom of usage. Most previous studies required the placement of smartphones in predefined orientation. The proposed approach is free from smartphone orientation constraints and is able to perform well with any arbitrary smartphone orientation by applying coordinate transformations. The results from the first case study confirmed, that in spite of locating devices in different orientations, the accuracy rate was higher that 85%. Furthermore, developing the proposed approach as a mobile application decreases the level of user interaction to a minimum for anomaly detection. That is, the entire process of detection is performed automatically without human interaction.

Moreover, previous studies attempting to classify road surface anomalies proposed hard classification approaches leading to a high rate of misclassification due to the fuzzy and unknown boundary between different anomalies sensed by smartphone sensors. The fuzzy classification approach proposed in this research study aids in the prevention of most misclassifications. In fact, the proposed probabilistic-based approach aids in the combining of data and provides more accurate inference from multiple detections.

The performance evaluation results show that, in spite of facing different vehicles, devices, speeds and road surface conditions, the proposed approach performs with a high rate of detection in most circumstances. All case studies show that more than 80% rate of detection can be reached for each circumstance, which is evidence of the inclusiveness of this approach. Although previous studies demonstrated an overall detection rate of approximately 80 %. However, their accuracy assessment was done under some controlled situations such as driving over a few preselected potholes or bumps, driving with constant vehicle velocities at all times, using only a specific vehicle and testing a particular placement or orientation.

Road surface anomaly detection from smartphone sensors face critical challenges due to the variability of detection rate, accuracy of detected location, and measuring the anomaly intensity using different devices and vehicles. Further, road surface anomalies have varying properties and they may change from time to time. These uncertainty and variability exist in both the detection and nature of road surface anomalies leading to the proposing of a crowdsourcing technique to integrate detected road surface anomalies from various users and combine them to infer more robust and accurate detection information from multiple users. Previous studies that investigated the crowdsourcing techniques to aggregate road surface anomalies from multiple detections were only in a very early stage and not efficient for implementing in on-line mode but also suffered from the uncertainty and variable nature of road surface anomalies.

In fact, previous studies investigating crowdsourcing techniques for integrating road surface anomalies from multiple sources were unable to deal with the existing dynamic feature of road surface anomalies. They suffered from lack of considering both temporal changes of the road surface anomalies and handling the inherent uncertainties existed in detecting road surface anomalies from smartphone sensors. Moreover, due to the critical weaknesses of the crowdsourcing approaches proposed in previous studies, the detection rate did not exceed more than 90% even after ten repetitions of the survey.

In this study, a probabilistic crowdsourcing approach was proposed to aggregate various detections of road surface anomalies from different users in the spatiotemporal domain. This approach consisted of three major steps. First, the road surface anomalies of each road segments are classified to different classes based on the severity level of anomalies sensed by vehicles. Second, each new detected anomaly either combined with existing clusters composed of preceding detections in different times or generated a new cluster. These processes also considered the location uncertainty of each detected anomaly for clustering assignment purposes. Third, the probability distribution of each clusters is updated whenever a new road surface anomaly assigned to that cluster. This step considers the spatiotemporal domain of detected anomalies existing in every cluster to infer the updated probability distribution. The results and the accuracy of detection analysis indicated that the proposed probabilistic-based crowdsourcing approach was highly capable of merging multiple detections and inferring robust interpretation of each road surface anomaly.

Chapter 5 Web-based GIS Prototype for Road Surface Monitoring System

A GIS is a computer-based information system, designed to locate, manipulate, process, and visualize geospatial data. GIS-based applications are the tools that allow users to create interactive queries, analyze and visualize the geospatial information on maps, which can be widely used for decision making. With the emergence of novel means of communications including Wi-Fi and mobile networks, the GIS system has been evolved from static processing to more dynamic and complex processing by analyzing vast amount of geospatial data generated in real-time.

For example, Wireless Sensor Networks (WSN) are widely used for environmental monitoring and intelligence transportation as a component of smart cities. There is a huge amount of data generated by these sensors, which can be sent to the server for further analysis and visualization. As a result, the amount of observations to provide the most up-to-date information for publics or authorities are increasing dramatically. The networks of sensors keep generating enormous amount of data, and the service providers aggregates and fuses those data to generate more valuable and understandable information for the public. Weather forecast, earthquake reports, traffic conditions and floods are some of the examples of using sensors data and GIS for decision making.

The primary objective of this chapter is to demonstrate and develop a web-based GIS prototype which is able to deliver a real-time and cost-effective platform to monitor road surface conditions.

5.1 System Architecture Design

The conceptual architecture of the proposed prototype was based on the client-server architecture (three-tier architecture) model. The user interface (client-side), server-side and database were developed and maintained as independent components (Figure 5.1). Clients send their requests to a web-based server to either receive appropriate georeferenced information in response or transfer applicable georeferenced information. The client-server architecture model was chosen in order to facilitate the maintenance of the application and allow its functionality to be accessible and modified at any time without considering the end user to configure their computer system (Sugumaran et al., 2004). Figure 5.1 illustrates the proposed web-based GIS system architecture to monitor road surface condition.

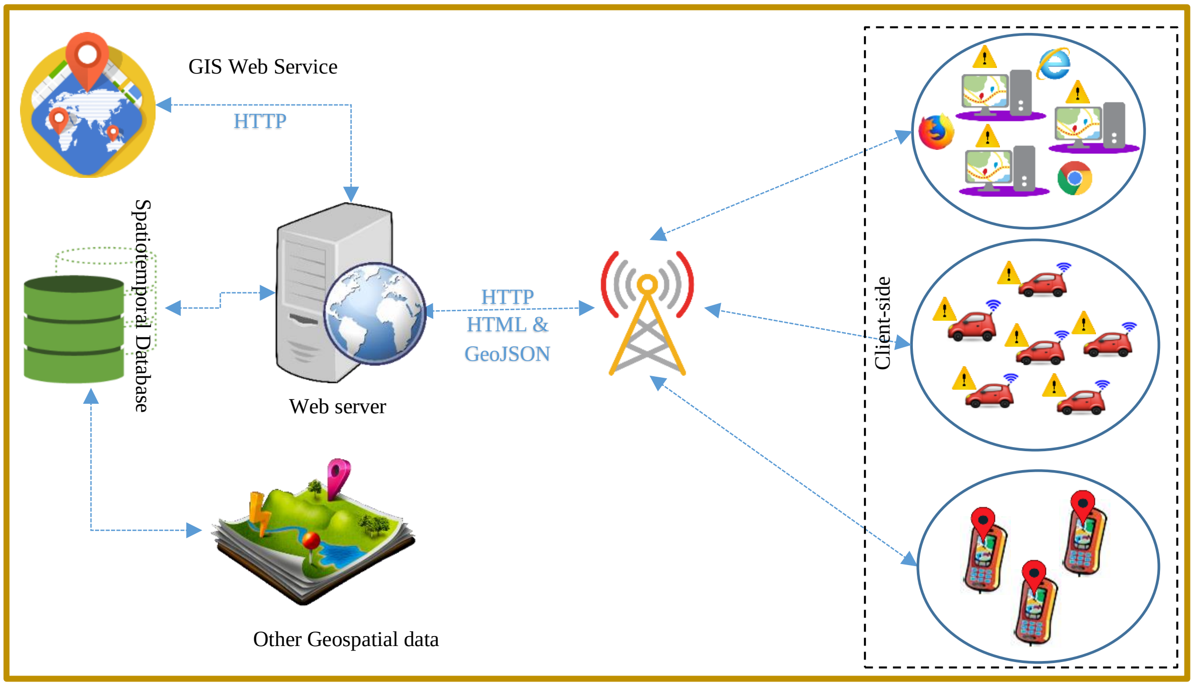

Figure 5.1: The web-based GIS system conceptual architecture to monitor road surface condition

According to Figure 5.1, on the client-side, there are two components: mobile GIS app and web-based GIS interface. The developed mobile app is able to automatically detect road surface anomalies from smartphone sensors and subsequently transfer the anomaly data to the central server. In addition, users are able to report existing road surface anomalies by capturing geotagged images using the app, which is the other suitable means of reporting road surface anomaly. Then, on the server-side, the event streams which are transferred from users are pushed to the complex event processing engine to infer high-level events (road surface anomalies) by improving the accuracy of previously-detected road surface anomaly locations, their reliability through the continuous event-stream, detecting anomalies which are newly created, or performing spatial statistics analysis (such as hotspot analysis). The outcomes from the complex event-processing engine were stored and updated continuously in a spatiotemporal database, which populates the

GIS service for web-based geo-visualization and push notification functions. The entire system is designed to perform as an S&R GIS system.

5.1.1 User Interface (Front-end)

This component includes a mobile GIS app and a web-based GIS interface (refer to Figure 5.2). The mobile GIS app should have various functionality, including a function to automatically detect and report road surface anomalies from smartphone sensors, a function to capture and transfer geotagged images from users' inputs, a routing capability that enables road users to navigate to their desired destinations and a warning system to notify road users concerning the oncoming road surface anomalies.

The other component of the user interface is a web-based GIS interface to illustrate the road surface anomaly information reported by the users. The Google Maps JavaScript API provides multiple functions to support queries, manipulation of maps and editing spatial data. With the combination of the Google Maps API and open source software, it becomes possible to develop a web-based GIS application, which uses the geo-data infrastructure of Google Maps and requests all GIS-functions within a web browser, which are then performed on a cloud-based processing environment. Also, the API provides the ability to set up various interactive functionalities (Google Maps Events) to respond to the users' interactions with map such as click, double click, mouse over, etc., while map overlay functions (Google Maps Overlays) are designed to overlay objects (e.g., points, line, polygon) that need to be visualized on the map. Further, the web-based GIS portal should have the capability to query data based on the selected area or time ranges.

In addition, the web-based GIS interface should have other functionalities, such as a tool panel to turn on/off different data layers, a date range tool panel to specify any desired date periods for querying anomaly data, and a search box to explore users' interested places or locations.

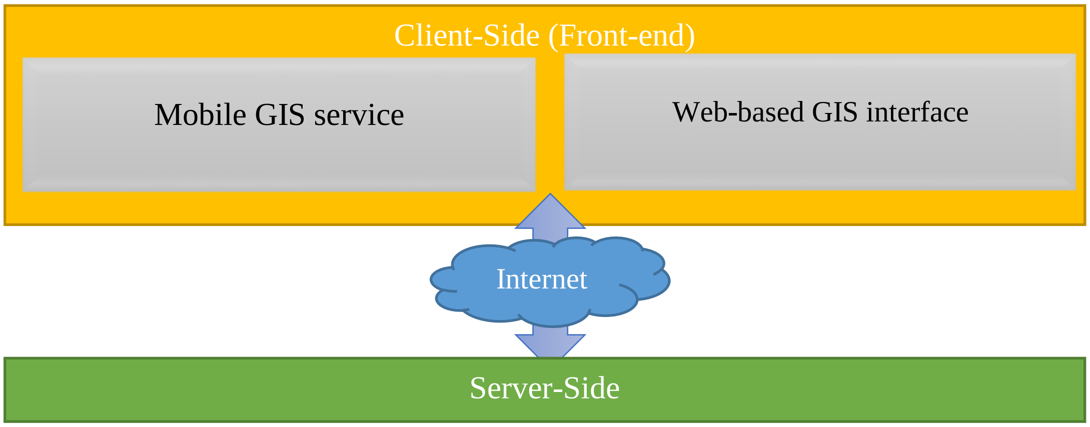

Figure 5.2: The client-side components

5.1.2 Server-Side (Back-end)

This component of the web-based GIS prototype should handle different capabilities such as collecting reported events, including captured geotagged images and detected road surface anomalies from the developed mobile app, real-time processing of the collected events, and data management. Figure 5.3 shows server-side components required to handle aforementioned capabilities. According to Figure 5.3, Apache server, which handles Hypertext Transfer Protocol (HTTP) requests sent from either mobile app or web-based GIS interface was implemented on the server. The requests are either in the form of a request of storing and/or processing collected data including detected road surface anomalies and geotagged images transmitted from the developed mobile app or in the form of evoke functions to browsers and queries to the database in response to the requests made within the web-based GIS interface.

According to Figure 5.3, several other functions need to be implemented to carry out the requests received from the mobile app or web-based GIS interface:

1) “Store/query geotagged images” function is responsible for storing captured geotagged images from mobile GIS application. This function also handles the requests from the web-based GIS interface (client-side).

2) “Road surface anomaly classification” function is responsible for classifying road surface anomalies detected and reported from the developed mobile app.

3) “Store/query detected road surface anomaly” function handles the required action for storing classified road surface anomalies (outcomes of “road surface anomaly classification” function) to the database, as well as queries the stored anomaly data for data visualization and integration purposes.

4) “Store/query/update formed clusters” function is responsible for storing, updating and querying the formed or newly formed clusters by accumulating multi-time detected road surface anomalies.

5) “Cluster assignment process” function assigns new classified road surface anomalies to the appropriate retrieved cluster (based on the proposed methodology described in Section 3.3.3.

6) ”Road surface anomaly integration” function handles the functionality to integrate detected road surface anomalies which were clustered.

7) “Google map API service request and response handler” function handles the requests for desired GIS processing which should to be processed by Google Map cloud.

Google Map API provides a wide variety of desired GIS services processed on the cloud. In fact, Google’s cloud platform provides a reliable and highly scalable infrastructure for GIS analysis particularly for big-data. There are different GIS services available in Google Maps API such as Google Roads API, which can be widely utilized to develop the anticipated research prototype.

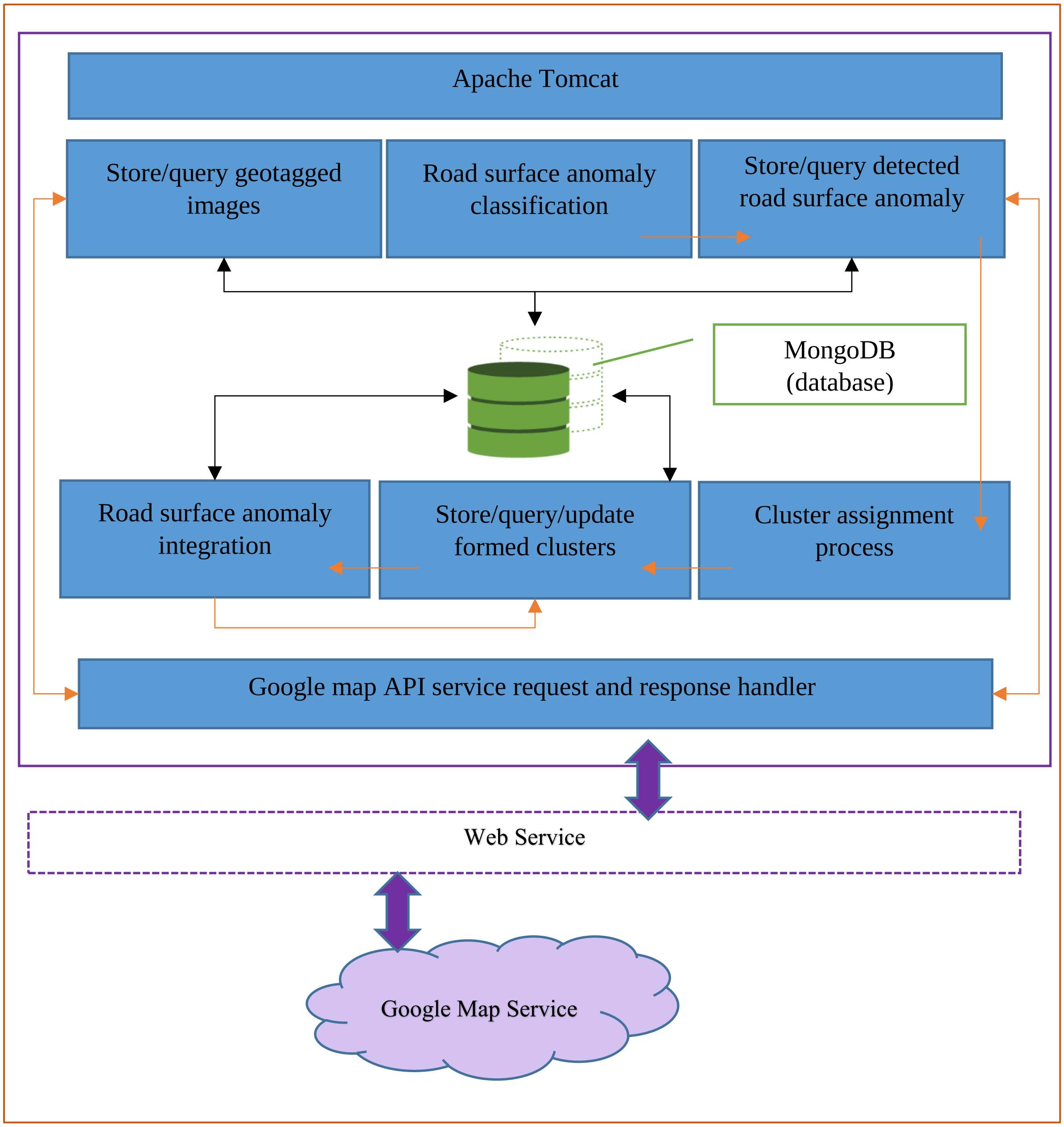

Figure 5.3: The server-side component of the proposed web-based GIS prototype architecture

5.1.3 Database

A spatiotemporal database model is widely used in Geo-information system. Spatiotemporal events can be described along four aspects: attribute, spatial, temporal and thematic. The attribute dimension of the spatiotemporal events describes the properties of the event. It contains the information such as feature ID, name, length, etc. The spatial dimension represents the location of the occurred event, while the temporal dimension represents the temporal domain of the occurred event and thematic dimension explains the motivation behind the event. Spatial and temporal data storage and management play an important role in the analysis and monitoring of any spatiotemporal phenomenon such as road surface conditions in order to assist transportation agencies to better optimize road surface maintenance scheduling and budgeting.

In order to properly manage the spatiotemporal data utilized in this prototype, MongoDB, which is an open-source and big-data based data management system, can be employed to develop the database. This database management system is a document-oriented database program known as NoSQL or non-relational database program using JSON-like file format for storing and retrieving data. In addition, MongoDB supports the GeoJSON format to store geospatial data and uses 2dsphere Indexes to support geospatial queries, such as intersect, nearest neighbor, etc.

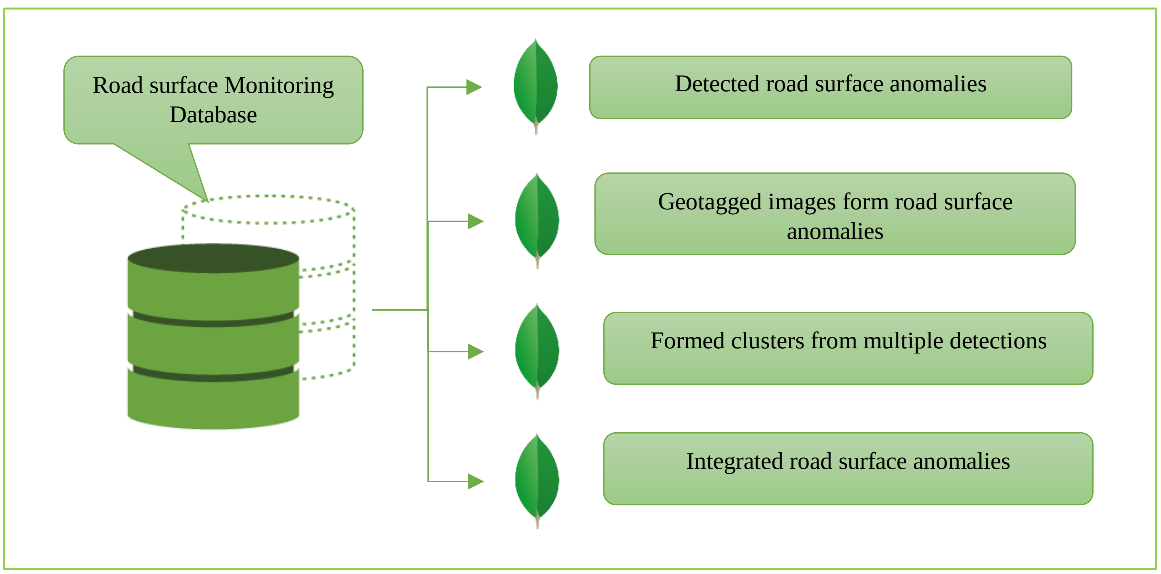

Figure 5.4: The desired database management schema for developing the web-based GIS prototype

In Mongo DB, each set of data, known as documents, is stored in various collections. A collection is similar to a table of a relational data base management system. Figure 5.4 illustrates the required collections to manipulate and manage the spatiotemporal data required for this proposed web-based GIS prototype.

As shown in Figure 5.4, four different collections are defined to store and manage incoming and processed spatiotemporal data. “Detected road surface anomalies” collection stores and manages the detected road surface anomalies from the developed mobile GIS app. “Geotagged images form road surface anomalies” collection aims to manage geotagged images captured and transferred by users from the developed mobile app. “Formed clusters from multi-time survey” collection manages the formed clusters from multi-time surveys of road surface conditions. Finally, “Integrated road surface anomalies” collection aims to manage outcomes from the integrating process of road surface anomalies.

5.2 System Implementation

According to the proposed system architecture, a web-based GIS research prototype has been implemented. In fact, the web service framework was applied into the GIS system design to extend the GIS functionality of the system to be reachable at any time without involving the end user to configure computer system and regardless of the users’ knowledge. GIS web services can provide server-hosted spatial data and GIS functionality in the form of services and integrate them to easily develop a web-based interactive GIS interface to perform basic geo-processing tasks, such as address matching, spatial data visualization, and performing various spatial analysis including hotspot analysis, without maintaining GIS tools or the associated spatial data on local computers. In this section, the procedure of implemented web-based GIS prototype is described and illustrated.

5.2.1 User Interface (Front-end)

A user interface (UI) includes two different components: mobile GIS app and web-based GIS interface. To develop mobile GIS app, an Android studio environment, which is built on JetBrains[3] IDE (Integrated Development Environment), was utilized. The developed mobile app had various functions provided as web services, including detecting and reporting road surface anomalies from mobile sensors, capturing and transferring geotagged images, and navigating users to their desired places. The process of the road surface

[3] https://www.jetbrains.com/

anomaly detection can be run in the background concurrently with the daily-required navigation functionality which road users rely on in their daily life. Google Maps SDK for Android application was utilized to provide a base map services provided by Google Maps and other GIS functionalities, such as navigation service and address matching. In addition, the Google Maps SDK provides a wide variety of mapping interactions besides displaying Google Maps tiles, including panning, zooming, adding markers on the map, and response to map gestures. The developed mobile app as described in Chapter 4 was modified in order to be runnable as a background service of the developed mobile app. In addition, to capture and report geotagged images from existing road surface anomalies, another background service was developed to handle the users' requests for activating camera sensor in order to capture geotagged images and transfer them to the central server for data processing and visualization.

This mobile app was developed in such a way that the intensive functions, including accessing sensor data, processing sensors data, capturing geotagged photos and data transferring performed asynchronously in different threads (multi-thread processing concept) of the smartphones in order to minimize the processing intensity and the battery usage. For instance, the developed service for detecting road surface anomalies from smartphone sensors, which was a long-running, data-intensive operation, is carried out in different threads to increase the speed and efficiency of the service and prevents any possible crashing or freezing caused by this intensive processing on the UI thread.

Moreover, to enhance the performance of the mobile app and reduce the network usage for data transferring in order to be more suitable for crowdsourcing purposes, a novel data structure and communication technology was employed. GeoJSON, which is a lightweight data-interchange format comparing to the Geography Markup Language (GML) and Keyhole Markup Language (KML) (which both have XML (Extensible Markup Language) formats) which ultimately results in reduced data file sizes, was utilized for required data storage or transferring (between multiple developed asynchronous services and central web-server). GeoJSON's lightweight data size allowed the system to have faster loading time for high volumes of data and its simplicity of data structure facilitated the parsing process for geometry data and their attributes, leading to the most suitable data structure to use for the mobile app which was a part of the road surface monitoring system. Figure 5.5 presents an example of GeoJSON data format. Representational State Transfer (REST) technology, which is a novel architectural style built based on HTTP, was employed for data transferring purposes. The REST technology is advanced compared to the regular Simple Object Access Protocol (SOAP) employed for data transferring by minimizing the bandwidth usage.


```
[
 {
  "Ratio": 3.073872053,
  "GbarInMax": 12.0460571,
  "LocBearing": 169,
  "Long": -79.3700231,
  "Lat": 43.7982436,
  "Speed": 16.5,
  "LocAccuracy": 10,
  "TimeOfDetect": "'21/03/2018 23:18:18'",
 },
 {
  "Ratio": 3.214517103,
  "GbarInMax": 12.99552948,
  "LocBearing": 174,
  "Long": -79.3694283,
  "Lat": 43.7959047,
  "Speed": 16.25,
  "LocAccuracy": 10,
  "TimeOfDetect": "'21/03/2018 23:18:35'",
 }
]
```


Figure 5.5: The GeoJSON data file format template

The web-based interface on the client-side was implemented as a simple web page application using Java Server Page (JSP). JSP is a server-side programming technology that has been widely utilized to develop web-based applications in order to be dynamic and platform-independent. The JavaScript API for Google Maps services was utilized to retrieve the map tiles from Google Maps and handle different functionalities, including dynamic interaction with the map and required GIS analysis, such as heat map analysis and access to the attribute information of any spatial object. JQuery, which is a cross-platform, lightweight JavaScript library, was employed to handle the requests for querying data from the central server. JQuery also has the capability to parse the GeoJSON file format, which is retrieved from the server. In addition, HTML and CSS languages were employed to structure the overall web-based user interface.

5.2.2 Server Side (Back-end)

The server-side component of the web-based GIS prototype integrated GIS web service and Servlet/JSP functions based on the framework of Java platform and Enterprise Edition (J2EE) infrastructure. The developed system was a distributed, platform independent system architecture that can be accessed by different devices including desktop computers, tablets, and smartphones in a network with different kinds of operating systems.

The functions developed on the server-side mainly serve two purposes: 1) data integration that integrates incoming road surface anomalies detected from multi-time surveys and 2) data query that processes the data requests from web-based GIS interface and mobile app. Table 5.1 lists all the functions developed on the server-side, with brief descriptions. Functions 1-6 are triggered in sequence when the newly detected road surface anomaly information was reported from the mobile app.

Table 5.1: The developed functions on the server-side

Functions	Descriptions
Road surface anomaly classification	To classify incoming detected road surface anomalies from mobile app
Google map API service request and response handler	To perform required GIS processing (e.g., obtaining road ID and snapping to the road)
Store/query detected road surface anomaly	To store/query classified road surface anomalies
Cluster assignment process	To assign new detected anomalies to existing clusters
Store/query formed clusters	To discover any possible formed clusters from the previous road surveys
Road surface anomaly integration	To integrate anomalies grouped in a cluster
Store/query geotagged images	To Store/query geotagged images

Google Road API was utilized to perform anticipated GIS functionalities. For example, road segment information such as road segment’s ID is retrieved from the API to label each road surface anomaly according to the road segment where it was detected. Also, the API provides the functionality to snap the location of captured geotagged images to the most probable location on the surface of the road with respect to their captured locations, since the geotagged images were primarily captured from off-street locations such as side-walks.

5.2.3 Database

MongoDB asynchronous Java Drive was utilized to handle the storing, updating, or querying tasks in the database. As described in Section 5.1.3, MongoDB uses JSON-like file format for storing and retrieving data. Figure 5.6, Figure 5.7, Figure 5.8 and Figure 5.9 present examples of data schema used for the implemented collections, including detected road surface anomaly collection, geotagged images collection, integrated road surface anomaly collection, and formed clusters collection, respectively. Table 5.2, Table 5.3, Table 5.4 and Table 5.5 summarize the description of all fields within each collection of the four collections listed above.


```
{
  "_id":{"$oid":"5ae6012e0f2d9997d8a56be0"},
  "location":{"type":"Point","coordinates":[{"$numberDouble":"43.7981592"},{"$numberDouble":"-79.3699985"}]},
  "Speed":{"$numberDouble":"17.1805706"},
  "Bearing":{"$numberInt":"170"},
  "Accuracy":{"$numberInt":"10"},
  "LinAccValue":{"$numberDouble":"3.900362385"},
  "StdNormal":{"$numberDouble":"0.97808711"},
  "StdEvent":{"$numberDouble":"1.112968534 "},
  "V":{"$numberDouble":"4.773311642 "},
  "Probability":[{"$numberDouble":"4.643817288711917e-    11"},
{"$numberDouble":"0.9934235240152408"},{"$numberDouble":"0.006576475938321099"}],
  "PlaceId":"ChIJdfS6ky_T1IkRJfQMdUi9Ick",
  "TimeOfDetect":"21/03/2018 23:19:02"
}
```


Figure 5.6: An example of the GeoJSON data schema format for storing detected road surface anomalies

Table 5.2: The description of the data schema used for storing detected road surface anomalies

Field	Data type	Description
_id	Object ID	Generated by MongoDB and is unique for each record (object I.D.)
location	Geometry	The geographic location of the detected road surface anomaly
speed	Double	The speed of moving direction of the vehicle in the time of detection
Bearing	Integer	The bearing of moving vehicle in the time of detection
StdNormal	Double	The standard deviation value of the normal road condition
StdEvent	Double	The standard deviation value in the event period
V	Double	The computed vertical component value according to the Equation 2
Probability	Array of Doubles	The probability distribution of the classified road surface anomaly
PlaceId	String	The road segment I.D. related to the detected anomaly retrieved from Google Road API
TimeOfDetection	Date	The time and data of detection


```
{"
   _id":{"$oid":"5b1069cd70142904a4524f46"},
   "location":{"type":"Point","coordinates":[{"$numberDouble":"43.794177999999995"},{"$numberDouble":"-79.38604736111112"}]},
   "Snplocation":{"type":"Point","coordinates":[{"$numberDouble":"43.79419321053428"},{"$numberDouble":"-79.38592236819571"}]},
    "TimeOfCapture":"Sun May 13 12:59:44 2018",
     "Image_name": "IMG_20180531_181833.JPEG"
}
```


Figure 5.7: An example of the GeoJSON data schema format for storing geotagged images

Table 5.3: The description of the data schema used for storing the geotagged images

Field	Data type	Description
_id	Object ID	Generated by MongoDB and is unique for each record (object I.D.)
location	Geometry	Geographic location of the captured image
Snplocation	Geometry	The snapped location of the captured image (on the surface of the road)
TimeOfCapture	Date	The time and the data of the captured image
Image_name	String	The local name of the uploaded image which stored on the server


```
{
"_id":{"$oid":"5b181d7c701429c9ecf7e485"},
"Integlocation":{"type":"Point","coordinates":[{"$numberDouble":"43.79277286"},{"$numberDouble":"-79.3919411"}]},
"NoVisit":{"$numberInt":"4"},
"IntegratedProbablity":[{"$numberDouble":"0.012282717"},{"$numberDouble":"0.451373978"},{"$numberDouble":"0.140730936"},{"$numberDouble":"0.39
5612369"}],
"TimeOfIntegrated": “2018-03-30 23:24:43.000"
}
```


Figure 5.8: An example of the GeoJSON data schema format for storing integrated road surface anomaly

Table 5.4: The description of the data schema used for storing integrated road surface anomaly

Field	Data type	Description
_id	Object ID	Generated by MongoDB and is unique for each record (object)
Integlocation	Geometry	The geographic location of the cluster (centroid's location)
NoVisit	Integer	The number of times which the anomaly has been detected (or visited)
IntegratedProbability	Array of Doubles	The probability distribution of the integrated road surface anomalies
TimeOfIntegration	Date	Date and time in which the integration process was applied

{

"_id":{"$oid":"5ae6012e0f2d9997d8a56bea"},

"MemOfCluster":["5ae6012e0f2d9997d8a56bea","5ae601570f2d9997d8a56c43","5b09892f70142988cc536be8","5b09b72b7014292df4495579","5b09b859701 4292df4495e2c"]

}

Figure 5.9: An example of the GeoJSON data schema format for storing formed clusters

Table 5.5: The description of the data schema used for storing formed clusters

Field	Data type	Description
_id	Object ID	Generated by MongoDB and is unique for each record (object)
Integlocation	Geometry	The centroid location of the cluster which calculated by taking average of the geographic locations of all members within the cluster
MemOfCluster	Array of object ID	Array of Object IDs associated with the cluster's members. These I.D.s are similar to the anomalies' I.D.s stored in the detected road surface anomalies collection (which used for anomaly's information retrieval)

5.3 Implementation Results

A web-based GIS research prototype with a simple and intuitive user interface was implemented that would enable any user without GIS background to use the system with minimal instructions. The user interface was composed of two different components: Android-based GIS mobile app and a web-based map GIS interface.

5.3.1 User Interface (Mobile GIS Application)

Figure 5.10 illustrates the main interface of the developed mobile application, in which base map tiles are provided by Google Maps API. The following briefly introduces all functions that can be accessed through this interface, together with illustrating screenshots.

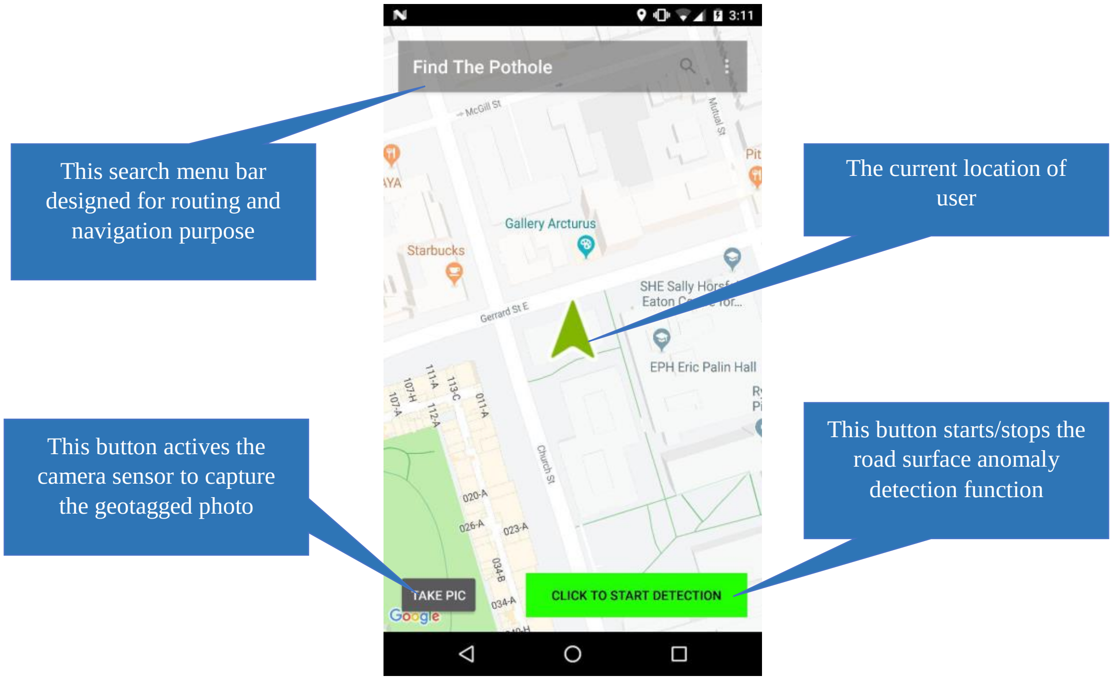

Figure 5.10: The main interface of the developed Mobile GIS application and its functionalities

- **Road surface anomaly detection from smartphone sensors**

An on-click GUI (Graphical User Interface) button was implemented to handle the start/stop service request from users ("CLICK TO START DETECTION" and "CLICK TO STOP DETECTION"). By clicking on the "CLICK TO START DETECTION" button, the developed detection service starts the processing in the background. By starting the service, a popup message is triggered to notify the users which of the service is started and in the meantime the GUI button automatically changes to "CLICK TO STOP DETECTION" to handle the requests for stopping the service whenever the user needs to stop the process (see Figure 5.11a). The "CLICK TO STOP DETECTION" button stops the service and the button changes back to the "CLICK TO START DETECTION" status automatically (see Figure 5.11b). The information about the road surface anomaly detected from this service are either sent to the server if the device has access to an internet connection or stored locally on the internal storage of the device if the device dose not have access to the internet connection. The stored files are sent to the server automatically every time the device connects to an internet connection.

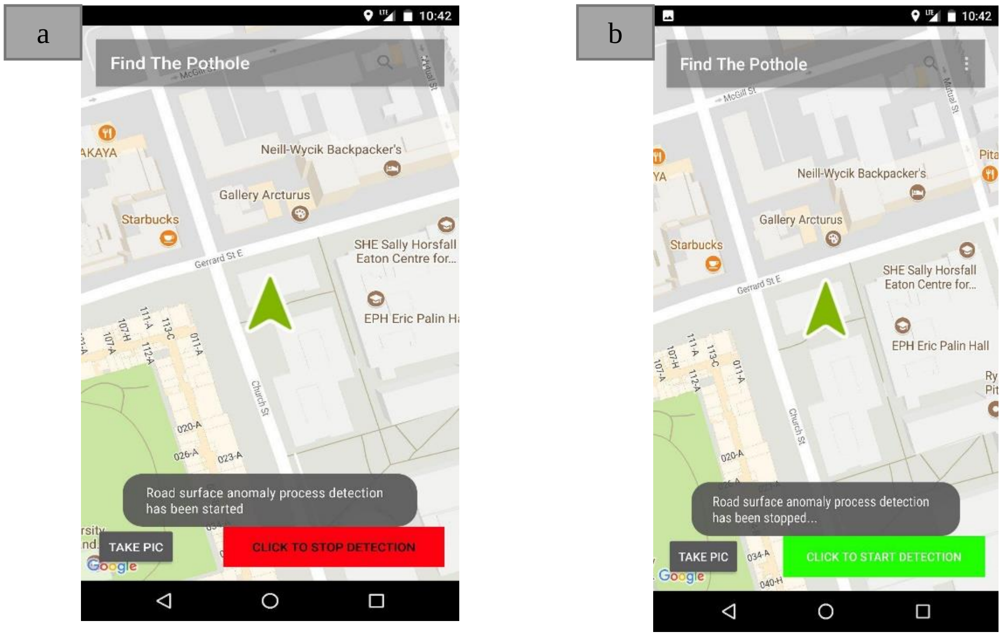

Figure 5.11: (a) The screenshot of the developed mobile app when the service for detecting road surface anomalies start processing, and (b) the screenshot of the developed mobile app when the service for detecting road surface anomalies stop processing

- **Geotagged photographs**

An on-click GUI ("TAKE PIC") button activates the camera sensor to take geotagged images. After the device captures the photo, users can review the captured image before reporting. The geotagged images either be transferred to the server if the device has accessed to the internet or stored locally on the internal memory of the device if the internet network is not available. The locally stored geotagged images are then sent to the server every time when the device has access to an internet connection. This process is performed automatically without any user interaction.

- **Routing**

The developed mobile app has an integrated routing facility that leverages the functionality of the mobile application (Figure 5.12). The "Address Search Menu" bar is implemented to help users to search and find their interested locations or places by typing either the address or the place name. This geocoding service, which is provided by Google Maps API, finds the best route considering the shortest path and minimum traffic congestion (i.e., minimizing the cost) between the user's current location and users' selected location. The routing function also provides turn-by-turn directions to guide users to their desired destinations.

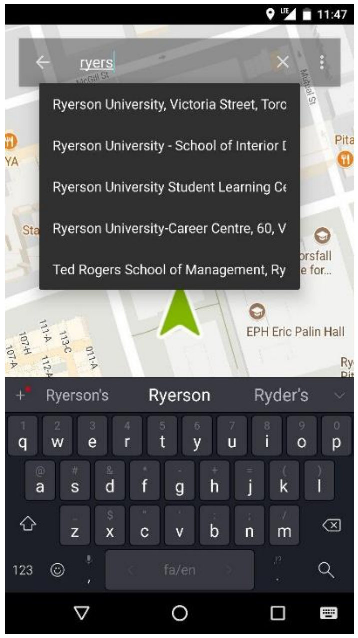

Figure 5.12: The screenshot of the mobile app showing the place search functionality

5.3.2 Server Side (Web-Map portal)

Figure 5.13 illustrates the main interface of the developed web-based GIS interface and its associated components (functions).

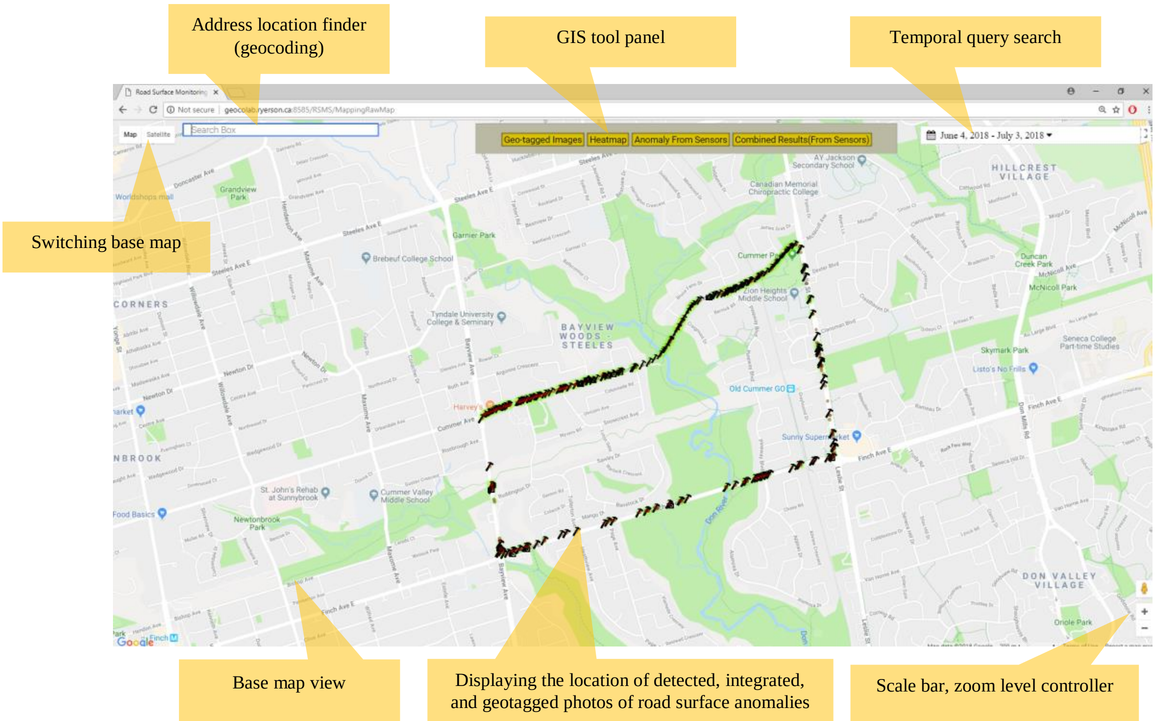

Figure 5.13: The screenshot of the developed web-based GIS interface

As shown in Figure 5.13, the web-based GIS interface shows the base map tiles (road network) provided by Google Map API. The base map also can switch to different other base map layers provided by Google Map API such as satellite map or terrain map. The available zoom and navigation functions enable users to navigate the map dynamically. The web-based GIS portal also includes a GIS tool panel which facilitates users to toggle (turn on/off) between different layers of events overlaid on the base map. The developed web-based GIS interface also has following functionalities:

- **Displaying Symbolized Spatial data**

  Different types of events are symbolized by different types of markers in order to illustrate them dynamically (see Figure 5.14). For example, the road surface anomalies detected from the smartphone sensors are symbolized by (•), the integrated road surface anomalies are symbolized by ( ), and the captured geotagged images are symbolized by ( ). The reason of the biases that exist between overplayed events and the base map's road network could be explained by the difference of the Google Maps framework and the framework which the GPS sensor of the smartphone devices in which such an issue can be solved by map matching technique.

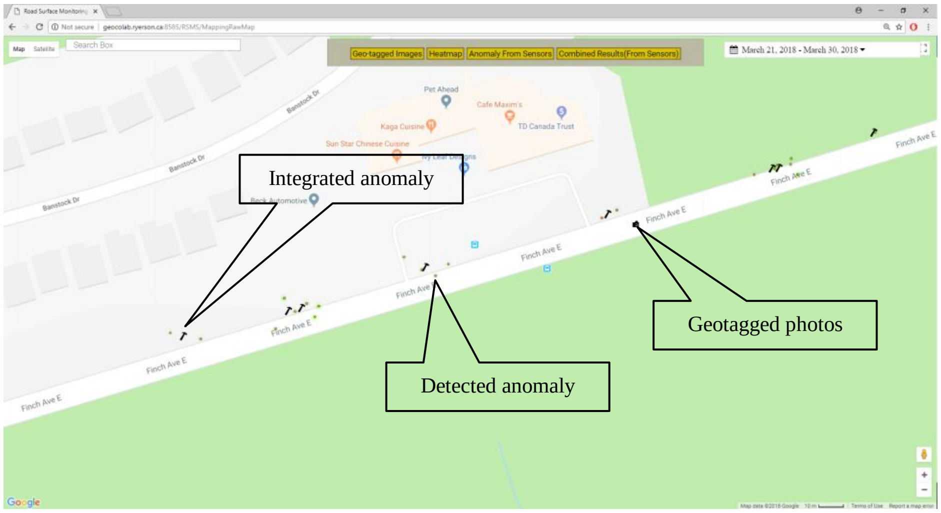

Figure 5.14: Utilizing different symbols to illustrates different types of events

- **Accessing Attribute data**

The attribute data of each event can be accessed by clicking on each marker that represents an event, including geotagged image, detected road surface anomaly from any user and integrated road surface anomaly. By clicking on each data event, a pop-up window is displayed to show the relevant attribute information for each data event. Table 5.5 summarizes the attribute data displayed for each data event.

Table 5.6: The attribute data describing each data event

Data event	Attribute data
Geotagged image	Geographic location, time of capture
Road surface anomaly	Geographic location, probability distribution, time of detection
Integrated road surface anomaly	Geographic location, probability distribution, time of last visit, number of visits

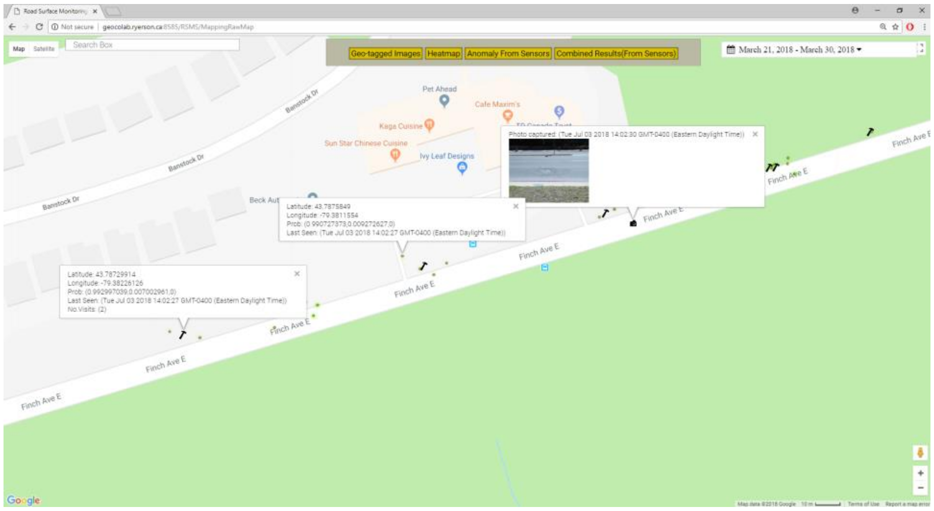

Figure 5.15: Representing the pop-up windows which contain the attribute data for each data event

- **Geocoding Search**

This tool allows the transformation of the address name or place name into the coordinates of the interested locations (geocoding process) and shows them on the map. The implemented geocoding search menu within the web-based GIS prototype allows user (i.e., public or authorities) searches for any interested location or area. Figure 5.16 shows the results for locating an interested location (Ruddington Park) with its surrounding road segments.

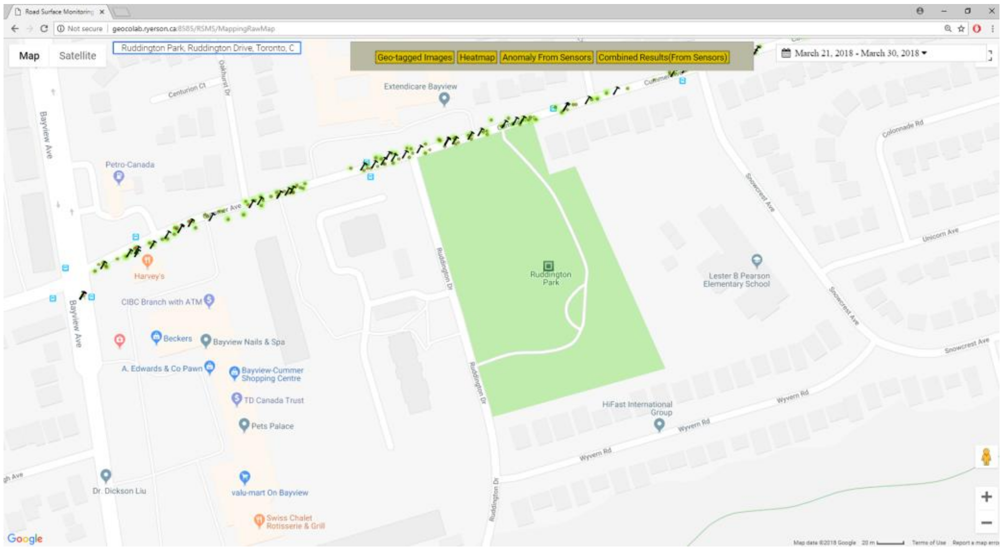

Figure 5.16: The geocoding result for Ruddington Park and its surrounding road segments

- **Heat map generation**

The heat-map tool embedded in the tool panel of the developed web-based interface allows for generating weighted heat maps for better visualization of the detected road surface anomalies by considering not only the level of concentration of the spatial distribution of the detected road surface anomalies, but also by considering level of severity (discomfort level) of each detected anomaly. Figure 5.17 shows the generated heat map from detected road surface anomalies (from the third phase of data collection). The generated heat map indicates that there were more defective areas (i.e., detected road surface anomalies) along the Cummer Avenue than the other surveyed road segments. This is due to the congestion of detected road surface anomalies with a higher level of severity along Cummer Avenue. Therefore, the heat map analysis can facilitate the monitoring of the road surface condition by generating the hotspot areas.

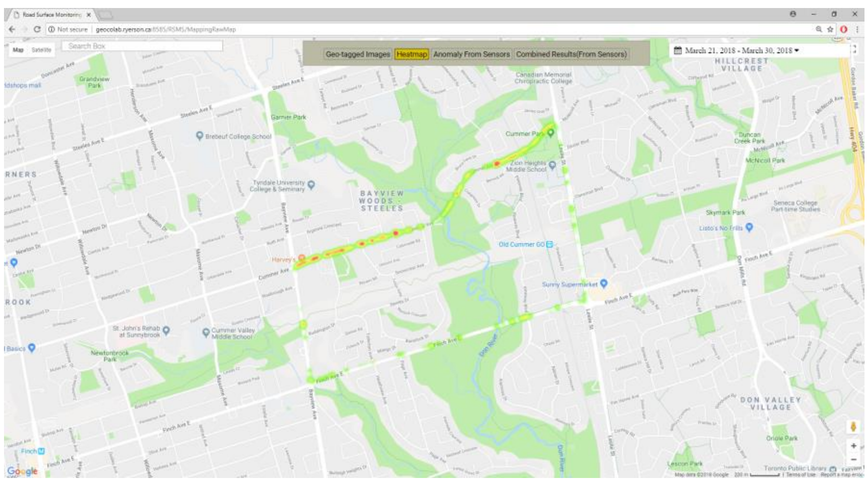

Figure 5.17: The generated heat map based on the detected road surface anomalies

- **Temporal query**

To enhance the query option of the data event, a time-range tool panel was implemented to enable users to define any desired time range in order to query data events. Further, this tool has some predefined time ranges such as, last 30 days, last 7 days, today, and yesterday to reduce and simplify the user’s interaction for choosing time ranges. By defining any time range, the web-based GIS interface sends an appropriate request to the server to query the data events based on the defined time range and visualize the results on the map. Figure 5.18 shows the time-range tool panel for selecting any desired time range from user input.

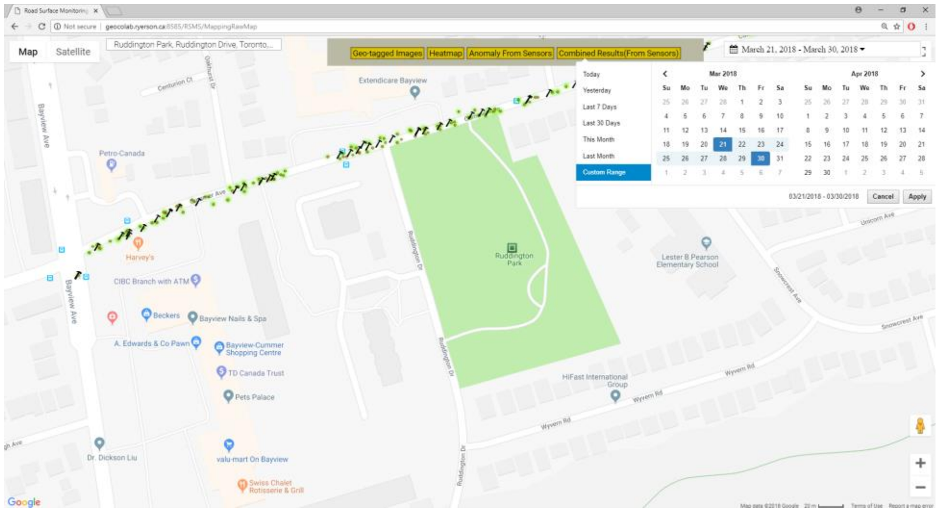

Figure 5.18: The implemented time-range tool panel to select any desired time range to query data

5.4 Discussion

This chapter presents a web-based GIS decision support prototype in the field of road surface monitoring. The purpose of the developed platform is to assist authorities (such as municipalities, ministry of transportation, or any decision maker) in monitoring road surfaces conditions and support them through their decision-making for the purpose of road surface maintenance. In addition, this system provides a participative platform for citizens to assist their communities for monitoring road surface conditions with minimal cost. Road surface condition data can be monitored and stored on the central server by leveraging on the broad coverage of the cellular mobile networks.

The developed web-based GIS prototype had three major components: client-side, server-side and database. The client-side consists of an Android based mobile app and a web-based GIS interface. The mobile app has two major functions: detecting and reporting road surface anomalies from smartphone sensors in a moving vehicle and capturing geotagged images by user inputs. The web-based GIS interface was developed to query and visualize the road surface anomalies based on user’s interests. The developed web-based GIS interface is an intuitive and efficient application, which enables non-specialist users to operate the system without any additional training or GIS background knowledge. The developed interface is a web-based and functions on any network devices with various operation systems. The server-side component of the developed web-based GIS prototype aims to collect and integrate road surface anomalies from various users. The developed spatiotemporal database model also aims to manage the collected and integrated road surface anomalies in spatiotemporal domain.

Web-based GIS development faces new challenges such as technology innovations, big-data transfer rates, GIS analysis of massive amounts of data and non–professional consumers (Alesheikh et al., 2002). The development of the web-based GIS prototype has taken into account some of these challenges by leveraging on web-based GIS architecture and strategies such as minimizing both client-side and server-side processing using Google Maps cloud computing and reducing the volume of transferred data between clients and server by utilizing GeoJSON file format and RESTful technology for data transferring. GeoJSON, which is a lightweight data-interchange format, was utilized, resulting in faster system load time for high volumes of data and faster parsing process for geometry data and their related attributes. Moreover, RESTful web services technology was employed for data communication between clients and server, which helps reduce the bandwidth usage substantially.

Chapter 6 Conclusions and Future Work

6.1 Conclusions

As described in Chapter 1, substantial efforts have been made to implement various methods to detect road surface anomalies using data collected from smartphone sensors. However, these approaches continue to face certain challenges. For many threshold-based approaches, the way the threshold being determined still remains unclear. In addition, those methods based on either supervised or unsupervised learning require a large amount of data to train their detection models. Therefore, a hybrid approach, which can continuously detect and distinguish various road surface anomalies using real-time data streaming from smartphone sensors and other geographic data, was developed. Sensor data were first being smoothed and reoriented to allow smartphone users to have more freedom, as well as to increase the accuracy of detection. Ideally, the approach should be self-adapting and self-learning, capable of reconciling itself to any platform, dynamic behaviors of different vehicles, and different road surface conditions.

Data collection and integration are the key components of any intelligent transportation system. This thesis research proved that the effectiveness of the road surface monitoring system could be substantially improved using crowdsourcing techniques. Data aggregation on the central server not only increases the accuracy of the entire system by data classification and integration, but also provides further services such as, driver warning system of upcoming road surface anomalies and notifying government agencies about the current road surface conditions for potential maintenance and rehabilitation. In fact, as ascribed by the significant increase in the number of smartphone holders and use of mobile devices, continuous monitoring and reporting of events such as road surface anomalies can be reached by on-road users, including the public and transit drivers. The main contributions of this thesis research include the following:

1. **Developed and tested a near real-time road surface anomaly detection approach for road surface monitoring.**

   A hybrid approach, which can continually detect and classify different road surface anomalies from the real-time data streams obtained from smartphone sensors, was developed (which was the improved version of an existing approach). Such an improved version of the developed approach is fully automatic without any user interaction and offers freedom of usage to smartphone users in terms of phone placements. This thus increases serviceability and detection rate. In fact, the developed approach is self-adapting and self-learning so that it can reconcile itself to any platform, and dynamic behaviors of different vehicles and road surface conditions. In addition, based on the developed approach, a free Android-based mobile phone app was developed. The developed mobile application reduces user interaction during the detection process, which is a prerequisite for developing any public participation application. That is, the complete process of detection is performed automatically without any human interaction. To ensure the efficiency of the proposed approach as a mobile app, three different case studies were conducted. The results indicated that the developed mobile app is capable of detecting road surface anomalies in different scenarios, including different device orientations, using various vehicles and different speeds, with reasonably high accuracy yielding up to 80%.

2. **Developed and tested a probabilistic-based crowdsourcing method for road surface anomaly integration**.

   To integrate the detected road surface anomalies from various road users in spatiotemporal domain, a probabilistic-based crowdsourcing method was developed to cluster and integrate multiple detections. The method considers both spatial and temporal characteristics of the detected road surface anomalies. For example, the location uncertainty of the detected anomalies due to poor location information data was considered in data integration process. In addition, the dynamic changes of the road surface anomalies are also considered. The outcomes from the developed probabilistic-based data integration method justified the efficiency of the proposed approach for clustering and combining multiple detections from various users for road surface anomaly detection using smartphone sensors. Experimental results demonstrated that the drastic improvement of road surface anomaly detection rate could be achieved after a few rounds of surveys, with an improvement ranging from 5 to 20%.

3. **Developed and tested a web-based GIS prototype for visualizing and monitoring road surface anomalies in real-time**.

   The developed web-based GIS prototype provides an efficient means for monitoring road surfaces with the following advantages. Firstly, the hosted spatial data (reported road surface anomalies or geotagged photographs) and GIS functionalities can be accessed and integrated to meet the practical need in the process of road surface monitoring system. Secondly, the prototype system is accessible anywhere. The web-based GIS service not only makes the system widely available through the internet, but also delivers the accurate georeferenced data for the public and authorities, including municipalities and transportation authorities dealing with planning to improve the driving comfort and road safety. Thirdly, the prototype system is a spatiotemporally enabled system for querying, analyzing and visualizing spatiotemporal data in a real-time mode. While the road surface conditions have dynamic characteristics, the developed web-based GIS prototype can deal with the space-time characteristics, which is critical in this type of application.

The participatory web-based GIS prototype can be beneficial to both authorities such as ministry of transportation or municipalities to monitor, improve and maintain road surface conditions with a low cost by using road user supplied data. In the City of Toronto, traditionally, citizens can report potholes by filling up an online form, calling 311 (the service line of the City of Toronto), or sending emails to authorities reporting the exact location of identified potholes. However, these reporting methods require considerable human interactions and may lead to faulty reports, which are costly for communities.

However, the developed web-based GIS platform facilitates reporting and monitoring of road surface anomalies since it is fully automated and needs a minimum level of human interaction. For instance, drivers can run the developed app on their smartphone to help detect road surface anomalies from smartphone sensors without any human interaction, or they can report potholes by capturing geotagged images and automatically report them for further inspections. Pavement officers can review the reported geotagged images from road surface anomalies. The integrated road surface anomalies detected from multiple road users through the developed web-based GIS interface in order to measure the severity level of the anomalies before dispatching the repair crews for maintenance purposes. In fact, the developed platform can substantially save time and resources for authorities dealing with road surface maintenance.

Furthermore, drivers can be beneficial from the system by receiving alerting them to oncoming potholes in future. Severe potholes can cause major damages to the vehicle, such as tire puncturing or suspension system failures. Road users can use the developed application to serve their daily navigation needs and to simultaneously notify them of any potential severe potholes (which caused driving discomfort) before approaching them.

6.2 Future Work

The research presented in this thesis provides a crowdsourcing-based and web-based GIS platform for road surface monitoring. Despite the considerable improvement in detecting and monitoring road surface anomalies from smartphone sensors, the results are not purported to be the last word in the subject of crowdsourcing techniques for the road surface monitoring using smartphone sensors. The developed approach has certain limitations that can be further investigated in future research. Several potential areas for future work are listed as follows:

Integration of other geographic data: Some of the detected road surface anomalies are caused by manholes, catchment basins, speed bumps and road joints, which are inevitable on every road surface. These anomalies usually generate similar patterns of signals generating by other types of road surface anomalies, such as cracks, potholes and bumps. If the map data storing all types of manholes, catchment basins, speed bumps and road joints are available, these undeniable road surface features can be either filtered out or treated distinctly from other types of anomalies.

Map Matching: Due to the poor quality of GPS data derived from the smartphone sensors, and the need to acquire more precise location of detected road surface anomalies a straight-forward averaging approach was employed in this study. However, map matching techniques, which have been investigated by many researchers, such as Kim (1996), Kim and Kim (2001), Quddus et al. (2003), Yuan et al. (2010), Brakatsoulas et al. (2005) and Greenfeld et al. (2002), can be utilized to reduce location uncertainties and to precisely associate the detected locations to the surface of the road network. This method is more robust and accurate comparing to the averaging approach, which can be potentially employed in order to associate the detected location of road surface anomalies suffered from location uncertainty to the most probable location on the surface of the roads. To perform the map matching, for instance, the geometrical similarities between series of detected locations and the digital map of the road networks can be calculated in order to correlate the detected location from GPS sensor of the smartphones to the actual location on the surface of road networks. However, this approach is highly dependent on the quality of road map data in order to perform accurately.

Reliability of participators: The reliability of different users' reports is critical for every mobile crowdsourcing system. However, in this research, the reliability of detection from different users who are participating were not considered as a part of the data integration. In fact, different contributors may have discrepancies caused by various data qualities generated by various devices, which have different sensor properties and also other conditions, such as different user preferences for placing their smartphone while they are driving (Ouyang et al., 2016). As a result, future direction can be emphasized in developing a filtering process to select and propagate the data from trusted users through building the trust metrics (Massa and Avesnai, 2004).

Sensor fusion: Other smartphone sensors, such as camera, gyroscope and microphone also can be integrated to improve the accuracy of detection. For example, in this study, the captured geotagged images from the developed mobile app are only stored on the developed database for verification. However, by developing an approach to detected and classify captured geotagged images or videos (i.e., vision-based approach) and integrate the results with the proposed detection approach can improve the detection rate. Vision-based approaches were extensively evaluated by Koch et al. (2013), Jog et al. (2012), Huidrom et al. (2013), Lokeshwor et al. (2013), and Yan et al., (2018). Gyroscope also is another sensor which can be utilized to detect road surface anomalies. For example, Yagi et al., (2010) and Douangphachanh et al., (2014) attempted to combine gyroscope and accelerometer sensor data and processed them in frequency domain to increase the detection accuracy using a data fusion technique.

References

Alesheikh, A.A., Helali, H. & Behroz, H.A. 2002, 'Web GIS: technologies and its applications', Symposium on geospatial theory, processing and applications, vol. 15.

Alessandroni, G., Klopfenstein, L. C., Delpriori, S., Dromedari, M., Luchetti, G., Paolini, B. D., & Bogliolo, A. (2014). Smartroadsense: Collaborative road surface condition monitoring. Proceedings of the UBICOMM, 210-215.

Bhoraskar, R., Vankadhara, N., Raman, B., & Kulkarni, P. (2012, January). Wolverine: Traffic and road condition estimation using smartphone sensors. In Communication Systems and Networks (COMSNETS), 2012 Fourth International Conference on IEEE, pp. 1-6.

Brakatsoulas, S., Pfoser, D., Salas, R., & Wenk, C. (2005, August). On map-matching vehicle tracking data. In Proceedings of the 31st international conference on Very large data bases, VLDB Endowment, pp. 853-864.

Burke, J. A., Estrin, D., Hansen, M., Parker, A., Ramanathan, N., Reddy, S., & Srivastava, M. B. (2006). Participatory sensing. Center for Embedded Network Sensing.

Buza, E., Omanovic, S., & Huseinovic, A. (2013, October). Pothole detection with image processing and spectral clustering. In Proceedings of the 2nd International Conference on Information Technology and Computer Networks pp. 48-53.

Canny, J. (1986). A computational approach to edge detection. IEEE Transactions on pattern analysis and machine intelligence, (6), 679-698.

Chen, K., Lu, M., Tan, G., & Wu, J. (2013). CRSM: Crowdsourcing based road surface monitoring. In High Performance Computing and Communications & 2013 IEEE International Conference on Embedded and Ubiquitous Computing (HPCC_EUC), 2013 IEEE 10th International Conference on IEEE, pp. 2151-2158.

Christopher, M. B. (2016). PATTERN RECOGNITION AND MACHINE LEARNING. Springer-Verlag New York.

Dennis, E., Hong, Q., Wallace, R., Tansil, W., & Smith, M. (2014). Pavement condition monitoring with crowdsourced connected vehicle data. Transportation Research Record: Journal of the Transportation Research Board, (2460), 31-38.

DMG. (2014). Monitoring highway assets with remote technology. Tech. rep., Michigan Department of Transportation. “RC- 1607”

Douangphachanh, V., & Oneyama, H. (2013, November). Estimation of road roughness condition from smartphones under realistic settings. In ITS Telecommunications (ITST), 2013 13th International Conference on IEEE, pp. 433-439.

Douangphachanh, V., & Oneyama, H. (2014, September). Exploring the use of smartphone accelerometer and gyroscope to study on the estimation of road surface roughness condition. In Informatics in Control, Automation and Robotics (ICINCO), 2014 11th International Conference on IEEE, 1, pp. 783-787.

Dunkel, J., Bruns, R., & Stipkovic, S. (2013, March). Event-based smartphone sensor processing for ambient assisted living. In Autonomous Decentralized Systems (ISADS), 2013 IEEE Eleventh International Symposium on IEEE, pp. 1-6.

Eriksson, J., Girod, L., Hull, B., Newton, R., Madden, S., & Balakrishnan, H. (2008, June). The pothole patrol: using a mobile sensor network for road surface monitoring. In Proceedings of the 6th international conference on Mobile systems, applications, and services, ACM, pp. 29-39

Fernandez, J. A., Borries, K., Cheng, L., Vijaya Kumar, B., Stancil, D. D., & Bai, F. (2012). Performance of the 802.11 p physical layer in vehicle-to-vehicle environments. Vehicular Technology, IEEE Transactions on, 61(1), 3-14.

Fox, A., Kumar, B. V., Chen, J., & Bai, F. (2015, June). Crowdsourcing undersampled vehicular sensor data for pothole detection. In Sensing, Communication, and Networking (SECON), 2015 12th Annual IEEE International Conference on IEEE, pp. 515-523.

Google and Open Handset Alliance (n.d.) Android API Guide. http://developer.android.com/guide/index.html. Accessed Sep. 19, 2017.

Greenfeld, J. S. (2002, January). Matching GPS observations to locations on a digital map. In 81th annual meeting of the transportation research board, 3 (1), pp. 164-173.

Gustafsson, F. (2010). Statistical Sensor Fusion, Studentlitteratur. ISBN 978-91-44-05489-6.

Harikrishnan, P. M., & Gopi, V. P. (2017). Vehicle Vibration Signal Processing for Road Surface Monitoring. IEEE Sensors Journal, 17(16), 5192-5197.

Hou, Z., Wang, K. C., & Gong, W. (2007). Experimentation of 3D pavement imaging through stereovision. In International Conference on Transportation Engineering 2007 (pp. 376-381).

Huidrom, L., Das, L. K., & Sud, S. K. (2013). Method for automated assessment of potholes, cracks and patches from road surface video clips. Procedia-Social and Behavioral Sciences, 104, 312-321.

Jain, M., Singh, A. P., Bali, S., & Kaul, S. (2012). Speed-Breaker Early Warning System. In NSDR.

Jog, G. M., Koch, C., Golparvar-Fard, M., & Brilakis, I. (2012). Pothole properties measurement through visual 2D recognition and 3D reconstruction. In Computing in Civil Engineering (2012), pp. 553-560.

Kelvin, C. P. (2004). Automated pavement distress survey through stereovision. Technical Report of Highway IDEA Project, (88).

Kim, J. S. (1996). Node based map matching algorithm for car navigation system. In International Symposium on Automotive Technology & Automation (29th: 1996: Florence, Italy). Global deployment of advanced transportation telematics/ITS.

Kim, S., & Kim, J. H. (2001). Adaptive fuzzy-network-based C-measure map-matching algorithm for car navigation system. IEEE Transactions on industrial electronics, 48(2), pp.432-441.

Kim, T., & Ryu, S. K. (2014). Review and analysis of pothole detection methods. Journal of Emerging Trends in Computing and Information Sciences, 5(8), pp.603-608.

Koch, C., & Brilakis, I. (2011). Pothole detection in asphalt pavement images. Advanced Engineering Informatics, 25(3), pp.507-515.

Koch, C., Jog, G. M., & Brilakis, I. (2013). Pothole detection with image processing and spectral clustering. Journal of Computing in Civil Engineering, 27(4), pp.370-378.

Lokeshwor, H., Das, L. K., & Goel, S. (2013). Robust method for automated segmentation of frames with/without distress from road surface video clips. Journal of Transportation Engineering, 140(1), pp.31-41.

Lou, S. M., Wang, Y. D., & Xu, C. S. (2007). Study of calculation of IRI based on power spectral density of pavement surface roughness. Journal of Highway and Transportation Research and Development, 24, pp.12-15.

Madli, R., Hebbar, S., Pattar, P., & Golla, V. (2015). Automatic detection and notification of potholes and humps on roads to aid drivers. IEEE Sensors Journal, 15(8), pp.4313-4318.

Malley, B., Ramazzotti, D., & Wu, J. T. Y. (2016). Data Pre-processing. In Secondary Analysis of Electronic Health Records, Springer, Cham, pp. 115-141.

Massa, P., & Avesani, P. (2004). Trust-aware collaborative filtering for recommender systems. In OTM Confederated International Conferences" On the Move to Meaningful Internet Systems", Springer, Berlin, Heidelberg, pp. 492-508.

Mednis, A., Strazdins, G., Zviedris, R., Kanonirs, G., & Selavo, L. (2011). Real time pothole detection using android smartphones with accelerometers. In Distributed Computing in Sensor Systems and Workshops (DCOSS), 2011 International Conference on IEEE, pp. 1-6.

Minka, T. (2000). Estimating a Dirichlet distribution. https://tminka.github.io/papers/dirichlet/minka-dirichlet.pdf. Accessed Sep. 13, 2018.

Moazzam, I., Kamal, K., Mathavan, S., Usman, S., & Rahman, M. (2013, October). Metrology and visualization of potholes using the Microsoft Kinect sensor. In Intelligent Transportation Systems-(ITSC), 2013 16th International IEEE Conference on IEEE, pp. 1284-1291

Mohan, P., Padmanabhan, V. N., & Ramjee, R. (2008). Nericell: rich monitoring of road and traffic conditions using mobile smartphones. In Proceedings of the 6th ACM conference on Embedded network sensor systems, ACM, pp. 323-336.

Mok, E. C., Shea, G. Y., & Yan, W. Y. (2004). Geolocation positioning with wireless cellular network in Hong Kong. Hong Kong Surveyor, 15(2), pp. 23-30.

Nomura, T., & Shiraishi, Y. (2015). A method for estimating road surface conditions with a smartphone. International Journal of Informatics Society, 7 (1), pp. 29-36.

Noureldin, A., Karamat, T. B., & Georgy, J. (2013). Basic Navigational Mathematics, Reference Frames and the Earth's Geometry. Fundamentals of Inertial Navigation, Satellite-based Positioning and their Integration. Springer, Berlin, Heidelberg. pp. 21-63.

Ouyang, R. W., Srivastava, M., Toniolo, A., & Norman, T. J. (2016). Truth discovery in crowdsourced detection of spatial events. IEEE transactions on knowledge and data engineering, 28(4), pp. 1047-1060.

Perttunen, M., Mazhelis, O., Cong, F., Kauppila, M., Leppänen, T., Kantola, J., & Riekki, J. (2011). Distributed road surface condition monitoring using mobile phones. In Ubiquitous Intelligence and Computing. Springer Berlin Heidelberg. pp. 64-78.

Pun-Cheng, L. S., Mok, E. C., Shea, G. Y., & Yan, W. Y. (2007). EASYGO - A public transport query and guiding LBS. In Location based services and tele-cartography. Springer, Berlin, Heidelberg. pp. 545-556

Quddus, M. A., Ochieng, W. Y., Zhao, L., & Noland, R. B. (2003). A general map matching algorithm for transport telematics applications. GPS solutions, 7(3), pp. 157-167.

Rasmussen, C. E. (2004). Gaussian processes in machine learning. In Advanced lectures on machine learning. Springer, Berlin, Heidelberg. pp. 63-71.

Rinner, C., Kumari, J., & Mavedati, S. (2011). A geospatial web application to map observations and opinions in environmental planning. Advances in web-based GIS, mapping services and applications, 9, 277-292.

Salari, E., Chou, E., & Lynch, J. J. (2012). Pavement distress evaluation using 3d depth information from stereo vision (No. MIOH UTC TS43 2012).

Sebestyen, G., Muresan, D., & Hangan, A. (2015, May). Road quality evaluation with mobile devices. In Carpathian Control Conference (ICCC), 2015 16th International. IEEE. pp. 458-464.

Shoaib, M., Bosch, S., Incel, O. D., Scholten, H., & Havinga, P. J. (2015). A survey of online activity recognition using mobile phones. Sensors, 15(1), 2059-2085.

Singh, G., Bansal, D., Sofat, S., & Aggarwal, N. (2017). Smart patrolling: An efficient road surface monitoring using smartphone sensors and crowdsourcing. Pervasive and Mobile Computing, 40, pp. 71-88.

Sinharay, A., Bilal, S. M., Pal, A., & Sinha, A. (2013). Low Computational Approach for Road Condition Monitoring Using Smartphones.

Smith, S. M., & Brady, J. M. (1997). SUSAN—a new approach to low level image processing. International journal of computer vision, 23(1), pp. 45-78.

Strutu, M., Stamatescu, G., & Popescu, D. (2013). A mobile sensor network-based road surface monitoring system. In System Theory, Control and Computing (ICSTCC), 2013 17th International Conference on IEEE, pp. 630-634

Sugumaran, R., Meyer, J. C., & Davis, J. (2004). A web-based environmental decision support system (WEDSS) for environmental planning and watershed management. Journal of Geographical Systems, 6(3), pp. 307-322.

Sun, S., Paisley, J., & Liu, Q. (2017, September). Location Dependent Dirichlet Processes. In International Conference on Intelligent Science and Big Data Engineering. Springer, Cham. pp. 64-76.

Tanaka, N., Okamoto, H., & Naito, M. (2000). Detecting and evaluating intrinsic nonlinearity present in the mutual dependence between two variables. Physical D: Nonlinear Phenomena, 147(1), pp. 1-11.

Vijay, S., & Arya, K. (2006). Low Cost–FPGA based system for pothole detection on Indian Roads. Indian Institute of Technology, Bombay.

Wallin, J., & Zachrisson, J. (2013). Sensor fusion in smartphones: With application to car racing performance analysis.

Wang, H. W., Chen, C. H., Cheng, D. Y., Lin, C. H., & Lo, C. C. (2015). A Real-Time Pothole Detection Approach for Intelligent Transportation System. Mathematical Problems in Engineering, 2015.

Wang, K. C. (2004). Challenges and feasibility for comprehensive automated survey of pavement conditions. In Applications of Advanced Technologies in Transportation Engineering (2004), pp. 531-536.

Yagi, K. (2010). Extensional smartphone probe for road bump detection. In 17th ITS World Congress.

Yan, W. Y., & Yuan, X. X. (2018). A low-cost video-based pavement distress screening system for low-volume roads. Journal of Intelligent Transportation Systems, 22(5), pp. 376-389.

Yan, W. Y., Shaker, A., & El-Ashmawy, N. (2015). Urban land cover classification using airborne LiDAR data: A review. Remote Sensing of Environment, 158, pp. 295-310.

Yi, C. W., Chuang, Y. T., & Nian, C. S. (2015). Toward crowdsourcing-based road pavement monitoring by mobile sensing technologies. Intelligent Transportation Systems, IEEE Transactions on, 16(4), pp. 1905-1917.

Yuan, J., Zheng, Y., Zhang, C., Xie, X., & Sun, G. Z. (2010). An interactive-voting based map matching algorithm. In Proceedings of the 2010 Eleventh International Conference on Mobile Data Management, IEEE Computer Society, pp. 43-52.

Zandbergen, P. A. (2009). Accuracy of iPhone locations: A comparison of assisted GPS, Wi-Fi and cellular positioning. Transactions in GIS, 13, pp. 5-25.

Zhang, L., Qi, G. J., Zhang, D., & Tang, J. (2018). Latent Dirichlet Truth Discovery: Separating Trustworthy and Untrustworthy Components in Data Sources. IEEE Access, 6, pp. 1741-1752.